Optimization of Organic-Inorganic Inter-phase in Hybrid Systems Based on Waterborne Polyurethanes and Silica Nanostructures

Haritz Sardon

2011

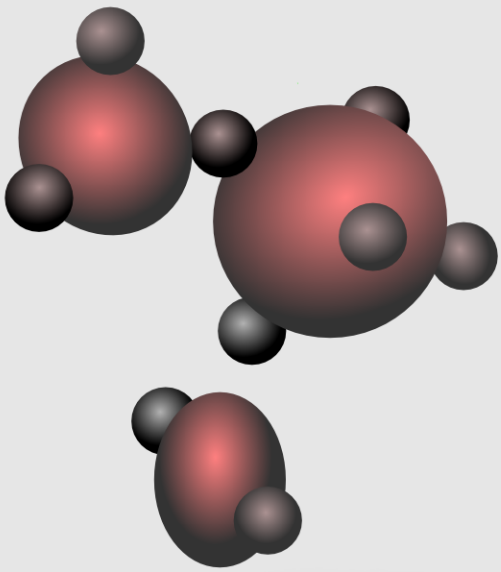

POLYMAT

eman ta zabal zazu

Universidad del País Vasco

Euskal Herriko Unibertsitatea

ISBN: 978-84-694-9479-0

ESKERRAK

Azkenean iritsi da tesi honen azken hitzak idazteko momentua, eta maila batean bizitzaren beste "etapa" bati amaiera emateko momentua. Zati hau idaztea zailena izan dela ezin da esan, baina pentsatzen nuena baino zailago egiten ari zait. Ezagutzen nauzuenek (eta asko zarete), badakizue bide luze hau jende askoren laguntzarik gabe ez zela posible eta zuei denoi eskertu nahi dizuet tesi hau.

Lehenik eta behin nire bi tesi zuzendariei (Josepi ta Luri) eskertu nahi diet eskainitako laguntza eta burututako esfortzua. Azken hilabete hauetan zuen oporretan ere zuekin egon naizelako, eta egindako lan izugarriagatik. Tesi hau maila handi batean zuen gidaritzagatik burutu da, eta zuek emandako konfiantzagatik, gutxinaka gutxinaka pausoak eman ditut aurrera eta azkenean iritsi da bukatzeko momentua. Beti hor egon zaretelako eta dakizuena erakusteko beti prest egon zaretelako, eskerrik asko.

Ezin ahaztu nire "herrikidea" (Yanko), eta gauza konplikatuenak ere ulergarri egiteko duen ahalmen hori. Edozein arazo bai kimiko bai burokratiko bai familiar konpontzeko daukazun erraztasunagatik, eskerrik asko. Orain agian bere proiektu gogorrenean murgilduta dago, gizarteari erakusten gauza kimikoak onak izan daitezkeela. Ea zortea daukazun eta gizartetik kentzen duzun hain garatua dagoen gaixotasun hori, "Kimifobia"; kimiko baten partez, animo !!!! (zure pedagogo dohain horiekin seguru lortuko duzula).

Baita ere gustatuko litzaidake eskertzea Txemari, Agustini eta Maria Eugeniari urte hauetan zehar emandako laguntza, nahiz eta lanez lepo egon niri laguntzeko denbora topatu duzuelako eskerrik asko.

Je voudrais aussi remercier mes supérieurs de Lyon (Elodie et Muriel). J'ai beaucoup appris avec vous à Lyon, ce fut une très bonne expérience personnelle et professionnelle. Je remercie aussi la petite famille que j'ai connue à Lyon (Veronique, Rémi, Ula, Franck, Messie Graillat, Pierre-Yves, Spitz, Vincent, Jean-Pierre, Elsa, Etienne…).

Eskerrak "nire" laborategiko lagunei ere, izugarriak izan dira urte hauek zuen ondoan. Hasieratik bukaerara nirekin egon den kubatar-euskaldunari: eskerrik asko eskainitako laguntza guztiagatik.

Badakit gure diskusioak faltan botatzen dituzula!! Hasieran sartu nintzenean ni "zaintzeagatik" eskerrak: Despiri (bai pupil bai), Alaitzi (gure amatxu) , Itziri (Errealeko sufrimenduak konpartitzen dituena), Javitxuri (la eterna juventud) eta Loretxuri (azkenean gehien agoantatu nauena !!!), eta nire ondoren sartu direnei ere eskerrak: Marinilla (la empresaria), Katherine (ai Karei Karei), Joseba (mi segundo pupilo), Robert (el del saxo), Izaskun (la feliciana), Edu (el Yanke), Alex (el patatero -con cariño-) eta Ibai (laborategiko ñoñostiarra).

Beste laborategietako lagunak ere ezin ditut ahaztu, ze azkenean Pupilen tesia laborategi askotatik pasatu da. Ezin ahaztu Erreologiako laborategiko jendea (Goretti, Arrate, Itsaso, Pablo, Maite, Jorge, Eneko, Mertxe, Antxon), transporte eta analisi termikoko laborategiko jendea (Alvaro, Sorkunde, Antton, Ana, Agurtzane, Marian, Ane, Maialen), propietate mekanikoetako laborategiko jendea (Asier, Imanol, Nora, Gonzalo, Izaro eta bereziki Pablori, tesi honetan egindako lan guztiagatik propietate mekanikoak neurtzeko garaian) eta ingeniaritza kimikoko jendeari (asko zarete eta beldurra daukat norbait ahaztea: Amai, Monika, Aitzi, Ainara, Gemma, Josetxo, Luis, Andoni, Ines, Ibon, Patx, Audrey, Edurne, Monica… eskerrik asko emandako laguntza guztiagatik). Bereziki Urkori (Lizeotik nirekin betidanik egon den lagunari) eta Pitxirriri (ostiral goizeko kafekideari), tesi guztian eskainitako laguntzagatik eta lagun oso onak izateagatik, milesker. Baita ere gustatuko litzaidake eskertzea Urkori, Iñakiri eta Sofiari egindako lan ona bai TEM-arekin ta baita RMN-arekin.

Beste alde batetik, nire lankide berriei, Histocelleko lagunei (Maria G, Maria M, Jon, Guille, Scott, Angel, María Mota, Idoia, Iker, Alba, Galder, Oihana, Javi, Itsaso, Diana, Ainara, Jone, Maite, Bego, Julio, Paola) eta Noraiko lagunei ere eskertu nahi dizkiet emandako animoak idazketako azken hilabete hauetan.

A mis padres también les quiero agradecer toda la ayuda que me han prestado durante todos estos años que han hecho posible todos los logros que he conseguido (os escribo esto para que al menos podáis entender algo de esta tesis).

Azkenik, eta agian esker handiena, Mirenentzat. Nire egun txar guztiak agoantatzeagatik, egun txar horiek on bihurtzeagatik eta azken hilabete luze hauetan beti hor egon zarelako. Milesker Maitti!!

GENERAL INDEX

CHAPTER I: INTRODUCTION

CHAPTER I: INTRODUCTION

1. POLYURETHANES

In 1937, Otto Bayer and coworkers in Germany were the first to discover polyurethanes (PU-s) in response to the competitive challenge arising from Carother's work on polyamides. The successful development of high molecular weight polyamides at E.I. Dupont encouraged Bayer to investigate similar materials not covered by Dupont's patent.[1-3] After some inefficient research, Bayer demonstrated that the reaction of an aliphatic isocyanate with a glycol produces new materials with interesting properties[4]. Dupont soon recognized the desirable elastic properties of PU-s.[1,5-6] In Figure 1.1 a schematic reaction between an alcohol and isocyanate in order to form urethane is shown.

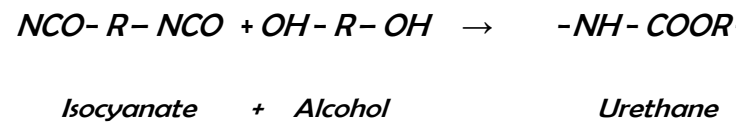

Figure 1.1. The reaction between isocyanate and alcohol to form urethane linkage.

The industrial scale production of PU-s started in 1940, but market growth of PU-s took until 1952, when isocyanates, especially toluene diisocyanate (TDI), became commercially available. In ensuing years, polyurethanes were developed for many different applications as shown in Figure 1.2, which illustrates the molecular structure features used to produce diverse polymer forms such as millable elastomers or rigid foams.[1-2]

Until the late 70s polyurethane production was negligible because of the high cost, and its use was limited only to high engineering materials. But in the 80s the situation changed due to the expansion of applications where thermoplastic elastomers had to be used.

The three important components of PU-s are macrodiol, diisocyanate and chain extender. The synthesis of PU-s involves a simple reaction between a di or polyisocyanate with a di- and/or polyol. These materials can be tailored, selecting appropriate monomers or even playing with the amount of the reagents, covering a wide range of

physical and chemical properties.[1-2,7-8] As a consequence modern technologies such as coatings, adhesives or leathers are continuously developing new materials based on PU-s.

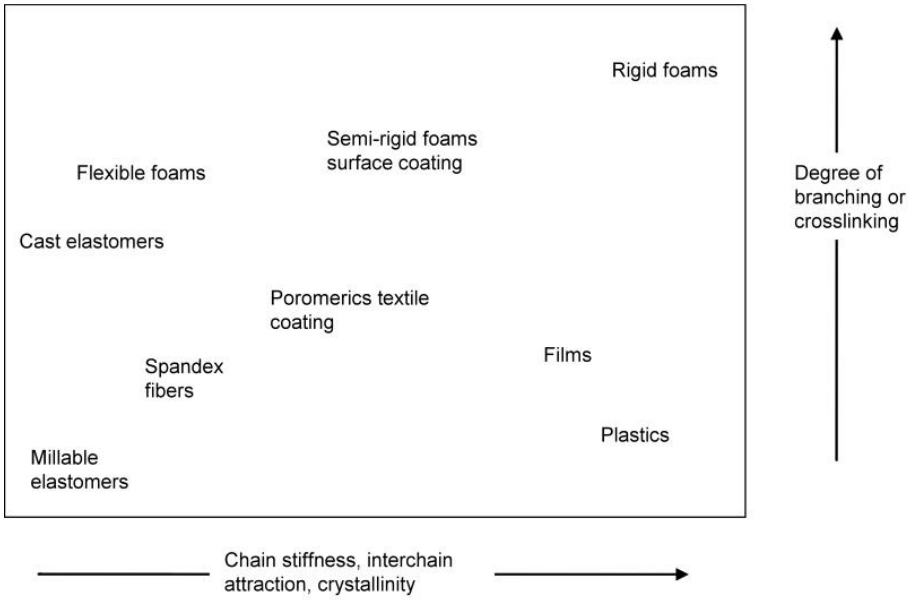

Figure 1.2. Structure-property relation in polyurethanes.

PU-s are usually synthesized in the presence of a solvent in order to obtain high molecular weight polymers due to the high viscosity of the final products.[1-2] However during the last decade, the environmental concerns have driven the coating technologists to explore newer chemistry and approaches to improve the efficiency of organic coatings at a minimum volatile organic component (VOC) and hazardous air pollutants (HAP).[9-15] The solvent use emitted products created around 26 % of the total VOC-s in the USA in 2005. In addition, it is important to point out that the VOC-s in paints and decorative coatings account for around 44 % of the total solvent use emitted (Figure 1.3). New regulations pushed by the European Union and the United States Environmental Protection Agency (EPA) are limiting the amount of VOC-s releasable to the atmosphere. Due to environmental advantages water-borne systems have attracted the attention of technologists and industry in order to replace solvent-borne ones.[11-14]

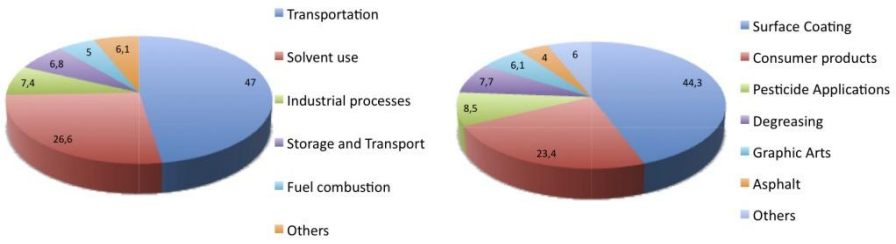

Figure 1.3. Main industries contributing to VOC released (left) together with the proportion of the VOC released from the solvent use products (right).

Not only is the amount of VOC-s and HAP-s reduced but also the use of water systems brings other advantages to formulation as well as clean-up ease, workers health and safety, odour reduction and the ability of the systems to form films at room temperature (if the minimum film formation temperature (MFT) is lower than room temperature).[8,11,16-17] However, the most important reason for using water-borne systems is that the quality of the obtained products can be maintained making them suitable for a myriad of application areas with much lower toxicity. Therefore, organic solvent-based polyurethanes (PU-s) are increasingly being restricted. In contrast, waterborne polyurethanes (WPU-s), prepared with low levels of organic solvent, are seeing even wider use than that of conventional polyurethanes in their time.

1.1. Waterborne Polyurethanes (WPU-s)

The first patent about the synthesis of waterborne polyurethanes was published by Schlack in the 40s and the first article in the 80s.[18] At the beginning these systems were rejected due to their poor properties compared to solvent-borne systems. However, because of the advances in waterborne systems and environmental awareness, the number of articles and patents related to the field of waterborne polyurethanes has considerably incremented as shown in Figure 1.4 which lists the number of publications related with the term waterborne polyurethanes published in the last years. Moreover, if term aqueous polyurethane is added the number of articles and patents increases substantially.

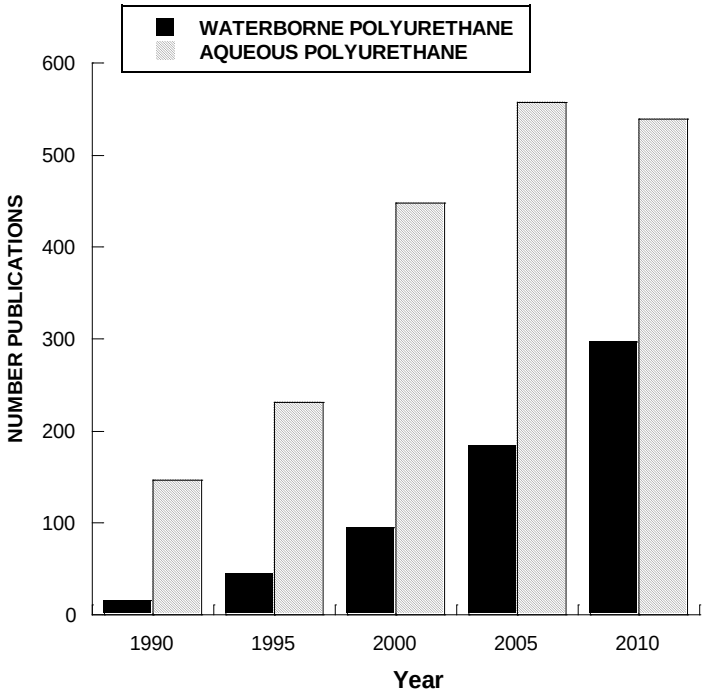

Figure 1.4. Number of publications and patents related to waterborne and aqueous polyurethanes obtained using Scifinder.

The main problem for synthesizing WPU-s, compared to other polymers, is the high reactivity of isocyanate groups towards water.[2,19] Therefore, it is not possible to obtain waterborne polyurethanes by conventional water synthesis methods such as emulsion or suspension polymerization and alternative synthesis routes have to be employed.[11-12,18]

Several processes have been developed for the synthesis of polyurethane water dispersions.[3,12,20-21] The first, and probably the most common one in the industry, is the prepolymer mixing process.[18,22] In the first stage low molecular weight polyurethane is prepared by a conventional synthesis method. In the next stage the prepolymer, which contains a group that improves its dispersability in water, is dispersed in water and finally the polymer is chain extended by the addition of a diamine. In this method, in order to obtain a stable dispersion, the viscosity of the prepolymer has to be sufficiently low.

Another interesting recent process to obtain PU water dispersions is miniemulsion

polymerization (Figure 1.5).[23] It has been proved that hydrophobic polyurethane dispersions can be synthesized in water in a one-step procedure using this method.[21,24] In this way, stable monomer droplets are obtained by intense shearing of a system containing water, surfactant, hydrophobe and the monomers. Each drop acts as a mini reactor where the polymerization occurs.

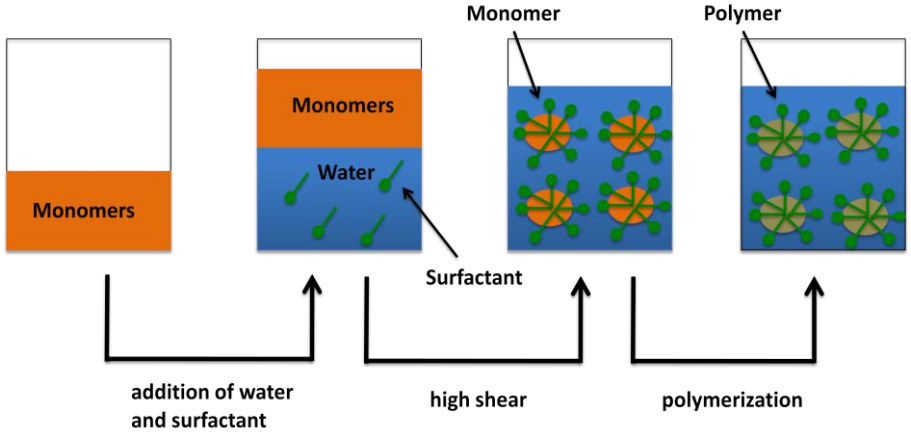

Figure 1.5. Scheme of miniemulsion polymerization.

The main issue of this system is that water can react easily with the isocyanate, leading to a significant decrease of the molecular weight. This can be avoided by a careful choice of the experimental parameters.

Another alternative is the formation of polyacrylic-polyurethane complex dispersions.[25-26] As in the prepolymer mixture process low molecular weight PU prepolymer is formed and blended with some acrylic monomers. This system is then dispersed in water and the polymerization is carried out via emulsion or miniemulsion polymerization.

Finally, one of the most successful polymerization routes is the acetone process.[18,22,27-29] The acetone process is a two-step route to obtain polyurethane dispersions. In the first step, during the polyurethane synthesis in acetone, hydrophilic groups are incorporated into the polymer backbone. These hydrophilic groups act as an internal emulsifier allowing the dispersion of the polymer in water; this emulsifier is usually a diol with ionic groups (carboxylate, sulfonate or quaternary ammonium salt) or with non-ionic groups such as

[poly(ethylene oxide)].[17,30-31] In the second step, water is added to the polyurethane/acetone mixture. Thanks to the hydrophilic groups incorporated previously in the polymerization process, polyurethane precipitation gives rise to stable dispersions. Finally, as acetone has a low boiling point, it can be easily removed, yielding a product containing either very low or no VOC-s. By properly fixing the conditions of the acetone process stable nanoemulsions can be obtained.[32]

However, because of the presence of hydrophilic functional groups, waterborne polyurethanes present lower water and weather resistance compared to solvent-based counterparts.[3,13,33-34] The major drawbacks of thermoplastic PU coatings are their poor resistance towards mechanical strains and high temperature deformation and/or degradation. Generally, their acceptable mechanical properties vanish above 80 °C and thermal degradation takes place above 200 °C. The presence of crosslinks provides thermoset coatings with enhanced tensile strength, abrasion resistance as well as acid, alkali and solvent resistance, which is lacking in thermoplastic WPU coatings. These performance criteria are essential for most industrial coatings. Therefore, in order to modify the properties of a segmented WPU for a high performance coating application, a calculated amount of crosslinker is needed. The presence of crosslinks by the deliberate addition of a crosslinker or by in situ generation due to the side product formation seriously hampers the phase separation and produces a polymer which shows both the phase-mixed and phase-separated behaviour, depending on the concentration of the crosslinker.[35-38]

A number of strategies have been suggested to modify WPU-s. Following the literature crosslinked WPU-s can be classified in two main groups: one component curable WPU-s (1K-WPU) and two component curable WPU-s (2K-WPU).[39-40]

A two-component waterborne polyurethane system utilizes hydroxyl functional coreactants, commonly polyesters or polyacrylates that form stable dispersions in water. Ideally, the polyol (component one) is formulated with all flow aids, thickeners, pigments and water incorporated into the mixture. A polyisocyanate (component two) is then mixed with component one prior to application, giving rise to a stable dispersion (only for a few hours). This is then applied to a substrate by conventional methods and, in most of

the cases, the dispersions are cured under ambient conditions (in especial cases an external source is employed to improve the curing rate).[3,35,37,41] In Figure 1.6, a schematic representation of the application route in 2K WPU-s is shown.

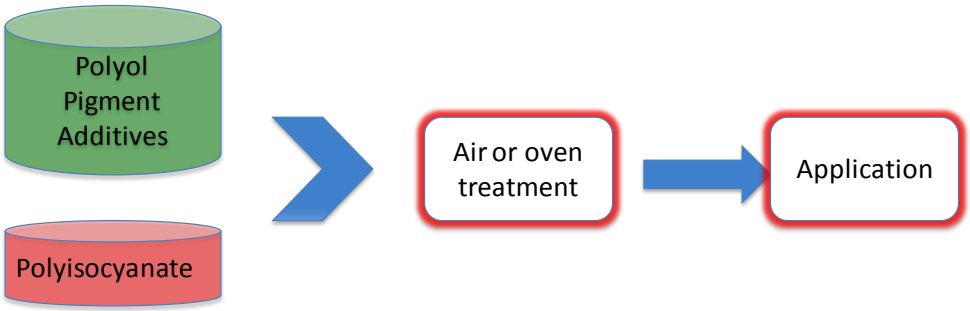

Figure 1.6. Schematic representation of the application route employed in 2K-WPU-s.

These materials have been used due to their high chemical resistance, exterior durability and high curing rate; however, they have many disadvantages over 1K coatings. Using one component coatings the risk of improper ratio of the components is eliminated and handling and capital costs for the applicator are reduced. Furthermore, waste resulting from mixing an amount of two components formulations larger than what can be used within the pot life time span is reduced, along with toxic hazard.[42]

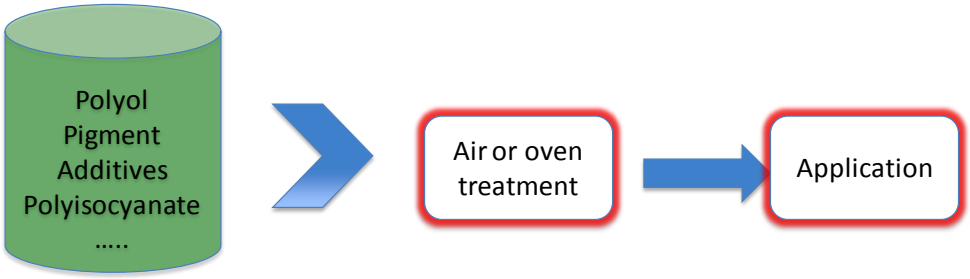

Figure 1.7. Schematic representation of the application route employed in 1K-WPU-s.

One-component polyurethane dispersions are fully reacted polyurethane polymers containing blocked reactive groups. However, for curing the blocked groups must be unblocked and this process normally requires an external energy source, such as temperature or UV radiation. The energy costs thus increase and heat-sensitive substrates, cannot be coated. In addition, in some cases blocking agents are hazardous. In

Figure 1.7 a schematic representation of 1K-WPU-s is shown, where all the additives, filler, etc. are introduced together with the polymer, avoiding the utilization of improper ratios.

Recently, room temperature self-curable waterborne polyurethanes have been developed in order to avoid the utilization of external sources. Among the different options available to self-cure polyurethanes, one of the most promising strategies is to employ the well-known Sol-Gel process in order to promote crosslinking. In this process, a low molecular weight alkoxysilane is introduced in the polymer chain. The alkoxysilane allows fast ambient curing by Sol-Gel process giving rise to a silicon dioxide network that considerably improves the properties of the WPU-s.[38,43-46] After curing, a crosslinked polyurethane/silica organic-inorganic hybrid material is obtained.

2. COLLOIDAL-BASED ORGANIC INORGANIC NANOSTRUCTURED MATERIALS

Waterborne organic/inorganic nanostructured materials with length scales in the order of a few to several tens of nanometers have attracted considerable attention in recent years as the intimate combination of the organic and inorganic components at the nanoscale offers the promise of novel properties.[47-49] As the working scale is in the range of nanometers, these materials possess high surface-to-volume ratio. In addition, their multifunctional character makes them particularly attractive in various fields of material science, such as catalysis, microelectronics, coatings , biology , medicine , etc.[50-53]

One of the main problems of organic-inorganic materials is the incompatibility between phases. This incompatibility can produce phase separation considerably reducing the expected properties of the obtained products. Therefore, the simple blending of the phases is not sufficient and the success mainly depends on the union between phases, which must be settled in order to minimize the negative effect of the interface in the final properties.[47-48,54-56]

Because of the interest in this emerging class of materials, a variety of synthetic routes have been developed in recent years. Organic-inorganic materials can be tailor-made

with an infinite number of architectures and in diverse forms (monoliths, thin films, powder, particles...).[57-58]

Following the synthesis route organic-inorganic hybrid materials can be classified in four main groups[59] as shown in Figure 1.8.

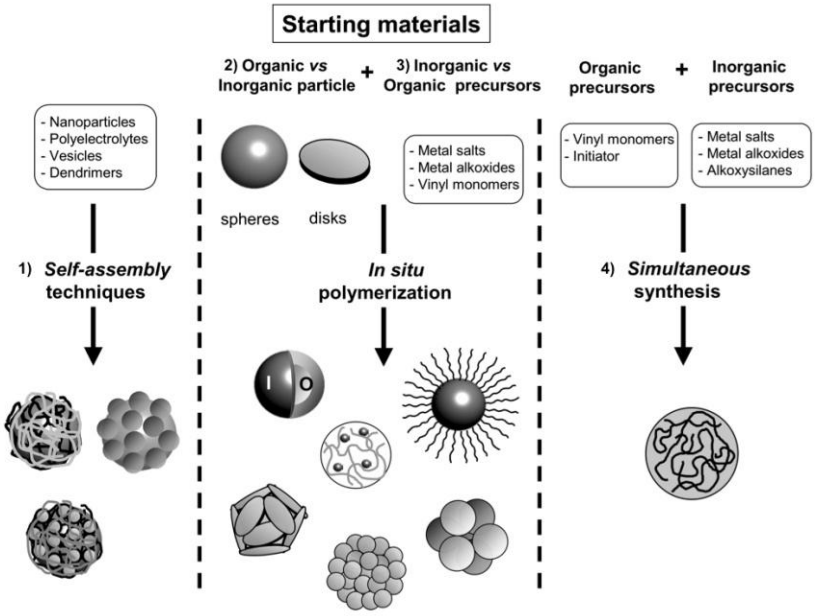

Figure 1.8. Schematic representation of the different strategies available in order to generate organic-inorganic hybrids (Bourgeat Lami et al.[59]).

2.1. Post-synthetic routes

The first strategy (Figure 1.8.1) consists on the achievement of the organic and inorganic polymers separately. Once the polymerization is finished a post-synthetic method is employed to build up organic-inorganic nanostructures. Preformed polymer latexes, inorganic particles and surfactant can be assembled into colloidal systems employing even electrostatic, chemical or biological interactions.[47-48,59-62] The self-assembly can be briefly described as the spontaneous 2D or 3D organization of molecules, aggregates or

nanoparticles. In Figure 1.9 a typical example of layer-by-layer self assembly by means of electrostatic interactions is shown.

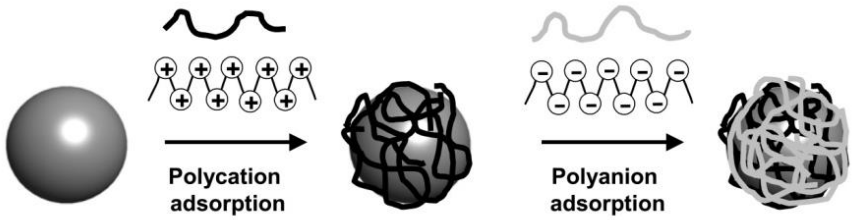

Figure 1.9. Layer by layer assembly by means of electrostatic interactions using preformed organic and inorganic materials (Bourgeat Lami et al.[59]).

2.2. "In situ" polymerization of inorganic precursors in the presence of preformed polymer particles

The second strategy (Figure 1.8.2) is the in situ formation of minerals in the presence of polymer colloids.[47-48,59-60] The immobilization of metal colloids onto nanoparticles surfaces is receiving a great deal of attention because of the potential use of metal-decorated particles in optics, electronics and heterogeneous catalysis. Polymer latex particles can be decorated by mineral components through layer-by-layer self-assembly, Sol-Gel nanocoating or metal precipitation.

A general approach for preparation of polymer core/inorganic shell particles consists of performing a Sol-Gel polycondensation in the presence of polymer latex particles used as templates. The surface of organic colloid spheres must be functionalized either during their synthesis or modified by grafting an appropriate compound, to enhance the coupling of the inorganic precursor on the polymeric colloid surfaces.[49,55,57-59,62]

The elementary Sol-Gel process involves the inorganic polymerization of organometallic precursors of the type metal + alkoxy group $M(OR)_x$ into a three dimensional metal oxide network through hydrolysis and condensation reactions.[63-65] The main interest of this process arises from the mild synthesis conditions and the possibility of creating specific organic-inorganic interactions. A thorough and comprehensive description of the Sol-Gel

chemistry and its application to the construction of Sol-Gel hybrid materials can be found in diverse books and reviews.[47-48,55,59-60] In Figure 1.10 a schematic representation of the Sol-Gel process for a silicon alkoxide is shown.

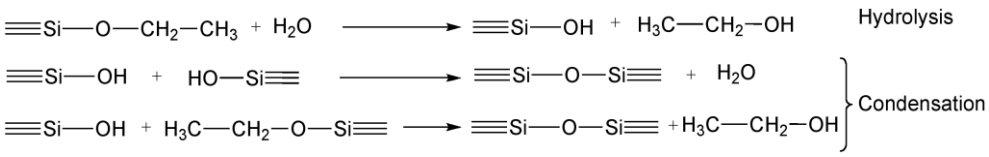

Figure 1.10. Sol-Gel process in an alkoxysilane inorganic precursor.

Although, in principle, a variety of metal alkoxides (tellurium, zirconium, tin...) can be involved in the synthesis of hybrid materials through the Sol-Gel process the nanocoating technology has been so far mainly restricted to the use of titanium and silicon alkoxides.

2.3. "In situ" polymerization of organic precursors in the presence of preformed inorganic particles

The third strategy (Figure 1.8.3) employed is the polymer formation on the surface of the inorganic particles by in situ polymerization, starting from pre-formed inorganic materials in order to build up a protective layer, which avoids the aggregation of inorganic particles. In Figure 1.11 a typical process for the formation of hybrids starting from inorganic particles is shown.

The first step for carrying out the polymerization creating the protective layer, is the surface functionalization of the inorganic material to enhance its affinity towards the organic phase and promote polymer formation on the inorganic particle surface. Functionalization may involve surface chemical reactions, with the implication of a variety of molecular or macromolecular precursors, but it can also be performed through simple adsorption methods such as surfactant self-assembly.

Modification of the surface can be performed in two ways, either by synthesizing the nanoparticles and treating them by appropriate molecules, or "in situ" during particle synthesis by the one step approach[47-48,55,59-60,66-67].

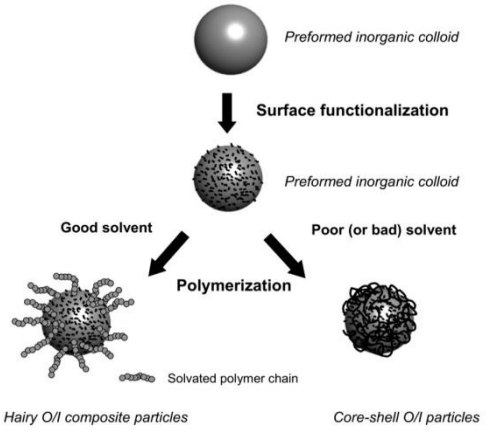

Figure 1.11. Process to form hybrids from inorganics particles (Bourgeat Lami et al[59]).

Organically substituted silane molecules with the general formula R_nSiX_{4-n} where X is a hydrolysable group (i.e., halogen, amine, alkoxy…) and R represents a non-hydrolysable organic group, have been widely used to alter the surface characteristics of inorganic oxides. The X ends of the silane undergo hydrolysis and condensation reactions with the silanol groups (Figure 1.12).

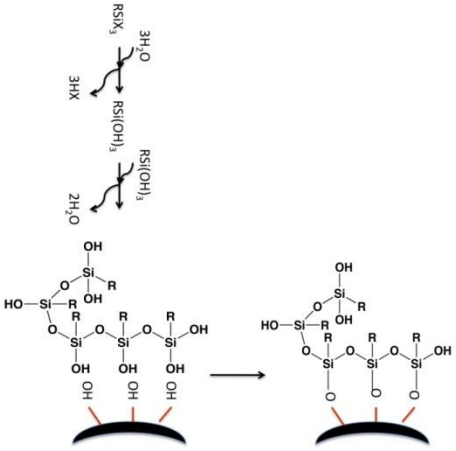

Figure 1.12. Modification process of inorganic particles using organic alkoxysilanes in order to enhance the formation of the organic phase.

The R group is selected to enhance the compatibility towards the organic phase. This R group can be designed so as to enable the subsequent polymerization reaction of the

organic phase (vinyl, epoxy, amino...), or to enhance the hydrophobicity of the colloid by means of the so called "grafting from" techniques into the inorganic surface.[47-48,55,60,68] However, another interesting alternative is the "grafting to" process. In this technique a previously functionalized polymer is reacted with silanol groups present on the inorganic surface or functionalized silica promoting the attachment of the polymer to the particle surfaces.[44,47-48,55,60,69] This technique can also be considered a post-synthetic route because the organic and inorganic moieties have already been synthesized.

2.4. "In-situ" polymerization of organic and inorganic precursors

The last strategy (Figure 1.8.4) is the in situ polymerization of organic and inorganic materials. Such materials are usually produced by the Sol-Gel technique and processed as thin films, powders, gels or monoliths. Surprisingly, there are only a few examples of nanoparticles synthesized by simultaneously reacting organic and inorganic precursor molecules to form O/I interpenetrated networks (IPN).[48,70-71] It is expected that the properties of these hybrid colloids will be significantly different from a simple combination of the properties of the two components. In Figure 1.13 a process where interpenetrated organic-inorganic hybrids are formed is shown.

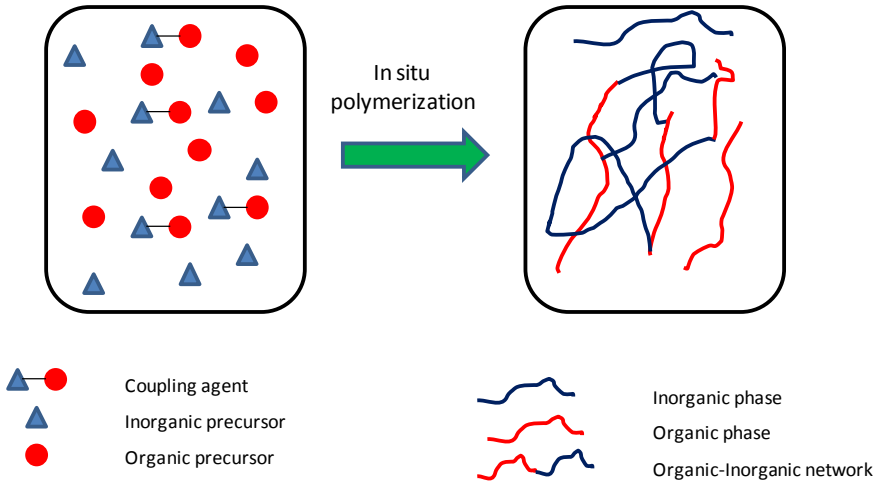

Figure 1.13. In-situ formation of the organic inorganic interpenetrated hybrid.

3. OBJECTIVES

This thesis has been developed in the group of Analysis and Characterization of Polymers in the Department of Polymer Science and Technology of the University of Basque Country. This group has a wide experience in the synthesis and characterization of segmented polyurethanes based on a great variety of diisocyanates (aromatic and aliphatic) as well as different molecular weight polyols (polyester and polyether). All these systems were synthesized using solution polymerization.

In the last decade, the research has been extended to the study of organic/inorganic hybrids where the organic component is a segmented polyurethane. In the frame of these hybrid systems, the first study was focused on the addition of inorganic clays in order to enhance physical and mechanical properties of polyurethanes. Although the results obtained confirmed the improvement of polyurethane properties, the importance of the compatibility between phases was clearly established.

As a way of improving phase compatibility, in a subsequent work, self curable covalently linked organic/inorganic polyurethane adhesives were developed, modifying polyurethane chain ends with alkoxysilane groups. These groups have the capacity of reacting under humidity conditions giving rise to stable polyurethane/silica interpenetrated networks with more resistance to environmental agents. Following this research line and being aware of the restrictions of using volatile organic solvents, this thesis has had a two-fold objective.

In the first place, the efforts have been centered in the synthesis of segmented polyurethanes in an aqueous medium, employing Isophorone Diiscocyanate (IPDI) as the diisocyanate and Polypropylene glycol (PPG) and Polybutylene adipate (PBAD) as the soft segment. This task has been an important challenge for the group due to its inexperience in water-based systems.

In the second place, different strategies have been tested for the achievement of waterborne polyurethane/silica nanostructures with good compatibility between the organic and inorganic phases.

Taking into consideration these two main objectives, this manuscript has been organized in the following chapters:

- *Chapter II* is devoted to the synthesis and characterization of water dispersible polyurethanes. After describing general considerations, the singularities of this type of synthesis are highlighted, emphasizing the acetone process. The results are discussed in terms of the catalytic activity and reactivity of IPDI isocyanate groups. The characterization of the final products is presented through the corresponding FTIR and NMR spectra. The last part of this chapter is dedicated to the description of the effect of different parameters on the phase inversion process followed by DLS and rheological measurements.

- *Chapter III* devoted to the synthesis of waterborne polyurethane hybrid dispersions, summarizes the methodology employed in the functionalization process of polyurethane chain ends with 3-aminopropyltriethoxysilane (APTES), as well as the effect of this coupling agent on the dispersion and final product characteristics. In the last section of the chapter the synthetic strategies employed in the formulation of hybrid compounds are resumed, selecting the best experimental conditions in order to obtain properly distributed organic/inorganic hybrids.

- *Chapter IV* is centred in the evolution of the most relevant properties of these hybrid compounds. In this chapter the thermal, mechanical, adhesion and transport properties of PBAD and PPG based WPU-s are deeply studied. These properties are relevant in the world of sealants, adhesives and coatings. The relation between properties and structure is established and the effect of APTES and the origin and content of silica on the properties is determined.

- *Chapter V* summarizes the most relevant conclusions of this work.

4. BIBLIOGRAPHY

1 Frisch, K. 60 years of polyurethanes. (Kresta JE, 1998).

2 Hepburn, C. Polyurethane elastomers. (Elsevier Applied Science 1992).

3 Chattopadhyay, D. K. & Raju, K. V. S. N. Structural engineering of polyurethane coatings for high performance applications. Progress in Polymer Science 32, 352-418 (2007).

4 http://www.pur.bayer.com/bms/pur-internet.nsf/id/02_PUR_EN_1937_to_1949.

5 Petrovic, Z. S. & Ferguson, J. Polyurethane elastomers. Progress in Polymer Science 16, 695-836 (1991).

6 Fink, J. K. in Reactive polymers fundamentals and applications. 69-138 (William Andrew Publishing, 2005).

7 Wojcik, R. T. PU Coatings: From raw materials to end-products. (Technomic Publishing, 1998).

8 Noble, K. L. Waterborne polyurethanes. Progress in Organic Coatings 32, 131-136 (1997).

9 http://www.vocemission.com/VOC-Solvent-Directive-Eng.pdf.

10 http://www.coatings.org.uk/files/Technical/VOC%20leaflet.pdf.

11 Kim, B. K. Aqueous polyurethane dispersions. Colloid & Polymer Science 274, 599-611 (1996).

12 Barni, A. & Levi, M. Aqueous polyurethane dispersions: A comparative study of polymerization processes. Journal of Applied Polymer Science 88, 716-723 (2003).

13 Chattopadhyay, D. K. & Webster, D. C. Thermal stability and flame retardancy of polyurethanes. Progress in Polymer Science 34, 1068-1133 (2009).

14 Madbouly, S. A. & Otaigbe, J. U. Recent advances in synthesis, characterization and rheological properties of polyurethanes and POSS/polyurethane nanocomposites dispersions and films. Progress in Polymer Science 34, 1283-1332 (2009).

15 www.pcimag.com/Articles/Industry News/bc0006395c6a7010VgnVCM100000f932a8c0

16 Rosthauser, J. W. & Nachtkamp, K. Waterborne polyurethanes. Journal of Industrial Textiles 16, 39-79 (1986).

17 Kim, B. K. & Lee, Y. M. Aqueous dispersion of polyurethanes containing ionic and nonionic hydrophilic segments. Journal of Applied Polymer Science 54, 1809-1815 (1994).

18 Dieterich, D. Aqueous emulsions, dispersions and solutions of polyurethanes; synthesis and properties. Progress in Organic Coatings 9, 281-340 (1981).

19 Król, P. Synthesis methods, chemical structures and phase structures of linear polyurethanes. Properties and applications of linear polyurethanes in polyurethane elastomers, copolymers and ionomers. Progress in Materials Science 52, 915-1015 (2007).

20 Tielemans, M., Roose, P., Groote, P. D. & Vanovervelt, J. C. Colloidal stability of surfactant-free radiation curable polyurethane dispersions. Progress in Organic Coatings 55, 128-136 (2006).

21 Barrère, M. & Landfester, K. High molecular weight polyurethane and polymer hybrid particles in aqueous miniemulsion. Macromolecules 36, 5119-5125 (2003).

22 Nanda, A. K. & Wicks, D. A. The influence of the ionic concentration, concentration of the polymer, degree of neutralization and chain extension on aqueous polyurethane dispersions prepared by the acetone process. Polymer 47, 1805-1811 (2006).

23 Asua, J. M. Miniemulsion polymerization. Progress in Polymer Science 27, 1283-1346 (2002).

24 Crespy, D., Stark, M., Hoffmann-Richter, C., Ziener, U. & Landfester, K. Polymeric nanoreactors for hydrophilic reagents synthesized by interfacial polycondensation on miniemulsion droplets. Macromolecules 40, 3122-3135 (2007).

25 Ahn, B. U., Lee, S. K., Lee, S. K., Jeong, H. M. & Kim, B. K. High performance UV curable polyurethane dispersions by incorporating multifunctional extender. Progress in Organic Coatings 60, 17-23 (2007).

26 Ahn, B. U., Lee, S. K., Lee, S. K., Park, J. H. & Kim, B. K. UV curable polyurethane dispersions from polyisocyanate and organosilane. Progress in Organic Coatings 62, 258-264 (2008).

27 Wei, Y. Y., Luo, Y. W., Li, B. F. & Li, B. G. Phase inversion of UV-curable anionic polyurethane in the presence of acetone solvent. Colloid and Polymer Science 283, 1289-1297 (2005).

28 Delpech, M. C. & Coutinho, F. M. B. Waterborne anionic polyurethanes and poly(urethane-urea)s: influence of the chain extender on mechanical and adhesive properties. Polymer Testing 19, 939-952 (2000).

29 Lee, S. K. & Kim, B. K. High solid and high stability waterborne polyurethanes via ionic groups in soft segments and chain termini. Journal of Colloid and Interface Science 336, 208-214 (2009).

30 Wang, H., Shen, Y., Fei, G., Li, X. & Liang, Y. Micromorphology and phase behaviour of cationic polyurethane segmented copolymer modified with hydroxysilane. Journal of Colloid and Interface Science 324, 36-41 (2008).

31 Lee, H. T., Wu, S. Y. & Jeng, R. J. Effects of sulfonated polyol on the properties of the resultant aqueous polyurethane dispersions. Colloids and Surfaces A: Physicochemical and Engineering Aspects 276, 176-185 (2006).

32 Chinwanitcharoen, C., Kanoh, S., Yamada, T., Hayashi, S. & Sugano, S. Preparation of aqueous dispersible polyurethane: Effect of acetone on the particle size and storage stability of polyurethane emulsion. Journal of Applied Polymer Science 91, 3455-3461 (2004).

33 Jena, K. K., Chattopadhyay, D. K. & Raju, K. V. S. N. Synthesis and characterization of hyperbranched polyurethane-urea coatings. European Polymer Journal 43, 1825-1837 (2007).

34 Chattopadhyay, D. K. & Webster, D. C. Hybrid coatings from novel silane-modified glycidyl carbamate resins and amine crosslinkers. Progress in Organic Coatings 66, 73-85 (2009).

35 Yang, Z., Wicks, D. A., Yuan, J., Pu, H. & Liu, Y. Newly UV-curable polyurethane coatings prepared by multifunctional thiol- and ene-terminated polyurethane aqueous dispersions: Photopolymerization properties. Polymer 51, 1572-1577 (2010).

36 Wicks, D. A. & Wicks, Z. W. Blocked isocyanates III: Part B: Uses and applications of blocked isocyanates. Progress in Organic Coatings 41, 1-83 (2001).

37 Wicks, Z. W., Wicks, D. A. & Rosthauser, J. W. Two package waterborne urethane systems. Progress in Organic Coatings 44, 161-183 (2002).

38 Subramani, S., Lee, J. M., Lee, J. Y. & Kim, J. H. Synthesis and properties of room temperature curable trimethoxysilane-terminated polyurethane and their dispersions. Polymers for Advanced Technologies 18, 601-609 (2007).

39 http://www.bayermaterialsciencenafta.com/processing/cas/1k-waterborne/index.html.

40 http://www.bayermaterialsciencenafta.com/processing/cas/2k-waterborne/index.html.

41 Otts, D. B. & Urban, M. W. Heterogeneous crosslinking of waterborne two-component polyurethanes (WB 2K-PUR); stratification processes and the role of water. Polymer 46, 2699-2709 (2005).

42 Pajerski, A. & Ahrens, G. www.lubrizol.com/1K-Polyurethane-Dispersion-Conventional-2K-Applications.pdf, 2009).

43 Subramani, S., Lee, J. M., Cheong, I. W. & Kim, J. H. Synthesis and characterization of water-borne crosslinked silylated polyurethane dispersions. Journal of Applied Polymer Science 98, 620-631 (2005).

44 Subramani, S., Lee, J. Y., Choi, S. W. & Kim, J. H. Waterborne trifunctionalsilane-terminated polyurethane nanocomposite with silane-modified clay. Journal of Polymer Science Part B: Polymer Physics 45, 2747-2761 (2007).

45 Wang, L., Shen, Y., Lai, X., Li, Z. & Liu, M. Synthesis and properties of crosslinked waterborne polyurethane. Journal of Polymer Research 1, 1-8, (2010).

46 Rekondo, A., Fernández-Berridi, M. J. & Irusta, L. Synthesis of silanized polyether urethane hybrid systems. Study of the curing process through hydrogen bonding interactions. European Polymer Journal 42, 2069-2080 (2006).

47 Bourgeat-Lami, E. in Encyclopedia of nanoscience and nanotechnology Vol. 8 (ed. Singh Nalwa Hayri) (American Scientific Publishers, 2004).

48 Bourgeat-Lami, E. Organic-inorganic nanostructured colloids. Journal of Nanoscience and Nanotechnology 2, 1-24 (2002).

49 Tissot, I., Novat, C., Lefebvre, F. & Bourgeat-Lami, E. Hybrid latex particles coated with silica. Macromolecules 34, 5737-5739 (2001).

50 Caruso, R. A. & Antonietti, M. Sol-Gel nanocoating: an approach to the preparation of structured materials. Chemistry of Materials 13, 3272-3282 (2001).

51 Schubert, U., Huesing, N. & Lorenz, A. Hybrid inorganic-organic materials by sol-gel processing of organofunctional metal alkoxides. Chemistry of Materials 7, 2010-2027 (1995).

52 Gómez-Romero, P. & Sanchez, C. Hybrid Materials, Functional applications. an introduction. (Wiley-VCH Verlag GmbH & Co. KGaA, 2005).

53 Livage, J., Coradin, T. & Roux, C. Bioactive sol-gel hybrids. (Wiley-VCH Verlag GmbH & Co. KGaA, 2005).

54 Chen, G., Zhou, S., Gu, G., Yang, H. & Wu, L. Effects of surface properties of colloidal silica particles on redispersibility and properties of acrylic-based polyurethane/silica composites. Journal of Colloid and Interface Science 281, 339-350 (2005).

55 Bourgeat-Lami, E., Herrera, N., Putaux, J. L., Perro, A., Reculusa, S., Ravaine, S. & Duguet E. Designing organic/inorganic colloids by heterophase polymerization. Macromolecular Symposia 248, 213-226 (2007).

56 Berra, I., Irusta, L., Fernández-Berridi, M. J. & de Miguel, Y. Comparison of synthetic procedures for the preparation of sol–gel derived phenoxy-silica hybrid materials. Journal of Sol-Gel Science and Technology 49, 19-28 (2009).

57 Judeinstein, P. & Sanchez, C. Hybrid organic-inorganic materials: a land of multidisciplinarity. Journal of Materials Chemistry 6, 511-525 (1996).

58 Sanchez, C., Julian, B., Belleville, P. & Popall, M. Applications of hybrid organic–inorganic nanocomposites. Journal of Materials Chemistry 15, 3559-3592 (2005).

59 Bourgeat-Lami, E. in Hybrid materials: synthesis, characterization, and applications. (ed Guido Kickelbick) (Wiley-VCH 2007).

60 Bourgeat-Lami, E. & Duget, E. in Functional coatings: by polymer encapsulation. (ed Swapan Kumar Ghosh) (Wyley VCH, 2006).

61 Caruso, F. Nanoengineering of particle surfaces. Advanced Materials 13, 11-22 (2001).

62 Castelvetro, V. & De Vita, C. Nanostructured hybrid materials from aqueous polymer dispersions. Advances in Colloid and Interface Science 108-109, 167-185 (2004).

63 Brinker, C. J. & Scherer, G. W. Sol-Gel science: The physics and chemistry of Sol-Gel processing. (Elsevier Editor, 1990).

64 Stöber, W., Fink, A. & Bohn, E. Controlled growth of monodisperse silica spheres in the micron size range. Journal of Colloid and Interface Science 26, 62-69 (1968).

65 Ding, X., Yu, K., Jiang, Y., Bala, H., Zhang, H., & Wang, Z. A novel approach to the synthesis of hollow silica nanoparticles. Materials Letters 58, 3618-3621 (2004).

66 Lai, S. M., Wang, C. K. & Shen, H. F. Properties and preparation of thermoplastic polyurethane/silica hybrid using Sol–Gel process. Journal of Applied Polymer Science 97, 1316-1325 (2005).

67 Lai, S. M. & Liu, S. D. Properties and preparation of thermoplastic polyurethane/silica hybrids using a modified Sol–Gel process. Polymer Engineering and Science 47, 77-86 (2007).

68 Böttcher, H., Hallensleben, M. L., Nuß, S. & Wurm, H. ATRP grafting from silica surface to create first and second generation of grafts. Polymer Bulletin 44, 223-229 (2000).

69 Subramani, S., Choi, S.-W., Lee, J.-Y. & Kim, J. H. Aqueous dispersion of novel silylated (polyurethane-acrylic hybrid/clay) nanocomposite. Polymer 48, 4691-4703 (2007).

70 Chattopadhyay, D. K., Zakula, A. D. & Webster, D. C. Organic-inorganic hybrid coatings prepared from glycidyl carbamate resin, 3-aminopropyl trimethoxy silane and tetraethoxyorthosilicate. Progress in Organic Coatings 64, 128-137 (2009).

71 Chen, G., Zhou, S., Gu, G. & Wu, L. Acrylic-based polyurethane/silica hybrids prepared by acid-catalyzed Sol–Gel process: Structure and mechanical properties. Macromolecular Chemistry and Physics 206, 885-892 (2005).

CHAPTER II: SYNTHESIS OF WATER-DISPERSABLE POLYURETHANES

CHAPTER II: SYNTHESIS OF WATER-DISPERSABLE POLYURETHANES

1. INTRODUCTION

1.1. General Considerations

There are two main routes to synthesize polyurethanes (PU-s): by the reaction of diisocyanates with dihydric alcohols and by reaction of bischloroformates with diamines at low temperature.[1-3] The former reaction is more advantageous since there is no formation of sub products. This is the one most commonly used in the synthesis of commercial polyurethanes.

Isocyanate groups can generally react with compounds containing active hydrogen atoms, and their high reactivity is a significant drawback for the synthesis of polyurethanes. For instance, isocyanate groups can react with alcohol, water, amine, acid, and so forth, giving rise to different products,[4-6] as summarized in Figure 2.1.

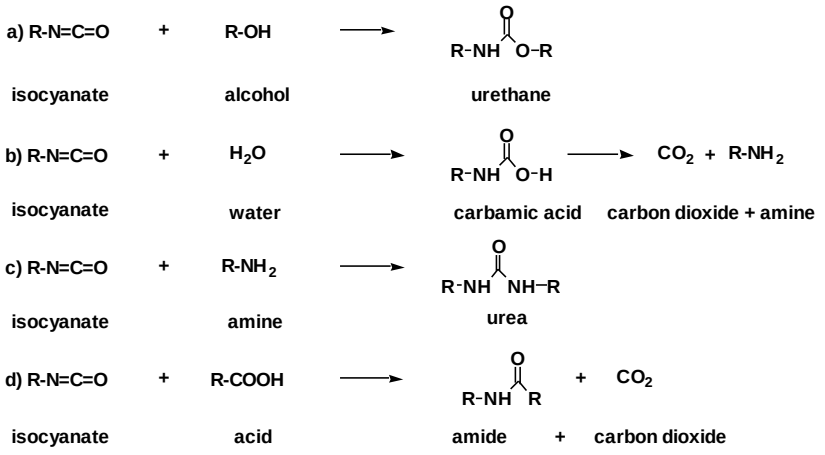

Figure 2.1. Possible reactions in the synthesis of polyurethanes.

In the synthesis of polyurethanes the most important reaction of isocyanate groups is obviously the addition of alcohol for the formation of the urethane group (reaction A). As shown in reaction B, water can react with isocyanate producing carbamic acid, which is unstable and decomposes in amine and carbon dioxide. Sometimes water is added to isocyanates to produce foamed polyurethanes. However, during the synthesis of

polyurethane elastomers, water has to be eliminated; otherwise amine groups will be formed. These are much more reactive than alcohols and will reduce the molecular weight (reaction C). Another reaction that must be taken into consideration is the one between the acid and isocyanate groups (D reaction) as in the synthesis of water-dispersable polyurethanes a diol containing an acid group (2,2-Bis(hydroxymethyl) propionic acid) is usually employed in order to improve the affinity of PU-s towards water. Although these groups are much less reactive than alcohols their reaction with isocyanate moieties must be avoided as much as possible to ensure the stability of PU-s in water.

Another parameter that affects the polyurethane polymerization process is the solvent. It has been confirmed that the rate of the reaction decreases as the dielectric constant of the solvent being increase when the solvent has the ability to hydrogen bond with alcohol[4,7].

1.2. Peculiarities in the synthesis of aqueous segmented polyurethanes

Segmented polyurethanes are block copolymers consisting of two segments. The first one is usually named as the hard segment and is formed by the reaction between the chain extender (usually a diol or diamine) and the diisocyanate. The other, commonly known as the soft segment, is built by a low molecular weight polyether or polyester that connects the hard segments. Figure 2.2 schematizes the structure of segmented PU-s.

Therefore, in the reaction of segmented polyurethanes three components are usually used:

- Polyol (polyester or polyether)
- Chain extender (diol or diamine)
- Diisocyanate

Based on the reaction methodology, there are at least two different routes to carry out the polymerization of polyurethanes:[8] batch reaction where all the reagents are

introduced at the same time in the reactor and semi-batch reaction in which the reaction is performed introducing the less reactive reagents first followed by the most reactive ones. This latter procedure offers a better control of the reaction.

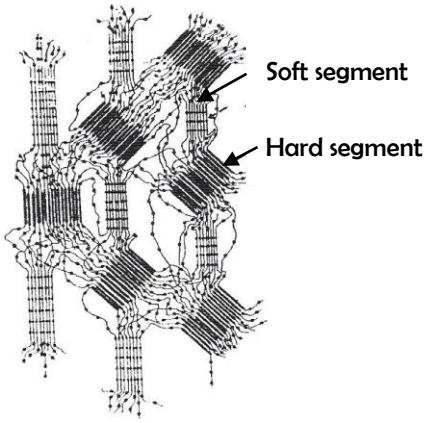

Figure 2.2. Schematic representation of segmented polyurethanes.

The main difference in the synthesis of water dispersible-segmented polyurethanes from that of traditional polyurethanes is that a part of the chain extender is replaced by a functionalized diol that improves polyurethane dispersability in water.

1.3. Waterborne polyurethanes: Acetone process

Waterborne polyurethanes (WPU-s) are versatile environmentally friendly materials that are increasingly being used in coatings and adhesives for wood and automobiles, as well as for numerous flexible substrates, such as textiles, leather, paper and rubber.[9-11]

Waterborne polyurethanes cannot be obtained by conventional synthesis methods, such as emulsion and suspension polymerizations, due to the high reactivity of isocyanate groups towards water.[6,12] Therefore, several processes have been developed for achieving aqueous polyurethane dispersions.[8,11,13-20] Among these synthetic methods, one of the most popular strategies is the acetone process, which consists in a two-step procedure.[11-12,18,21-22]

In the first step, during the polyurethane synthesis in acetone, hydrophilic and potentially charged groups are incorporated into the polymer backbone. As explained, the most

commonly employed strategy in order to obtain hydrophilic PU-s by the acetone process is the addition of an internal emulsifier containing an acidic group (2,2-Bis(hydroxymethyl) propionic acid (DMPA)).

In the second step, water is added to the PU/acetone mixture. Thanks to the hydrophilic groups previously incorporated during the polymerization process, stable dispersions can be obtained. This particle formation process has created controversy in terms of the particle formation mechanism. Nevertheless, it is generally accepted that the particle formation process can be divided in three distinctive stages.[23-27]

In the first stage, when water is initially added, the hydrated ionic groups allow PU/acetone to absorb a certain amount of water homogeneously. In the second stage, when the system cannot absorb more water, the solution becomes turbid. In the literature, two different hypotheses can be found in order to explain this turbidity, which is related to the particle formation process. Thus, PU particles can be formed by phase inversion or precipitation.[25-27]

In the phase inversion, (Figure 2.3), the hydrated portions enlarge gradually as the amount of water is increased. Finally, water slowly extends into the hydrophobic areas of the polymer matrix thus forming discrete water areas. The hydrophilic centres of the ionic groups occupy the PU–W interface as shown in Figure 2.3. Further water addition promotes the restructure of polymer-water interface to form a dispersion of spherical particles enclosed by a continuous aqueous phase.

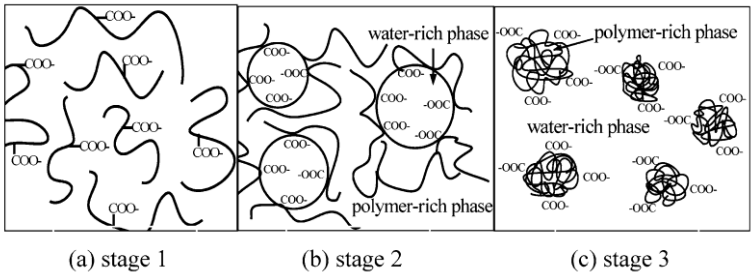

Figure 2.3. Polyurethane emulsification process for a system containing carboxylate groups in the main backbone.[27]

In the precipitation process, the transition from a one-phase to a two-phase system is a continuous process. The polyurethane particles are generated directly without passing through water in oil (W/O) to oil in water (O/W). The particles precipitate due to the change in the polarity of the solvent mixture, and they are stable due to the presence of DMPA.

In the last stage, after the formation of all polyurethane particles, the addition of water is just a dilution process. Finally, the low boiling point of acetone allows its easy removal, yielding a product containing either a very low content of VOC-s or none VOC.[6,28-30]

In this thesis WPU-s were synthesized by means of the acetone process. It is widely accepted that a minimum amount of ionic group content is required for the formation of stable PU dispersions, but this value depends on many variables such as the polymer nature and the neutralization degree.[11,21,27,31-32] The DMPA content affects the dispersion particle size and stability, but other parameters such as the PU content in acetone, the phase inversion temperature and the affinity of the solvent used towards water also have a significant effect on the final PU dispersions.

In this chapter, the insertion of DMPA units into the polyurethane chains is studied together with the best polymerization conditions in order to obtain water-dispersable polyurethanes. Moreover, the effect of different variables such as ionic group concentration, PU content, phase inversion temperature, solvent evaporation conditions and solvent affinity towards water on the particle size and stability are studied. In addition, viscosity curves during the water addition step as well as a ternary diagram are determined in order to better understand the particle formation mechanism.

2. EXPERIMENTAL PART

2.1. Materials for the synthesis of waterborne polyurethanes

Different reagents were used during the synthesis of water-dispersible polyurethanes. All were purchased from Aldrich and characterized by FTIR and NMR before use. The selection of the reagents is explained in this section.

2.1.1. Diisocyanate

The polyfunctional isocyanates used to prepare PU coatings can be aromatic, aliphatic, cycloaliphatic or polycyclic.[6] Aromatic isocyanates have higher reactivity than aliphatic or cycloaliphatic ones. Different diisocyanates contribute to PU properties in a variety of ways. For example, aromatic diisocyanates give more rigid PU-s than do aliphatic ones, but their oxidative and ultraviolet stabilities are lower. In addition, carcinogenic aromatic diamines, such as toluene diamine (TDA) or 4,4´-methylene dianiline (MDA) are reported to be the degradation products of the commonly used aromatic diisocyanates (TDI and MDI),[33-34] and therefore their use is being reduced throughout the polyurethane industry.

From the commercially available diisocyanates, isophorone diisocyanate (IPDI) was selected for this study. In spite of being a cycloaliphatic isocyanate, it provides good oxidative, ultraviolet and thermal stabilities. The two isocyanate groups are different because one is bonded directly to the cycle (NCO_{sec}) whereas the second one is bonded through a primary carbon (NCO_{prim}) as shown in Figure 2.4.

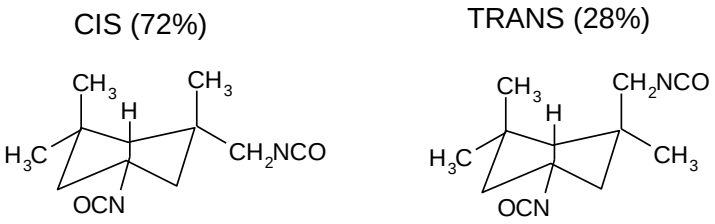

Figure 2.4. Structure of the two different isomers of IPDI.

The molecule consists of a mixture of two isomers, *cis* and *trans*, relative to the position of NCO_{sec} and NCO_{prim} on the cyclohexane ring. NMR and GC analysis indicate a 72 % of cis and 28 % of trans isomers.[35] Furthermore, secondary isocyanate is observed at higher chemical shifts in carbon ^{13}C NMR, which means that its electronic density is lower than that of the NCO_{prim}, and consequently it reacts better with nucleophilic species such as alcohols.

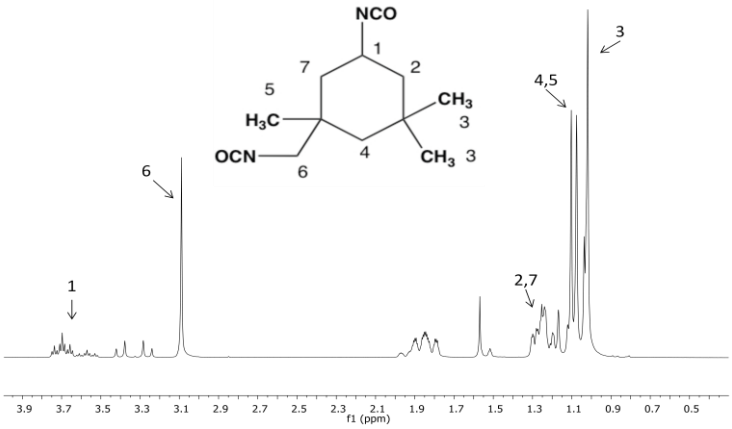

Figure 2.5. ^{1}H-NMR spectrum of IPDI.

The Figures 2.5 and 2.6 show the ^{1}H-NMR and ^{13}C-NMR spectra of IPDI respectively.

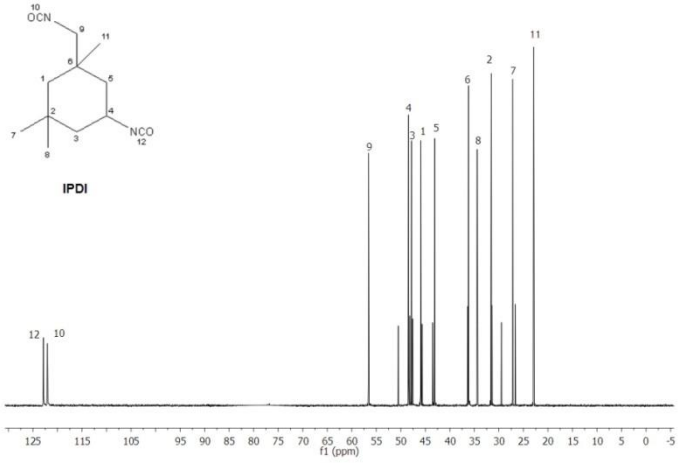

Figure 2.6. ^{13}C-NMR spectrum of IPDI.

2.1.2. Macrodiol

In this work polypropylene glycol (PPG) (Mn=1000 g.mol^{-1}) and poly(1,4-butylene adipate (PBAD) (Mn=1000 g.mol^{-1}) were used as macrodiols. The selection of the macrodiols was not arbitrary being the PPG an amorphous polyether (Tg ≈ -70 °C) and the PBAD a semicrystalline polyester (Tm ≈ 50-60 °C and Tg = -60 °C).

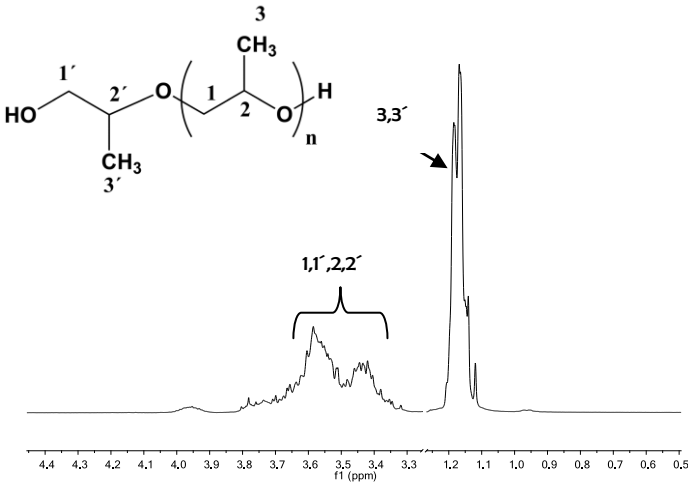

Figure 2.7. Chemical structure of PPG end capped diol and its ^{1}H-NMR spectrum.

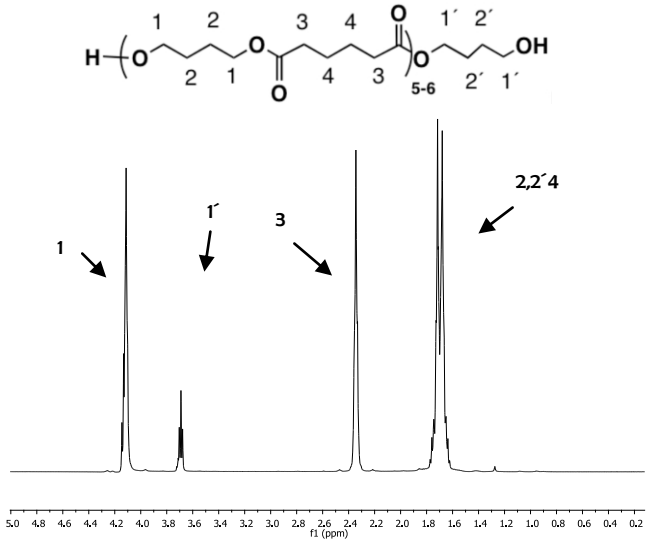

Figure 2.8. Chemical structure of PBAD end capped diol and its ^{1}H-NMR spectrum.

In Figures 2.7 and 2.8 the ^{1}H-NMR spectra and structures of PBAD and PPG are shown.

2.1.3. Chain extender

The reaction between the chain extender and the diisocyanate gives rise to the hard segment and fixes the properties of segmented polyurethanes. Diols or diamines can be used as chain extenders. Diamines are more reactive than diols and therefore more efficient for carrying out the polymerization; however, urea products, which are formed from the reaction between amine and isocyanate, decompose at relatively low temperatures.

In this work 1,4-butanediol was selected as the chain extender.

2.1.4. Functionalized diol

It is known that polyurethanes are not soluble in water and therefore, in order to obtain water dispersable polyurethanes, their chemical structure must be modified. The modification consists of adding either a surfactant or incorporating hydrophilic groups into the polymer backbone. These groups improve the stability of the dispersion by acting as internal emulsifiers. There are three primary types of stabilizing groups: anionic, cationic and nonionic groups.[9-11,36-38]

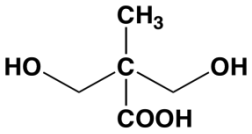

Figure 2.9. Structure of the internal emulsifier employed in the synthesis process.

In this work, the polyurethanes were obtained using an anionic stabilizing group (2,2-dimethylolpropionic acid (DMPA)). As shown in Figure 2.9, this molecule has two alcohol groups able to react with the isocyanate inserting the acid group into the polyurethane chain. It should be pointed out that as the acid group is attached to a quaternary carbon its reactivity towards isocyanate is substantially reduced, compared to other reagents.

2.1.5. Neutralizing agent

There are two principal types of neutralizing agents: ammonium- and alkali-metal containing cations. In literature it is well established that the size and polidispersity index of the obtained particles depend on the chemical nature of the neutralizing cation. Accordingly alkali metal cations produce particles with low polydispersity indexes while ammonium-containing cations give rise to higher polydispersities, but smaller particle sizes are obtained.[39]

In this work triethylamine (TEA) was used as the neutralizing agent.

2.1.6. Catalyst

Due to the low reactivity of isophorone diisocyanate[40] (Table 2.1) a catalyst has to be added in order to improve the polymerization rate.

Isocyanate	k_1	k_2
TDI	400	33
MDI	320	110
HDI	1	0.5
IPDI	0.62	0.23

Table 2.1. Uncatalyzed reactivities of different diisocyanates.

The most commonly used catalysts are the tin catalysts (dibutyltin dilaurate (DBTDL) and dibutyltin diacetate (DBTDA)), which are recognized as acting as a Lewis acid catalyst by complexing with the isocyanate. It is clear that these compounds catalyse the reaction; however, establishing a catalytic mechanism is complicated due to the catalytic effect of the urethane groups formed in the isocyanate/hydroxyl reaction.[6,41] The generally accepted mechanism is the one which involves the polarization of the carbonyl by the metal complex followed by nucleophilic attack to the hydroxyl group. It has been suggested that tin compounds can catalyse either complexing with alcohol or with isocyanate groups. Therefore tin catalysts act as a second order catalyst. The proposed catalytic mechanism is summarized in Scheme 2.1.

Amines and organometallics have shown a synergetic effect on the formation of polyurethanes. Although these catalysts are very toxic, there are not many examples in the literature which avoid the utilization of these compounds in order to obtain less toxic polyurethanes.

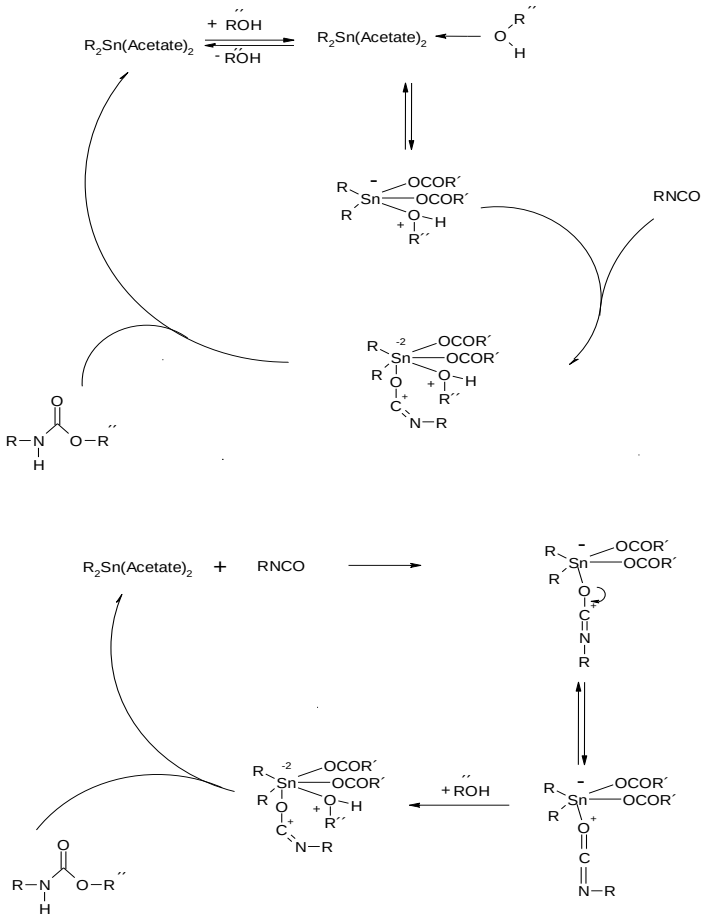

Scheme 2.1. Catalytic mechanism proposed for tin compounds.

Zirconium catalysts seem to be good candidates for replacing tin in polyurethane synthesis. They are much less toxic than tin compounds (many studies have demonstrated the non toxicity of these compounds) and promote a much higher selectivity of the isocyanate towards alcohol than towards water.[42-45] The mechanism of catalysis

suggested in the literature for this system is different to the one proposed for tin compounds. Different studies have been done to establish the mechanism and the one postulated by Werner Blank et al.[43,45] studied through NMR, is the most convincing one. Scheme 2.2 shows the catalytic mechanism proposed for Zirconium acetyl acetonate.

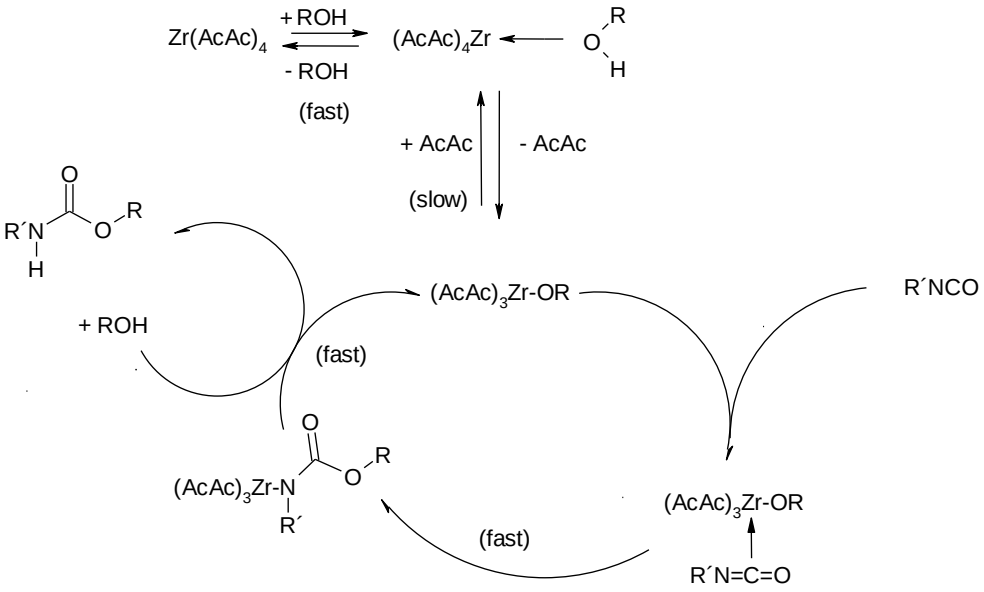

Scheme 2.2. Catalyst mechanism of Zirconium based catalysts in polyurethane synthesis.

2.2. Reaction equipment

WPU-s were synthesized in a 250 mL or 500 mL jacket glass reactor equipped with a mechanical stirrer, a nitrogen inlet and a condenser as shown in Figure 2.10.

A water bath was employed for fixing the reaction temperature. Moreover, an addition pump was used to control the addition rate of some reagents.

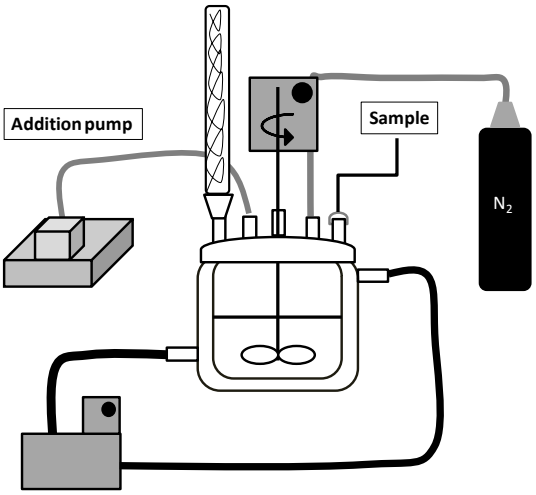

Figure 2.10. Schematic representation of the reaction equipment used in the synthesis process.

2.3. Preparation of water-dispersible polyurethanes (WPU-s)

WPU-s preparation was divided into two main steps. In the first the PU-s were prepared by polyaddition in acetone and in the second the dispersion process was carried out.

2.3.1. Polyurethane polymerization

Polyol (PBAD/PPG 45 mmol), internal emulsifier (DMPA from 52 to 7.5 mmol) and the required amount of TEA (from 69 to 0 mmol) (TEA was added at this point to increase DMPA solubility in acetone, avoiding the use of other organic solvents[11,46]) were fed into the reactor together with the catalyst (DBTDA/$Zr(acac)_4$) (400 ppm) and the solvents. In most of the cases acetone was used as a solvent, however, in some experiments chloroform and THF were also employed. Once the reaction temperature reached 60 °C, IPDI (113 mmol) was added drop-wise at 1 $mL.min^{-1}$. The reaction was carried out for 5 hours under nitrogen atmosphere and mechanical stirring (250 rpm), and finally the required amount of chain extender BD (from 60.5 to 16 mmol) was introduced to react with residual NCO groups.

The reaction was periodically monitored by FTIR, and was considered concluded when the infrared absorbance of the NCO groups (around 2260 cm^{-1}) was negligible. Scheme 2.3 shows the polymerization process.

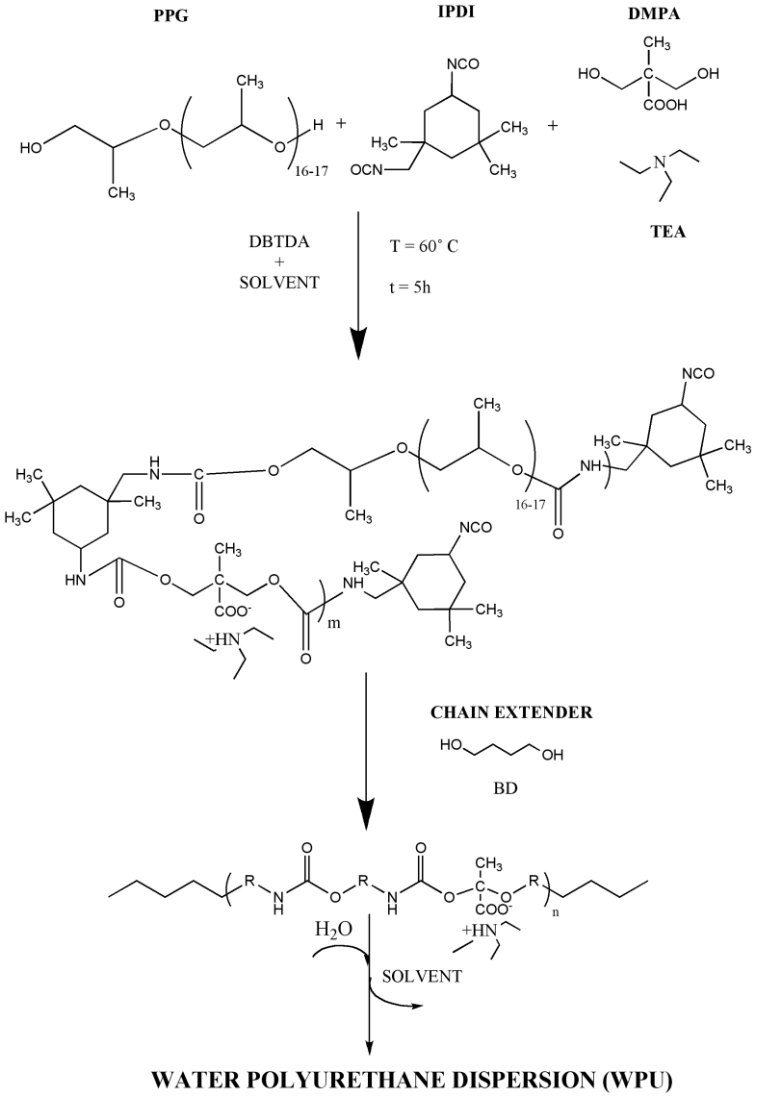

Scheme 2.3. Scheme of the process for obtaining waterborne polyurethanes.

2.3.2. Dispersion process

The dispersion process was carried out using different experimental conditions. Thus, the concentration of the PU-s solution was adjusted to the desired value and an aliquot of this solution was fed into the reactor. After setting the temperature and stirring rate (400 rpm), water was added at 1 $mL.min^{-1}$. Once the dispersion was achieved, the solvent was removed by means of a rotary evaporator at different temperatures in order to test the effect of this parameter on the final dispersion stability.

3. RESULTS AND DISCUSSION

Most of the studies referred to this chapter were performed with the PPG based systems. Nonetheless, the same characteristics were observed for the PBAD based polyurethanes.

3.1. Catalytic activity

Due to the low reactivity of isocyanate groups present in isophorone diisocyanate (IPDI)[40] towards hydroxyl groups, the use of a catalyst is needed to carry out the polymerization process. As previously mentioned, the most commonly used compounds are tin catalysts. However, being aware of their toxicity, we tested the catalytic activity of a zirconium catalyst in order to replace the tin catalyst in waterborne polyurethane synthesis.

Different polymerizations were performed using 400 ppm of both types of catalyst in the presence and absence of triethylamine (30 mmol). The concentration of PPG (45 mmol), IPDI (113 mmol), DMPA (22 mmol), and BD (46 mmol) were maintained constant. The reactions were carried out using 40 wt. % of acetone. Infrared spectroscopy was employed as a tool to follow the reaction.

Figure 2.11 shows the infrared spectra recorded at different reaction times for a reaction mixture catalyzed with 400 ppm of DBTDA with TEA. As expected, as the reaction advances, the relative absorption at 2270 cm^{-1} (isocyanate stretching) decreases, while the intensity of the absorptions assigned to urethane groups increase (Amide I at

1720 cm^{-1} and Amide II at 1550 cm^{-1}). In addition, a change is detected at 3300 cm^{-1} related to the formation of NH groups and the elimination of the band corresponding to the stretching of OH groups.

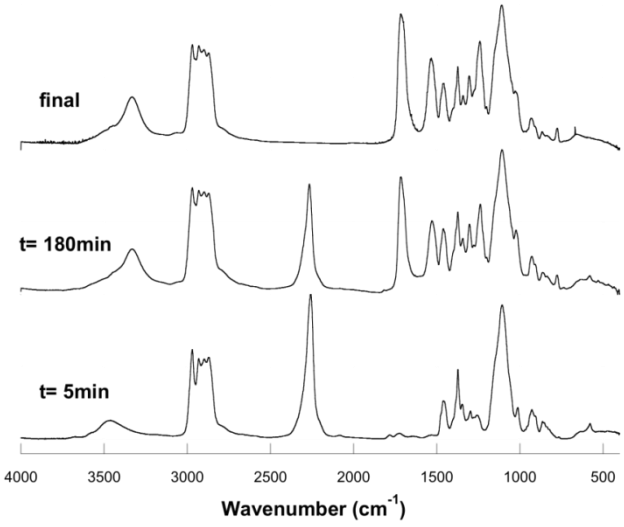

Figure 2.11. Infrared spectra recorded at different reaction times for a reaction mixture catalyzed with DBTDA for a PPG based PU.

The disappearance of the IR isocyanate band at 2272 cm^{-1} is a simple tool to determine the reaction rate. Consequently, the band absorption was measured at different reaction times. In order to take into account the path length of the samples, the obtained values were normalized to the absorbance of a band whose intensity did not change during the reaction (we selected the total C-H stretching band in the range 3000-2850 cm^{-1}). The same calculations were performed for the other three reactions and the results obtained for all systems are shown in Figure 2.12.

The results indicate that under these conditions $Zr(acac)_4$ catalyst does not catalyze the isocyanate/alcohol reaction. Nevertheless, when the zirconium compound is used in the presence of TEA, the reaction is conveniently catalyzed. In our opinion, when no TEA is

present in the reaction, DMPA acid groups hydrolyze the zirconium catalyst and therefore the reaction rate is negligible.[43] However, when TEA is present, the acid groups of DMPA are in the carboxylate form, and therefore the zirconium complex is not deactivated. This fact is very relevant in the synthesis of waterborne polyurethanes and according to this, if zirconium catalysts are used, internal emulsifier acid groups must be previously neutralized. Comparing the results obtained with zirconium and tin catalysts in the presence of TEA, the zirconium compound shows a slightly higher catalytic activity, in agreement to other results reported in literature in the absence of TEA.[35,45,47]

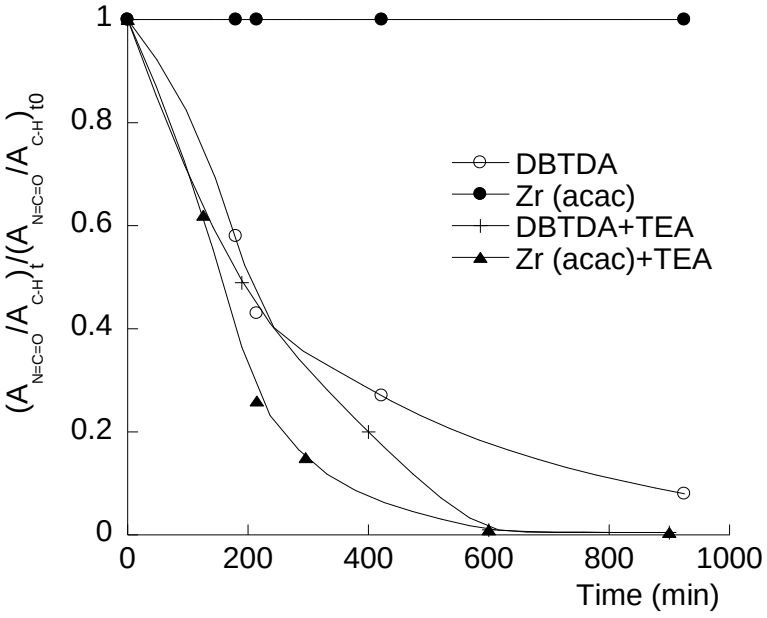

Figure 2.12. Isocyanate band reduction during the reaction using different catalysts.

The results obtained with the tin catalyst, depicted in Figure 2.12 show that the reaction rate is slightly higher when DBTDA is used in the presence of TEA. It is well known that ternary amines catalyze the isocyanate/alcohol reaction, although their catalytic activity is lower than that of organometallic compounds.[47] Accordingly, a synergetic effect of tin compounds with amines has been obtained. Similar effects have been reported in literature.[48]

3.2. Reactivity of IPDI primary and secondary isocyanate groups

IPDI is an asymmetric cycloaliphatic diisocyanate with two different isocyanate groups, as one is bonded directly to the cycle (secondary NCO), whereas the second one is bonded to a methylene group (primary NCO).

The presence of primary and secondary NCO groups in IPDI has attracted researchers to investigate differences in their reactivities. According to literature[41,49] their reactivities are catalyst dependent, the primary NCO being more reactive when the catalyst is a ternary amine, and the secondary NCO when tin catalyst and/or no catalyst is used.

In our case FTIR spectra, obtained at different reaction times for two different catalyzed systems, suggest that the reactivity of the two isocyanate groups is a function of the catalyst employed.

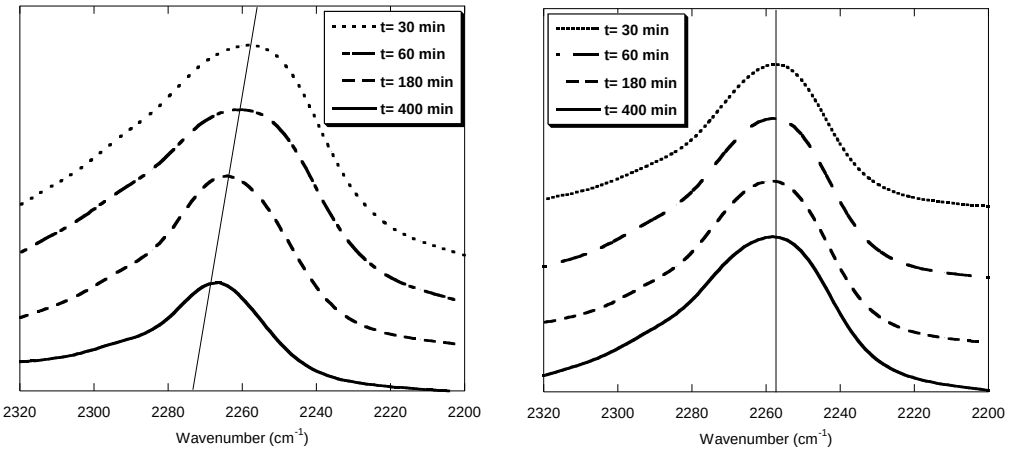

Figure 2.13. Scale expanded infrared spectra in the isocyanate stretching region of two reactions catalyzed with 350 ppm of Zr(acac) (right) and 350 ppm of DBTDA (left) as a function of reaction time.

As can be seen in Figure 2.13, at low reaction times the NCO stretching vibration gives rise to a single broad band, centred at 2258 cm^{-1} for the $Zr(acac)_4$ and DBTDA catalyzed systems. It must be pointed out that in both cases it is not possible to distinguish between

primary and secondary isocyanate groups. However, the situation changes when we register the evolution of this band as a function of reaction time. While the band maintains its initial position in the Zr catalyzed system, the band shifts towards higher wavenumbers in the system catalyzed by DBTDA. From this observation we can deduce that in the zirconium catalyzed reaction the reactivity of the two isocyanates (primary and secondary) is basically the same and therefore the position of the infrared absorption remains constant. However, in the tin catalyzed reaction, the infrared absorption shifts towards the position of the less reactive isocyanate (whose relative proportion increases with reaction time), indicating that the reactivity of the two isocyanates is not the same.

In order to determine the position of the infrared absorption of primary and secondary isocyanates, infrared spectra of two model compounds containing primary and secondary isocyanate groups, 1,3-bis(isocyanate methyl)-cyclohexane and trans-1,4-cyclohexane diisocyanate, were recorded using a liquid cell. The obtained spectra are shown in Figure 2.14.

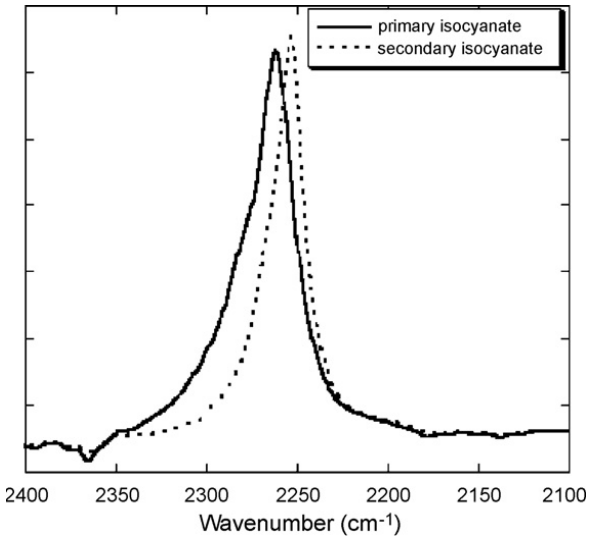

Figure 2.14. Scale expanded infrared spectra in the isocyanate stretching vibration region of trans-1,4-cyclohexane diisocyanate (secondary) and 1,3-bis(isocyanate methyl)-cyclohexane (primary).

As can be seen, the primary isocyanate band appears at higher wavenumbers than the secondary isocyanate. According to this, it seems that the shift observed in this absorption in the tin catalyzed reaction can be attributed to a higher reactivity of the secondary isocyanate group, as stated in literature for non and DBTDA catalyzed systems.[35,49]

In order to confirm these statements, the reactivity of both isocyanate groups of isophorone was also studied by ^{13}C-NMR. The spectra were recorded when the reaction reached about 50 % of molar conversion (before butanediol addition). Figure 2.15 shows the ^{13}C-NMR spectra in the NCO and urethane regions for the reactions catalyzed with tin and zirconium catalysts respectively.

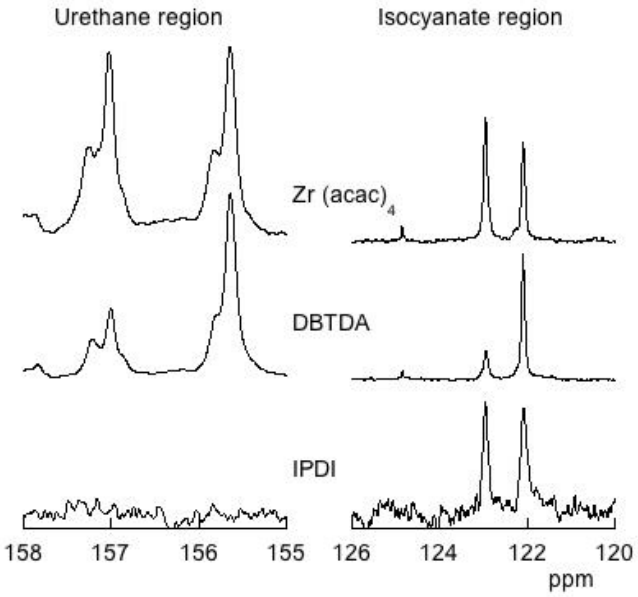

Figure 2.15. Scale expanded ^{13}C NMR spectra of IPDI and the reactions catalyzed with DBTDA and Zr(Acac) at ≈50 % molar conversion.

As can be seen in the isocyanate region, IPDI shows two different resonances at 123 and 122 ppm. According to literature[41] the carbon resonance shown at a lower magnetic field can be assigned to the secondary NCO groups (in cis and trans isomers), while the signal observed at a higher magnetic field corresponds to the primary isocyanate group. When the conversion of the reaction is ≈50 %, the signal at 123 ppm decreases in intensity compared to that at 122 ppm in the reaction catalyzed with DBTDA. However, in the

zirconium catalyzed reaction the intensity of the two signals remains similar. These results prove the selectivity of DBTDA towards secondary isocyanate, whereas using the zirconium catalyst the reactivity of both isocyanates is similar. These results can be confirmed analyzing the spectra obtained in the urethane region. As can be seen, two complex signals appear at 155 ppm and 157 ppm that can be assigned to secondary and primary urethane groups respectively. The shoulders in both peaks can also be assigned to E and Z isomers. In the reaction catalyzed by DBTDA, as the reactivity of the secondary isocyanate is higher, the intensity of the peak assigned to the secondary urethane (155 ppm) is higher than that of the primary urethane (157 ppm). In the other case, the two peaks show a similar intensity in the urethane region.

The results obtained by means of ^{13}C-NMR spectroscopy have confirmed those obtained from FTIR. Consequently, FTIR data can also be used in order to check the reactivity of IPDI primary and secondary NCO groups.

3.3. Chemical characterization of the final products

All the obtained systems were characterized employing ^{1}H NMR and FTIR in order to determine the polyurethane final structure. When the isocyanate band was negligible the reaction was considered concluded and the ^{1}H-NMR spectra were performed (Figures 2.16 and 2.17) for the cases of PBAD and PPG respectively. The ^{1}H-NMR spectra shown were obtained from the reaction mixture, using DBTDA as catalyst in the presence of TEA.

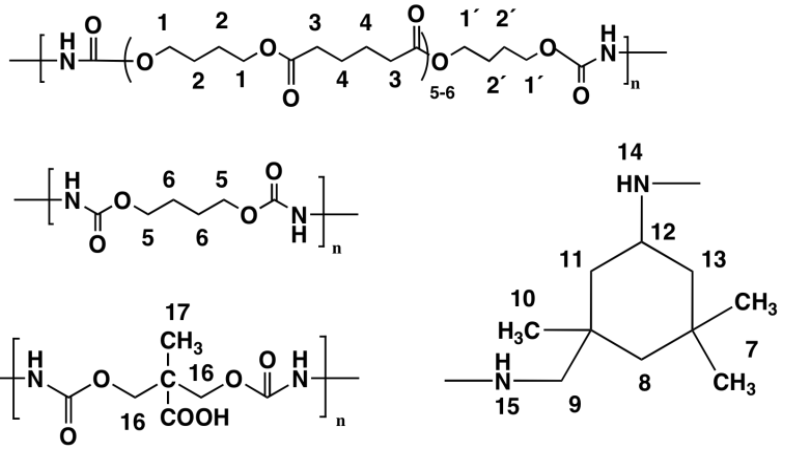

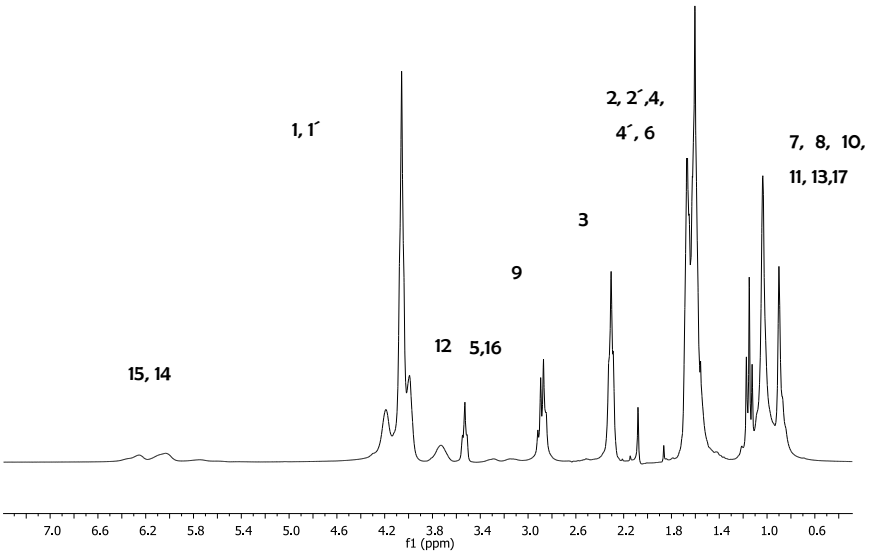

Figure 2.16. ^{1}H-NMR spectrum of PBAD based PU.

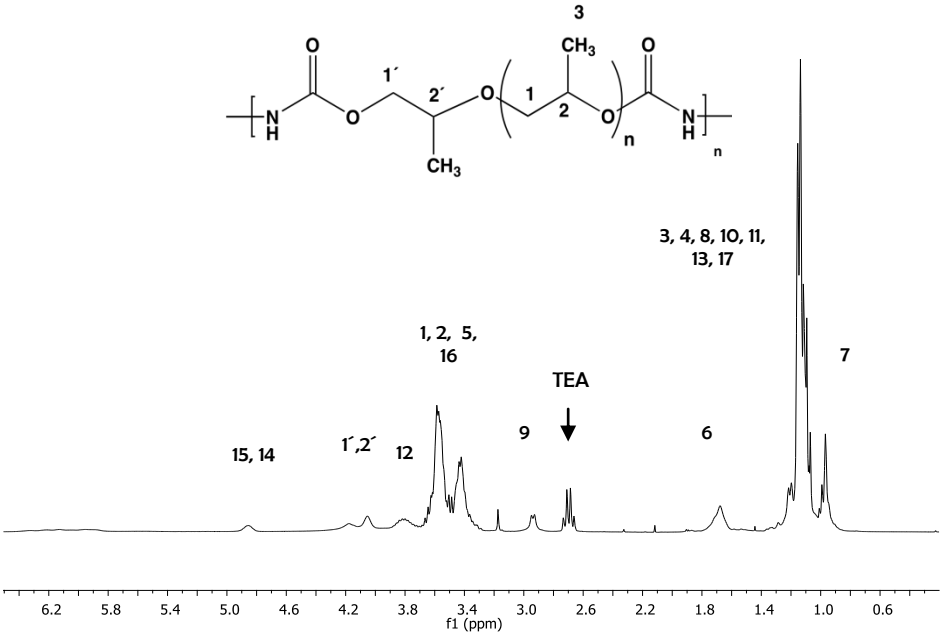

Figure 2.17. ^{1}H-NMR spectrum of PPG based PU.

The insertion of DMPA could not be easily confirmed using FTIR and ^{1}H-NMR spectra and therefore, ^{13}C-NMR studies were carried out in order to ensure its insertion in the polymer chain. Two different DMPA concentrations were employed, as shown in Table 2.2, keeping the other reagents concentrations constant (the TEA content was varied for neutralizing all the acidic groups and BD was varied in order to maintain equimolecularity).

DMPA *(mmol.g$^{-1}_{pol}$)*	*Polyether* *(mmol)*	*IPDI* *(mmol)*	*DMPA* *(mmol)*	*TEA* *(mmol)*	*DBTDA* *(ppm)*	*BD* *(mmol)*
0.58	45	113	52	69	400	16
0.16	45	113	11	15	400	57

Table 2.2. Reagent concentrations employed in the different reactions.

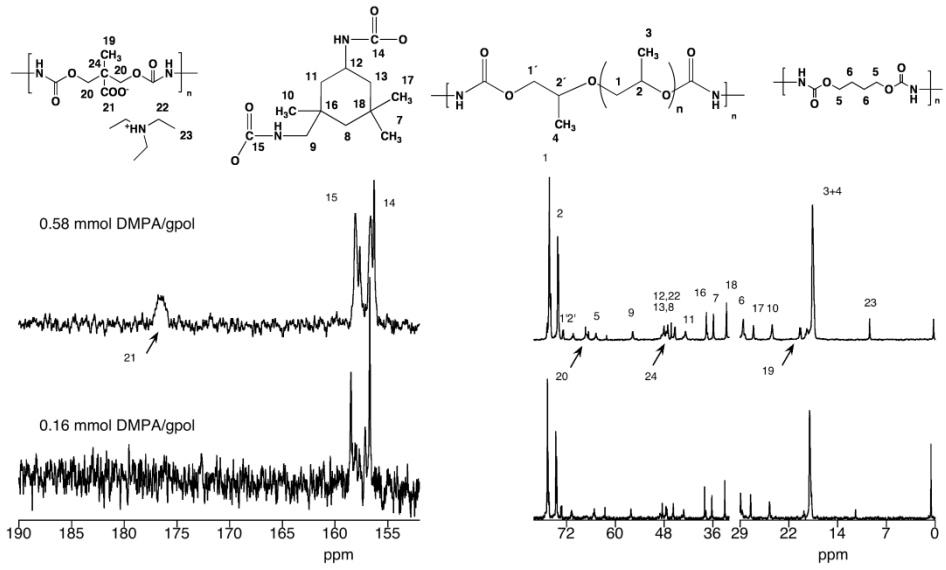

Figure 2.18. ^{13}C NMR spectra of WPU-s containing 0.16 and 0.58 mmol DMPA. g$^{-1}_{pol}$.

Figure 2.18 shows the ^{13}C NMR spectra of two of the synthesized systems containing 0.16 and 0.58 DMPA mmol.g$^{-1}_{pol}$ respectively, where all the signals have been assigned to their corresponding carbon atoms. With this technique the signals attributed to DMPA could

be detected. Specifically, the signals of carbons 19, 20, 21 and 24 of the spectrum of the system with the higher DMPA content are directly related to the insertion of DMPA into the polymer backbone.

3.4. Effect of various parameters on the characteristics of the PU dispersions

The average particle size of WPU dispersions is an important parameter that can be mainly controlled by varying the total amount of internal ionic surfactant: DMPA. However, it is also governed to some extent by the emulsification conditions such as solvent affinity towards water, PU content and temperature.

3.4.1. Effect of DMPA concentration and PU content on colloidal features of WPU-s based on PPG

In order to investigate the effect of DMPA concentration, seven dispersions were prepared varying the initial amount of DMPA, while maintaining the concentration of the other reagents and the emulsification conditions constant. All acidic groups were neutralized with triethylamine (TEA). The phase inversion was performed at 400 rpm and 25 °C by adding 45 g of water at 1 mL.min^{-1} to 35 g of a polyurethane solution in acetone (60 wt. %). Table 2.3 summarizes the reagents used in these reactions.

DMPA (*mmol.g$^{-1}_{pol}$*)	*Polyether* (*mmol*)	*IPDI* (*mmol*)	*DMPA* (*mmol*)	*TEA* (*mmol*)	*DBTDA* (*ppm*)	*BD* (*mmol*)
0.58	45	113	52	69	400	16
0.35	45	113	26	35	400	42
0.30	45	113	22	30	400	46
0.26	45	113	19	25	400	49
0.21	45	113	15	20	400	53
0.16	45	113	11	15	400	57
0.10	45	113	8	10	400	61

Table 2.3. Reagent concentrations employed in the different reactions.

In all the reactions the particle size was measured by Dynamic Light Scattering (DLS) during the water addition process. The stability of the final product was determined using a Turbiscan, a stable dispersion being one when no variation in the backscattering was observed for 48 hours.

Figure 2.19 shows the evolution of the particle size during the water addition process for samples containing different DMPA concentrations as a function of f (where f is defined as the ratio of the mass of added water to the total mass of solvents). The last points of the graph (f=1) were obtained after acetone removal at 25 °C under vacuum using a rotary evaporator.

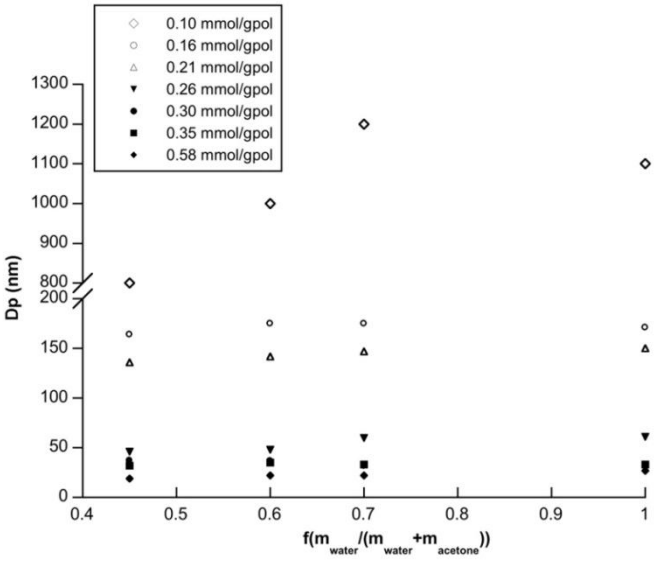

Figure 2.19. Particle size evolution during the phase inversion process for different DMPA concentrations and 60 wt. % PU content in acetone. The stable dispersions are represented with filled symbols.

As shown in Figure 2.19, for DMPA concentrations lower than 0.26 $mmol.g^{-1}_{pol}$ the resultant systems were highly unstable as they settled within a couple of hours[25-27].

In relation to the particle size, the system containing the lowest surfactant concentration (0.10 $mmol.g^{-1}_{pol}$) experiments a sharp increase during the water addition process. On the contrary, for higher DMPA amounts, particle size does not change during the whole process, although it decreases with DMPA content. However, for acid concentrations

higher than 0.30 mmol.g$^{-1}_{pol}$, no additional reduction of particle size is observed. Similar results have already been reported in literature[11] and attributed to the greater ability of the system to stabilize larger areas, eventually leading to smaller particle sizes.

Another parameter having a great effect on the phase inversion process is the initial PU content[27,32]. In order to study its influence, the same type of experiments were carried out at different initial PU contents. The results obtained are shown in Figure 2.20.

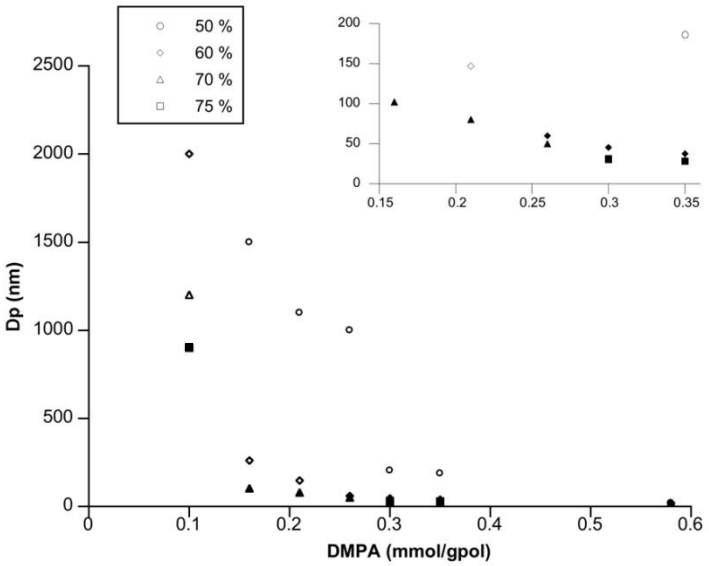

Figure 2.20. Final (f=1) particle size vs. DMPA concentration, for different initial PU contents. The stable dispersions are represented with filled symbols.

At low DMPA concentrations, the particle size clearly decreases when increasing the concentration of the starting solutions. However, at higher DMPA concentrations the effect of PU content is not so pronounced. Nevertheless, a small particle size does not imply dispersion stability. Thus, starting at 75 wt. % PU, stable dispersions with mean particle sizes around 800 nm can be obtained using a low DMPA concentration (0.10 mmol.g$^{-1}_{pol}$). In contrast, at concentrations of 50 wt. %, although mean particle size is about 200 nm, no stable dispersions are obtained even when threefold DMPA concentrations are employed. Indeed, the polydispersity index is very high and the dispersions contain aggregates (>1 μm) that precipitate rapidly. Nevertheless, as a

consequence of the presence of a large amount of small particles, the mean particle size is low.

Figure 2.21 shows photographs of stable and unstable dispersions containing different PU and DMPA concentrations. In all cases the appropriate amount of water was added in order to obtain final dispersions with a 30 wt. % of solids. The photographs were taken just after stirring for a few minutes (2.21A - left) and after leaving the samples 48 hours without stirring (2.21B - right). Figure 2.21A shows that, regardless of the initial PU content, either soluble or two- phase systems are obtained, and this is dependent on DMPA concentration.

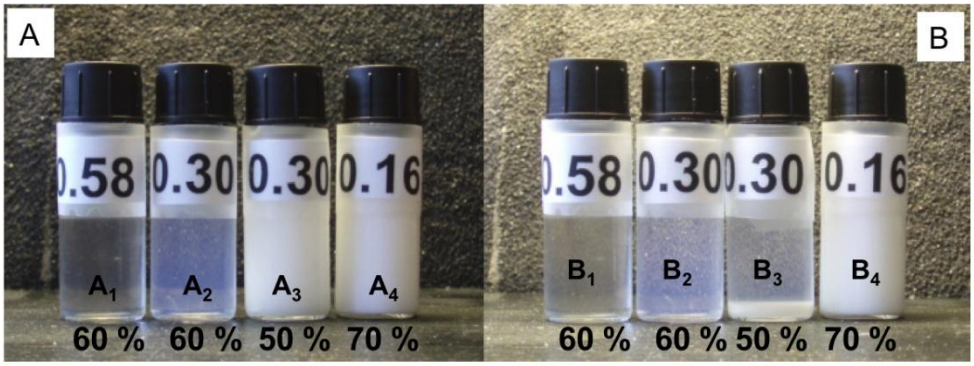

Figure 2.21. Photographs of samples with different DMPA concentrations and contents. Starting point (A-left) and after 48 hours without stirring (B-right).

In addition, dispersions containing the same DMPA concentration but with two different initial polyurethane contents (vials A2 and A3) present different particle size. Furthermore, after leaving the vials 48 hours without stirring (Figure 2.21B) the dispersion with 0.30 mmol.g^{-1}_{pol} and 50 wt. % PU precipitates, probably due to the presence of large aggregates (see A3/B3). Nevertheless, when PU content is increased (70 wt. %), stable dispersions are obtained with a lower DMPA concentration (0.16 mmol.g^{-1}_{pol}, vials A4/B4) and with similar mean particle sizes (A3 ≈ 225 nm/A4 ≈ 150 nm).

This result shows that DMPA minimum amount depends on polymer/acetone ratio. Therefore, in order to obtain stable dispersions both parameters (DMPA concentration

and polymer/acetone ratio) must be selected together and not separately as reported in literature.[11,27,32]

Figure 2.22 shows the minimum amount of DMPA required for obtaining a stable dispersion as a function of PU content. As can be observed, this amount decreases as PU content increases. This result agrees with literature data[27,32] where it is concluded that a high amount of acetone can alter the dispersion stability.

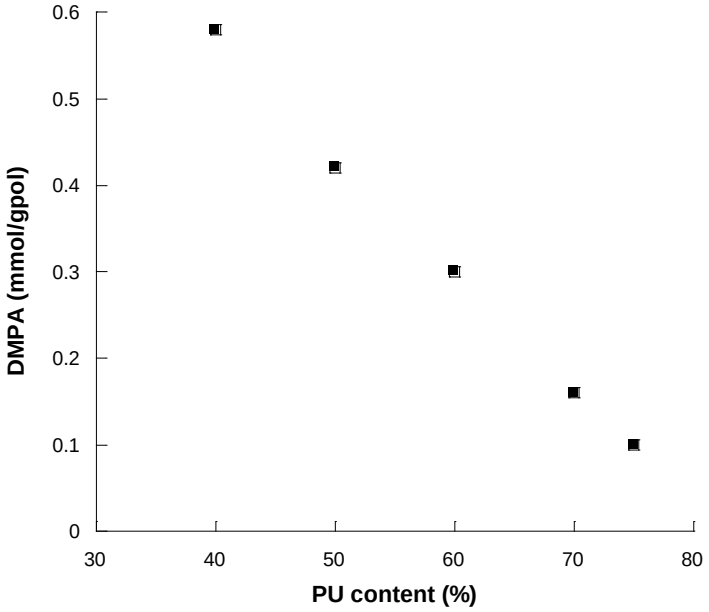

Figure 2.22. Minimum amount of DMPA for obtaining stable dispersions as a function of the initial PU content.

3.4.2. Effect of DMPA concentration and PU initial content on the colloidal features of WPU-s based on PBAD

The results shown in the previous section were obtained using poly (propylene glycol) as soft segment. The same type of experiments was performed using a polyester type glycol (PBAD). The prepared dispersions are summarized in Table 2.4.

DMPA ($mmol.g^{-1}_{pol}$)	*Polyester* (*mmol*)	*IPDI* (*mmol*)	*DMPA* (*mmol*)	*TEA* (*mmol*)	*DBTDA* (*ppm*)	*BD* (*mmol*)
0.41	45	113	30	40	400	38
0.30	45	113	22	30	400	46
0.21	45	113	15	20	400	53

Table 2.4. Amount of different reagents employed in the reactions.

The minimum amount of DMPA required for obtaining a stable dispersion as a function of PU content is represented in Figure 2.23. As shown, the trend is similar to the case of PPG where the minimum amount of DMPA needed to obtain a stable dispersion decreases as PU content increases.

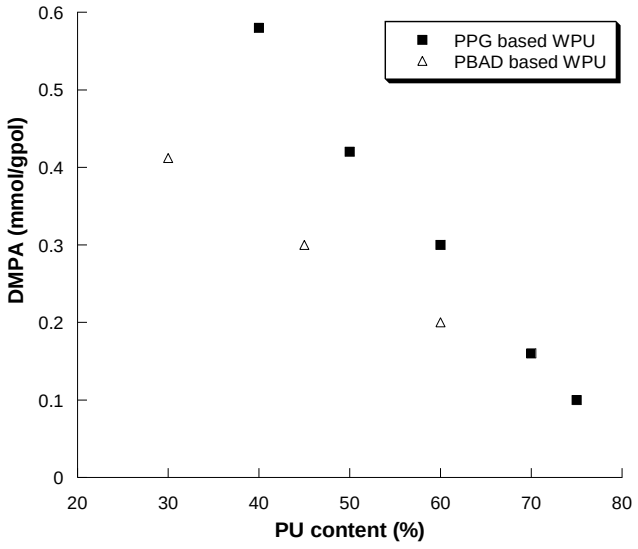

Figure 2.23. Minimum amount of DMPA for obtaining stable dispersions as a function of initial PU content for PPG and PBAD based polyurethanes.

Nevertheless, comparing both set of data, it can be observed that for a fixed PU content polyester based PU gives a stable dispersion at a lower DMPA concentration than PPG based systems. In our opinion, this behaviour can be explained taking into account the higher polarity of ester groups compared to ether groups and also due to the higher viscosities of polyester based PU's compared to polyether.

3.4.3. Effect of temperature on the phase inversion process

The effect of the precipitation temperature on both particle size and dispersion stability has not been clearly stated in literature so far. In order to study this effect, several experiments were carried out performing the phase inversion at different temperatures. The system employed was a PPG based PU with 0.30 mmolDMPA.g^{-1}_{pol} at a starting PU content of 60 wt. %.

Figure 2.24 shows the evolution of the particle size during the water addition process at different temperatures.

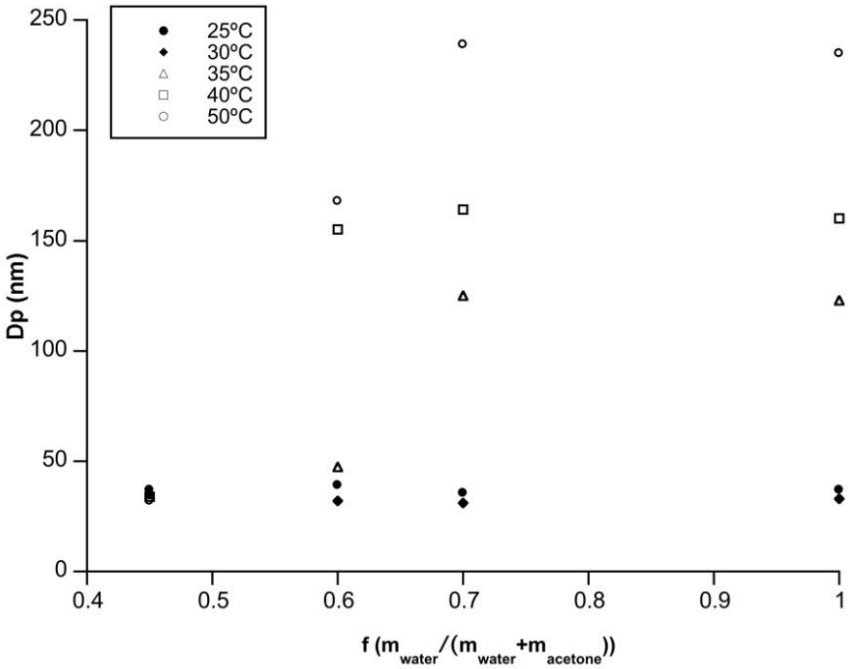

Figure 2.24. Particle size obtained during the water addition process carried out at different temperatures, DMPA concentration 0.30 mmol.g^{-1}_{pol} and PU content (60 wt. %). The stable dispersions are represented by filled symbols.

As can be seen, the temperature has an important effect on the phase inversion process in the higher temperature ranges, while at low temperatures (25-30 °C), the particle size remains stable, close to 40 nm. However, when the phase inversion temperature is set up

at 35 °C or higher, there is an important increase in the particle size and the dispersion becomes unstable, precipitating in a short period of time. According to our results, it is clear that not only does the DMPA content control the dispersion characteristics, but the initial content of PU and the phase inversion temperature also play an important role in the formation of stable polyurethane dispersions.

All the results shown so far were obtained by removing the acetone at room temperature. Although a higher removal temperature permits a faster solvent evaporation, it can strongly affect particle size and dispersion stability because of the formation of aggregates. In order to check this point, the acetone was evaporated at different temperatures for the system obtained using 0.30 $mmol.g^{-1}_{pol}$ and a starting PU content of 60 wt. %. The results are shown in Table 2.5.

Acetone evaporating temperature (°C)	Particle size (nm)	Polydispersity index
25	29±1	0.14±0.02
35	38±2	0.18±0.03
45	43±3	0.37±0.05

Table 2.5. Particle size and polydispersity values as a function of acetone removal temperature.

As can be seen, the higher the temperature of evaporation, the higher the particle size and polydispersity index, indicating the presence of large aggregates, probably due to the increase of the kinetic energy of the system, which promotes particle aggregation. According to these results, low temperatures have to be used in order to remove the acetone from the system.

3.4.4. Effect of catalyst on the emulsification process

As reported in previous sections, the IPDI/alcohol reaction rate and mechanism are catalyst dependent. In this section the effect of the catalyst on the polymer water dispersion process is described.

Two similar formulations obtained using zirconium and tin catalysts were selected for this experiment. The results obtained are summarized in Table 2.6.

The general behaviour of both systems is similar. When more water is added, the size of the particle maintains constant of about 40 nm. These results are in accordance to others reported in the literature.[43,45,50] It can be concluded that the catalyst does not have any relevant effect on the particle size and stability.

Water volume (mL)	PPG Dp Zr(nm)	PPG Dp Sn(nm)
30	43	35
60	42	37
120	43	36
180	40	38

Table 2.6. Particle diameter during the phase inversion process employing different catalysts.

3.4.5. Effect of the solvent miscibility with water

Two different organic solvents were tested in addition to acetone (totally miscible with water), i.e. chloroform (totally immiscible) and THF (totally miscible). The DMPA concentration and the initial PU content were maintained constant at 0.30 $mmol.g^{-1}_{pol}$ and 60 wt. %, respectively.

Figure 2.25 shows the evolution of the particle size during the water addition process for the three different solvents at 25 °C. The particle size variation during the phase inversion process is different depending on the solvent. When using a totally miscible solvent (acetone), the particle size remains constant during the whole process (around 30 nm). In our opinion this behaviour can be explained owing to the fact that most of the acetone is in the water phase and therefore does not swell the formed particles. When THF is used, the particle size does not change during water addition, and a similar tendency to that of acetone is observed, due to their similar solubility. Nevertheless, when THF is evaporated the particle size increases (from 34 to 180 nm) and consequently the evaporation conditions have to be controlled in order not to affect the particle size and distribution.

When employing a totally immiscible solvent (chloroform), the particle size fluctuates along the process. At the beginning large particles are obtained, but after solvent evaporation (f=1) the particle size decreases substantially. We suggest that this phenomenon occurs because the polyurethane particles are swollen due to the presence of chloroform and therefore after its evaporation the particle size is reduced.

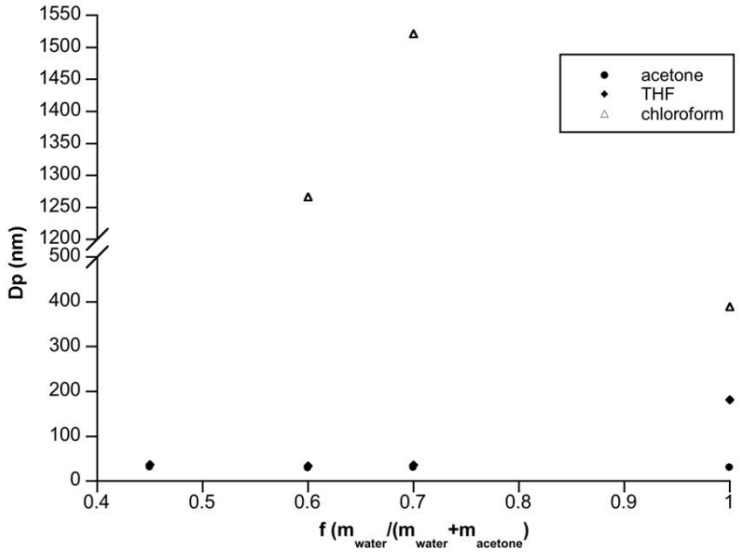

Figure 2.25. Particle size variation during the phase inversion process using different solvents. The stable dispersions are represented by filled symbols.

3.5. Rheological behaviour of PU-s during the phase inversion process

According to literature[25-27] the phase inversion process during the production of aqueous polyurethane dispersions follows three consecutive steps. In the first one, the first water drops are soluble in the PU/acetone solution and thus the viscosity reduces slightly. However, in the second one, the generation of polyurethane particles makes the viscosity rise sharply. After reaching a maximum, the viscosity finally drops again because the

effect of adding more water is just to dilute the dispersion and not to generate new particles.

3.5.1. Effect of PU content

3.5.1.1. PPG based systems

The phase inversion point was detected by measuring the viscosity during the water addition process as explained in Annex I. Figure 2.26 shows the viscosity evolution vs. f for three different initial PU containing systems at 25 °C and 0.30 mmol DMPA.g^{-1}_{pol}.

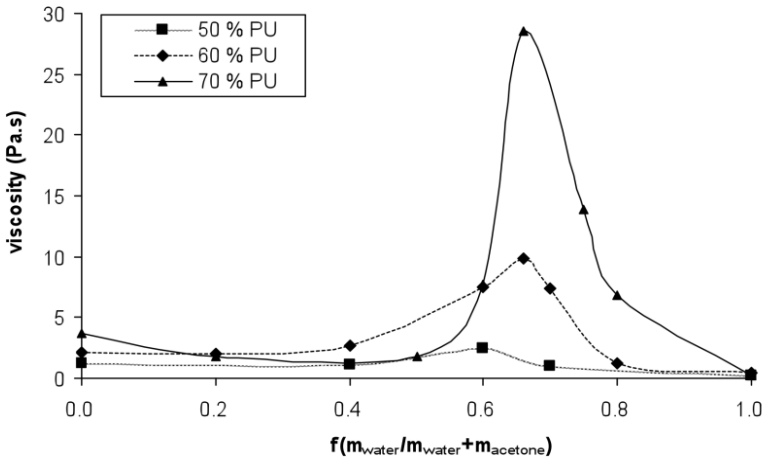

Figure 2.26. Viscosity evolution as a function of f for different initial PU contents and a fixed DMPA content of 0.30 mmol.g^{-1}_{pol} at 25 °C.

As can be seen, the three stages mentioned above are clearly observed only in the case of the system containing initially 70 wt. % of PU. However, the three systems present an increase of the viscosity, which is more pronounced at high initial PU contents. Although the effect of the initial PU content on the maximum viscosity has also been discussed in the literature,[27] there is no clear explanation to account for this phenomenon. From our point of view, two possible facts can be responsible for this result. First of all, as already mentioned, the higher particle size (200 nm) of the system with the lowest PU content (50 wt. %) reduces the possibility of particle interaction, leading to a lower increase of the viscosity at the maximum. However, the viscosity value corresponding to the phase inversion point is very different for the systems containing 60 and 70 wt. % of PU

although their particle sizes are almost identical (30 nm). Taking into account that the polymer concentration at the inversion points varies from about 35 wt. % to 43 wt. % of PU in these two systems, we believe that this factor can be responsible for the viscosity difference observed at the phase inversion points.

3.5.1.2. PBAD based systems

When PBAD as soft segment was employed the behaviour was similar. The phase inversion point was also detected by measuring the viscosity during the water addition process. Figure 2.27 shows the viscosity evolution vs. f for three different initial PU containing systems at 25 °C and 0.30 mmol DMPA.g^{-1}_{pol}.

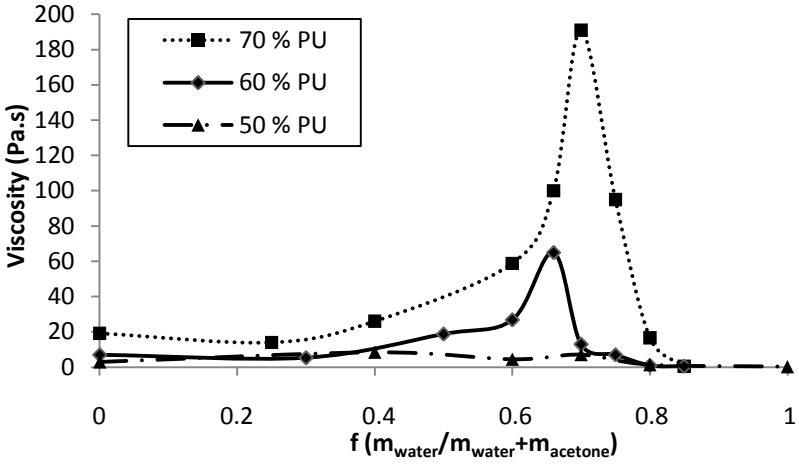

Figure 2.27. Viscosity evolution as a function of f for different initial PU contents and a fixed DMPA content of 0.30 mmol.g^{-1}_{pol} at 25 °C.

The viscosity value corresponding to the phase inversion point for the PU-s based on PBAD is much higher than in the case of PPG. Moreover, as in the case of PPG, very different viscosity curves are obtained for the systems containing 50, 60 and 70 wt. % of PU although their particle sizes are almost identical (30 nm). Taking into account that the polymer concentration at the inversion points varies from about 29 to 43 wt. % of PU

in these systems, we believe that this factor can be responsible for the viscosity difference observed at the phase inversion points such as in the case of PPG.

3.5.2. Effect of the phase inversion temperature

The effect of the phase inversion temperature was also studied. Figure 2.28 shows the viscosity evolution for three different phase inversion temperatures at 60 wt. % of initial PU content (in a PPG based PU) for a system containing 0.30 mmol DMPA.g^{-1}_{pol}.

As water content increases the viscosity reaches a maximum whose value decreases with temperature. Furthermore, this maximum is obtained at similar values for the experiments carried out at 35 and 45 °C and shifts towards lower f values at 25 °C. This result can be explained taking into account that polyurethane solubility in the acetone/water mixture increases with temperature.

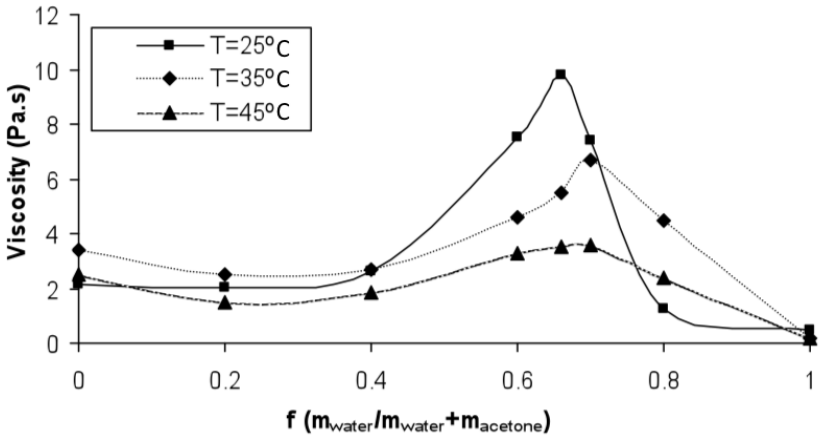

Figure 2.28. Evolution of the viscosity as a function of f for three different phase inversion temperatures (60 wt. % of initial PU; 0.30 mmol DMPA.g^{-1}_{pol}).

3.5.3. Effect of solvent affinity towards water

Rheological measurements were also performed using THF and chloroform. The phase inversion process was studied at 25 °C using 60 wt. % and a DMPA concentration of 0.30 mmol.g^{-1}_{pol}.

Figure 2.29 shows the viscosity curves during the phase inversion process with the three different organic solvents. When using chloroform as solvent, the viscosity curve shifts towards lower f values. In this case, due to the unsolubility of chloroform in water, less water can be absorbed by the chloroform/polyurethane system than in the other two cases, and therefore particle formation occurs using less water. For THF and acetone, the viscosity curves are similar indicating that the amount of absorbed water is the same in both systems leading to a similar phase inversion mechanism.

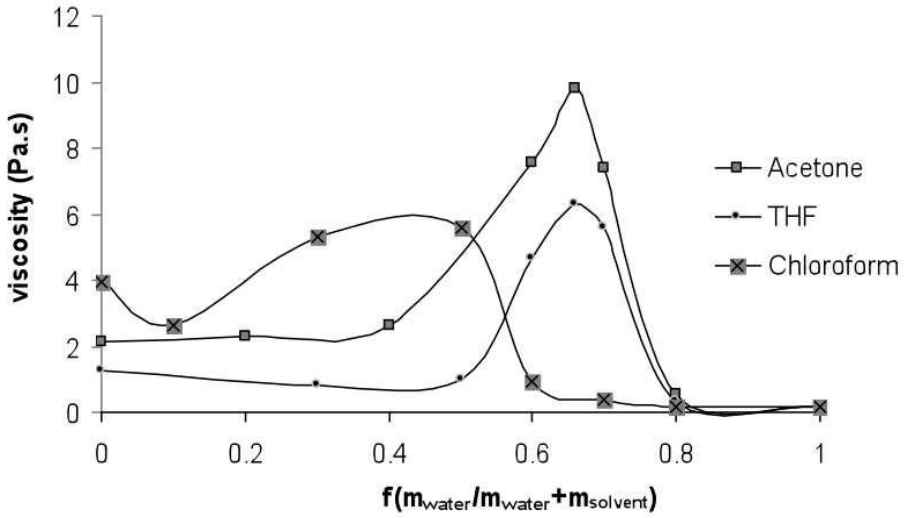

Figure 2.29. Evolution of the viscosity as a function of f for three different organic solvents at 25 °C (60 wt. % of PU; 0.30 mmol DMPA.g^{-1}_{pol}).

3.6. Ternary diagram for the acetone process

All these results can be represented using a ternary diagram (Figure 2.30 and 2.31). The initial PU concentration for achieving a stable polyurethane dispersion was determined at a fixed DMPA concentration and temperature. In addition, for a fixed PU content, it is possible to visualize the water content needed for obtaining particles (this point is defined in the ternary diagram as turbidity point). Finally, the maximum viscosity point was determined by means of rheological measurements. The connection of the turbidity points allows us to divide the diagram into homogeneous and heterogeneous regions. The

heterogeneous region can be further divided into stable (from 75 down to 60 wt. % of PU) and unstable sub-regions (from 60 down to 10 wt. % of PU). Furthermore, maximum viscosity points are those at which no more polyurethane particles are formed. The final dispersion point is taken when acetone is removed using a rotary evaporator.

According to the results summarized in Figure 2.30 for the PPG based WPU-s, 60 wt. % of PU is needed in order to obtain stable water dispersions using 0.30 mmol DMPA.g^{-1}_{pol} and working at 25 °C. However, if DMPA concentration is varied, the diagram changes because both polyurethane affinity towards water and the ionic strength increase with DMPA content. In addition, when the temperature is increased, polyurethane solubility in both solvents changes and consequently the phase diagram is also different.

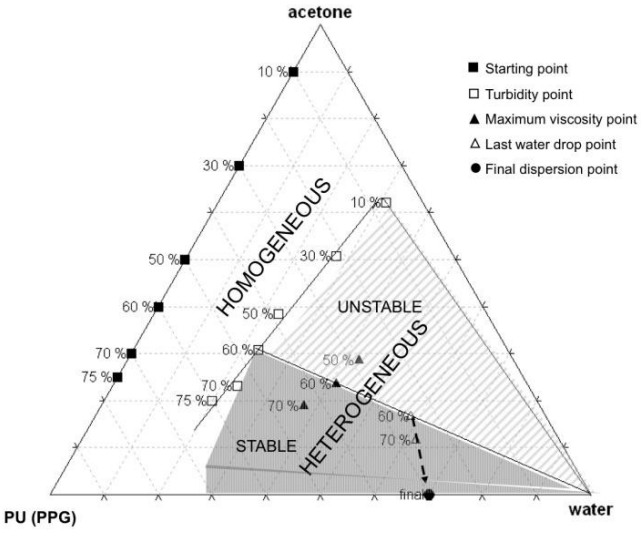

Figure 2.30. Schematic ternary diagram for the PPG based WPU-s containing 0.30 mmol DMPA.g^{-1}_{pol} at 25 °C.

Figure 2.31 shows the ternary diagram for the PU-s based on PBAD. As shown the stable region goes from 70 down to 45 wt. % of PU and unstable regions from 40 down to 10 wt % of PU. When the concentration of PU is greater than 70 wt. %, the system viscosity was high. Under these conditions, when emulsification was performed the reproducibility was

low, leading to nanoemulsions in some cases and big aggregates in others. Comparing this system (Figure 2.31) with the one based on PPG (Figure 2.30), it seems that in the later the stability window is higher and therefore stable dispersions can be obtained using larger acetone contents.

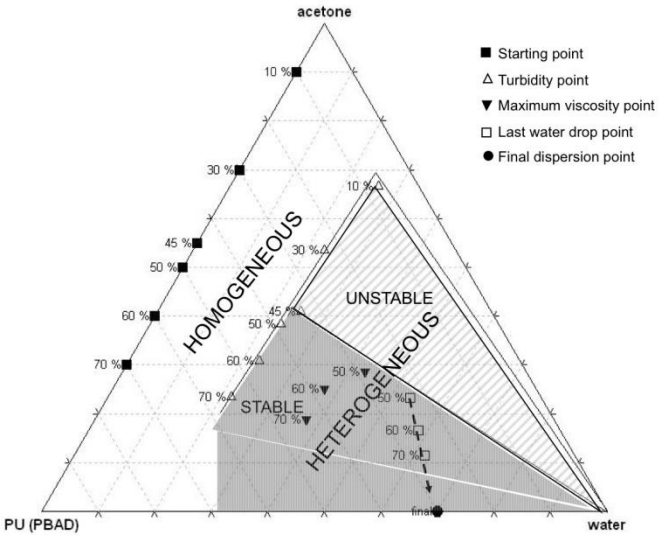

Figure 2.31. Schematic ternary diagram for the PBAD based PU-s containing 0.30 mmol DMPA.g^{-1}_{pol} at 25 °C.

It is not easy to explain the effect of acetone concentration on the emulsification process. Recently, Katz et al.[51-52] postulated a new mechanism where stable fine emulsions were obtained upon pouring water into a solution consisting of oil in a water-miscible solvent without the presence of surfactants. Known as the Ouzo effect, oil droplets are produced whose diameter is a function of the ratio of excess oil to water-soluble solvent. Figure 2.32 is a triangular three component ternary diagram showing the concentration of the solvent on the ordinate. The water concentration in the ternary diagram is calculated from the values of the oil and the co-solvent concentrations.

In this diagram, the binodal (miscibility-limit curve) and the spinodal (stability-limit curve) can be traced out. The binodal in a ternary diagram traces the thermodynamic minima in the Gibbs free energy as a function of mol fraction. The spinodal traces the limit of thermodynamic stability. It is possible for a system to exist for a very long time in states between the spinodal and the binodal, that is, a "state" for which the Gibbs free

energy is not minimum, if there are large kinetic barriers to the phase separation. The set of all such nonequilibrium but very long-lived "states" is called "the metastable region".

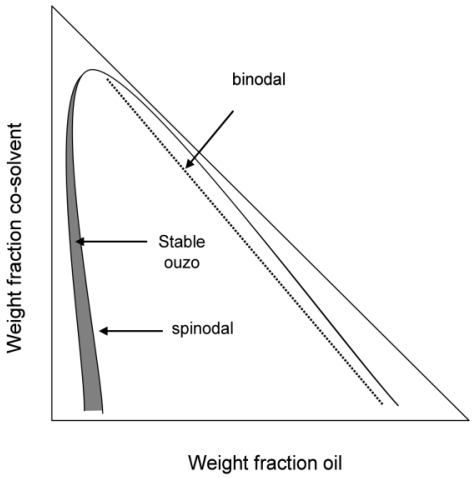

Figure 2.32. Triangular three-component phase diagram at constant temperature and pressure. The Ouzo effect occurs for solutions brought from the one-phase region into the metastable region between the binodal and spinodal curves.

The Ouzo effect occurs when solutions are brought rapidly into the metastable region by the addition of water. When the solubility of some of the solutes decreases faster than linearly with water concentration, the solution can become supersaturated in these components. If the supersaturation is large, nuclei form spontaneously from small local fluctuations in the concentration of solute molecules. Nucleation ends when there are no remaining regions with a high super- saturation. The final result of this process (which occurs on the millisecond or faster time scale) is a spatially, fairly uniform dispersion of very small liquid droplets suspended in the continuous liquid phase.

As shown in Figure 2.33, the Ouzo effect is a liquid-liquid nucleation process. In the first stage, water diffuses towards the oil containing solvent droplet causing super saturation of oil and particle nucleation. In the second stage, droplets grow to a limit where water phase is not further supersaturated with the oil. In the literature a short-review[51-52] of the processes that may occur by means of the Ouzo effect (Sol-Gel process, polyurethane dispersion...) are discussed together with its advantages as an alternative to ultrasonic and high-shear techniques. The review mentions some limitations, namely, the low oil

content that can be dispersed (typically 1 wt. %) and the requirement that the solvent used be soluble in water.

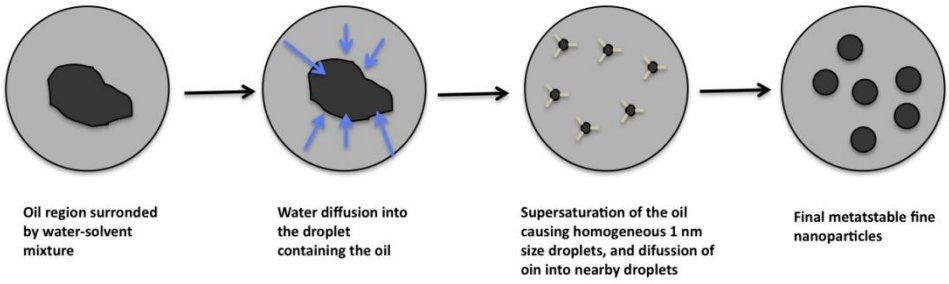

Figure 2.33. Schematics of the liquid–liquid nucleation process or Ouzo effect.

Katz el al[51-52] suggested that when a water soluble solvent exceeds a critical value (in our case when the acetone concentration exceeds a critical value for PPG based WPU-s 40 wt. % and for PBAD based WPU-s 55 wt. %) emulsification can take place by spinodal decomposition, producing coarse emulsions that separate rapidly. On the other hand, when the acetone concentration is lower than a certain value, particle stabilization occurs by means of spontaneous emulsification (Ouzo effect), generating stable nano emulsions. From our point of view, the Ouzo effect can explain the big differences observed in the PU emulsification process as a function of temperature, acetone content or solvent employed. However, more studies have to be carried out to prove this particle formation mechanism.

4. CONCLUSIONS

The synthesis of water dispersible polyurethanes based on isophorone diisocyanate and two different soft segments (PPG/PBAD) has been described in this chapter.

In addition, less toxic zirconium catalyst has proven to be a good candidate to replace the generally used tin catalyst in the synthesis process of polyurethanes. Zirconium catalyst shows a catalytic activity similar to that of tin based ones. Nevertheless, in order to overcome the hydrolysis of the zirconium complex, the acid groups of the functionalized diol must be previously neutralized. This catalyst presents the same selectivity towards primary and secondary isocyanate groups of IPDI, whereas tin catalyst has different behaviour. Thus, FTIR and ^{13}C-NMR results have shown that in the presence of triethyl amine (TEA) and the tin catalyst the secondary isocyanate groups present a higher reactivity than that of the primary group, while using the zirconium catalyst the two isocyanate groups show the same reactivity.

Stable polyurethane dispersions were obtained by means of the acetone process. The results showed that a minimum amount of ionic groups (DMPA) is required in order to obtain stable polyurethane dispersions. Nevertheless, this minimum amount of DMPA decreases when increasing the initial polyurethane concentration (before the water addition process). When the phase inversion was carried out at temperatures higher than 35 °C, the particle size increases and the dispersions become unstable. The same decrease in stability is generated when acetone is removed at high temperatures. Therefore, low phase inversion and mild evaporation temperatures must be used in order to obtain stable dispersions.

The viscosity behaviour during the phase inversion process provides interesting information in relation to the different steps during particle formation, although there are still some open questions about the particle formation mechanism. The elaboration of a ternary phase diagram makes possible to fix the optimal conditions needed to obtain stable polymer dispersions. However, different phase diagrams can be obtained by varying the concentration of the internal emulsifier, temperature and solvent nature.

As a general conclusion, the conditions for obtaining stable polyurethane dispersions based on PPG and PBAD were determined. This result can be of great interest in order to obtain different particle size dispersions that can be commercialized as low VOC polyurethane adhesives.

5. BIBLIOGRAPHY

1 Hepburn, C. Polyurethane elastomers. (Elsevier Applied Science 1992).

2 Mark, H. F., Bikales, N., Overberger, C. G., Menges, G. & Kroschwitz, J. I. in Encyclopedia of polymer science and engineering (eds Herman F. Mark) (Wiley-Interscience, 1986).

3 Kircher, K. Chemical reactions in plastics processing. (Oxford university Press, 1987).

4 Król, P. Synthesis methods, chemical structures and phase structures of linear polyurethanes. Properties and applications of linear polyurethanes in polyurethane elastomers, copolymers and ionomers. Progress in Materials Science 52, 915-1015 (2007).

5 Seneker, S. D. & Potter, T. A. Solvent and catalyst effects in the reaction of dicycloexyl-methane diisocyanate with alcohols and water. Journal of Coatings Technology 63, 19-26 (1991).

6 Chattopadhyay, D. K. & Raju, K. V. S. N. Structural engineering of polyurethane coatings for high performance applications. Progress in Polymer Science 32, 352-418 (2007).

7 Wong, S. W. & Frisch, K. C. Catalysis in competing isocyanate reactions. I. Effect of organotin–tertiary amine catalysts on phenyl isocyanate and N-butanol reaction. Journal of Polymer Science Part A: Polymer Chemistry 24, 2867-2875 (1986).

8 Wang, T. L. & Lyman, D. J. The effect of reaction conditions on the urethane prepolymer formation. Polymer Bulletin 27, 549-555 (1992).

9 Kim, B. K. Aqueous polyurethane dispersions. Colloid & Polymer Science 274, 599-611 (1996).

10 Lee, S. K. & Kim, B. K. High solid and high stability waterborne polyurethanes via ionic groups in soft segments and chain termini. Journal of Colloid and Interface Science 336, 208-214 (2009).

11 Nanda, A. K. & Wicks, D. A. The influence of the ionic concentration, concentration of the polymer, degree of neutralization and chain extension on aqueous polyurethane dispersions prepared by the acetone process. Polymer 47, 1805-1811 (2006).

12 Sardon, H., Irusta, L. & Fernández-Berridi, M. J. Synthesis of isophorone diisocyanate (IPDI) based waterborne polyurethanes: Comparison between

zirconium and tin catalysts in the polymerization process. Progress in Organic Coatings 66, 291-295 (2009).

13 Barrère, M. & Landfester, K. High molecular weight polyurethane and polymer hybrid particles in aqueous miniemulsion. Macromolecules 36, 5119-5125 (2003).

14 Li, C. Y., Li, Y. H., Hsieh, K. H. & Chiu, W. Y. High-molecular-weight polyurethanes prepared by one-step miniemulsion polymerization. Journal of Applied Polymer Science 107, 840-845 (2008).

15 Bouchemal, K., Briançona, S., Perrierb, E., Fessia, H., Bonnetb, I. & Zydowicet N. Synthesis and characterization of polyurethane and poly(ether urethane) nanocapsules using a new technique of interfacial polycondensation combined to spontaneous emulsification. International Journal of Pharmaceutics 269, 89-100 (2004).

16 Subramani, S., Cheong, I. W. & Kim, J. H. Synthesis and characterizations of silylated polyurethane from methyl ethyl ketoxime-blocked polyurethane dispersion. European Polymer Journal 40, 2745-2755 (2004).

17 Pérez-Limiñana, M. A., Arán-Aís, F., Torró-Palau, A. M., César Orgilés-Barceló, A. & Miguel Martín-Martínez, J. Characterization of waterborne polyurethane adhesives containing different amounts of ionic groups. International Journal of Adhesion and Adhesives 25, 507-517 (2005).

18 Barni, A. & Levi, M. Aqueous polyurethane dispersions: A comparative study of polymerization processes. Journal of Applied Polymer Science 88, 716-723 (2003).

19 Coutinho, F. M. B. & Delpech, M. C. Some properties of films cast from polyurethane aqueous dispersions of polyether-based anionomer extended with hydrazine. Polymer Testing 15, 103-113 (1996).

20 Tielemans, M., Roose, P., Groote, P. D. & Vanovervelt, J.C. Colloidal stability of surfactant-free radiation curable polyurethane dispersions. Progress in Organic Coatings 55, 128-136 (2006).

21 Wen, T.C., Wang, Y.J., Cheng, T.T. & Yang, C.H. The effect of DMPA units on ionic conductivity of PEG-DMPA-IPDI waterborne polyurethane as single-ion electrolytes. Polymer 40, 3979-3988 (1999).

22 Dieterich, D. Aqueous emulsions, dispersions and solutions of polyurethanes; synthesis and properties. Progress in Organic Coatings 9, 281-340 (1981).

23 Brooks, B. W. & Richmond, H. N. Phase inversion in non-ionic surfactant--oil--water systems--III. The effect of the oil-phase viscosity on catastrophic inversion and the relationship between the drop sizes present before and after catastrophic inversion. Chemical Engineering Science 49, 1843-1853 (1994).

24 Sajjadi, S., Zerfa, M. & W. Brooks, B. Dynamic behaviour of drops in oil/water/oil dispersions. Chemical Engineering Science 57, 663-675 (2002).

25 Saw, L. K., Brooks, B. W., Carpenter, K. J. & Keight, D. V. Different dispersion regions during the phase inversion of an ionomeric polymer-water system. Journal of Colloid and Interface Science 257, 163-172 (2003).

26 Saw, L. K., Brooks, B. W., Carpenter, K. J. & Keight, D. V. Catastrophic phase inversion in region II of an ionomeric polymer-water system. Journal of Colloid and Interface Science 279, 235-243 (2004).

27 Wei, Y.Y., Luo, Y.W., Li, B.F. & Li, B.G. Phase inversion of UV-curable anionic polyurethane in the presence of acetone solvent. Colloid & Polymer Science 283, 1289-1297 (2005).

28 Vogt-Birnbrich, B. Novel synthesis of low VOC polymeric dispersions and their application in waterborne coatings. Progress in Organic Coatings 29, 31-38 (1996).

29 Jena, K. K., Chattopadhyay, D. K. & Raju, K. V. S. N. Synthesis and characterization of hyperbranched polyurethane-urea coatings. European Polymer Journal 43, 1825-1837 (2007).

30 Chattopadhyay, D. K., Raju, N. P., Vairamani, M. & Raju, K. V. S. N. Structural investigations of polypropylene glycol (PPG) and isophorone diisocyanate (IPDI) based polyurethane prepolymer by matrix-assisted laser desorption/ionization time-of-flight (MALDI-TOF)-mass spectrometry. Progress in Organic Coatings 62, 117-122 (2008).

31 Delpech, M. C. & Coutinho, F. M. B. Waterborne anionic polyurethanes and poly(urethane-urea)s: influence of the chain extender on mechanical and adhesive properties. Polymer Testing 19, 939-952 (2000).

32 Chinwanitcharoen, C., Kanoh, S., Yamada, T., Hayashi, S. & Sugano, S. Preparation of aqueous dispersible polyurethane: Effect of acetone on the particle size and storage stability of polyurethane emulsion. Journal of Applied Polymer Science 91, 3455-3461 (2004).

33 Jahangir, R., McCloskey, C., McClung W.G., Brash, J.L, Labow, R.S. & Santerre, J.P. The influence of protein adsorption and surface modifying macromolecules on the hydrolytic degradation of a poly(ether-urethane) by cholesterol esterase. Biomaterials 24, 121-130 (2003).

34 Labow, R. S., Meek, E. & Santerre, J. P. Hydrolytic degradation of poly(carbonate)-urethanes by monocyte-derived macrophages. Biomaterials 22, 3025-3033 (2001).

35 Lomölder, R., Plogmann, F. & Speier, P. Selectivity of isophorone diisocyanate in the urethane reaction influence of temperature, catalysis, and reaction partners. Journal of Coatings Technology 69, 51-57 (1997).

36 Wang, H., Shen, Y., Fei, G., Li, X. & Liang, Y. Micromorphology and phase behaviour of cationic polyurethane segmented copolymer modified with hydroxysilane. Journal of Colloid and Interface Science 324, 36-41 (2008).

37 Kim, B. K. & Lee, Y. M. Aqueous dispersion of polyurethanes containing ionic and nonionic hydrophilic segments. Journal of Applied Polymer Science 54, 1809-1815 (1994).

38 Yoon Jang, J., Kuk Jhon, Y., Woo Cheong, I. & Hyun Kim, J. Effect of process variables on molecular weight and mechanical properties of water-based polyurethane dispersion. Colloids and Surfaces A: Physicochemical and Engineering Aspects 196, 135-143 (2002).

39 Chen, Y. & Chen, Y. L. Aqueous dispersions of polyurethane anionomers: Effects of countercation. Journal of Applied Polymer Science 46, 435-443 (1992).

40 Wojcik, R. T. PU Coatings: from raw materials to end-products. (Technomic Publishing, 1998).

41 Rochery, M., Vroman, I. & Lam, T. M. Kinetic model for the reaction of IPDI and macrodiols: study of the relative reactivity of isocyanate groups. Journal of Macromolecular Science, Part A: Pure and Applied Chemistry 37, 259-275 (2000).

42 Dobrzynski, P., Kasperczyk, J., Janeczek, H. & Bero, M. Synthesis of biodegradable copolymers with the use of low toxic zirconium compounds. 1. copolymerization of glycolide with l-Lactide initiated by Zr(Acac)4. Macromolecules 34, 5090-5098 (2001).

43 Blank, W. J., He, Z. A. & Hessell, E. T. Catalysis of the isocyanate-hydroxyl reaction by non-tin catalysts. Progress in Organic Coatings 35, 19-29 (1999).

44 Blank, W. J. & Tramontano, V. J. Properties of crosslinked polyurethane dispersions. Progress in Organic Coatings 27, 1-15 (1996).

45 Blank, W. J. New developments in catalysis. Macromolecular Symposia 187, 261-270 (2002).

46 Yang, J. E., Kong, J. S., Park, S. W., Lee, D. J. & Kim, H. D. Preparation and properties of waterborne polyurethane–urea anionomers. I. The influence of the degree of neutralization and counterion. Journal of Applied Polymer Science 86, 2375-2383 (2002).

47 Smith, H. A. Catalysis of the formation of urethanes. Journal of Applied Polymer Science 7, 85-95 (1963).

48 Sojecki, R. & Trzcinski, S. The synergetic effect of catalytic systems in 2,4-tolylene diisocyanate reactions with macrodiols--I. A reaction model with catalysts molar ratio 1:1. European Polymer Journal 34, 1793-1799 (1998).

49 Prabhakar, A., Chattopadhyay, D. K., Jagadeesh, B. & Raju, K. V. S. N. Structural investigations of polypropylene glycol (PPG) and isophorone diisocyanate (IPDI)-based polyurethane prepolymer by 1D and 2D NMR spectroscopy. Journal of Polymer Science Part A: Polymer Chemistry 43, 1196-1209 (2005).

50 Blank, W. J. Novel polyurethane polyols for waterborne and high solids coatings. Progress in Organic Coatings 20, 235-259 (1992).

51 Ganachaud, F. & Katz, J. L. Nanoparticles and nanocapsules created using the Ouzo effect: spontaneous emulsification as an alternative to ultrasonic and high-shear devices. Chemical Physics and Physical Chemistry 6, 209-216 (2005).

52 Vitale, S. A. & Katz, J. L. Liquid droplet dispersions formed by homogeneous liquid–liquid nucleation: "The Ouzo effect". Langmuir 19, 4105-4110, (2003).

CHAPTER III: SYNTHESIS OF WATERBORNE POLYURETHANE SILICA DISPERSIONS

CHAPTER III: SYNTHESIS OF WATERBORNE POLYURETHANE SILICA DISPERSIONS

1. INTRODUCTION

WPU-s have already been developed and studied in wide range of applications such as adhesives and coating materials.[1-6] However, some inferior properties of these materials such as low mechanical strength, solvent and chemical resistance restrict their utility for high performance applications to some extent.[7-11] It is important to modify WPU-s by various methods to improve the solvent and chemical resistance, thermal and mechanical properties.[12-17]

There are several options available to formulators for improving the performance of waterborne thermoplastic polyurethanes by crosslinking the polymer.[9,13,17-28] Among these, polyaziridines and polyisocyanates have found significant commercial application in contractor-applied wood floor coatings, mainly due to their cure effectiveness at ambient conditions in a reasonable length of time.[29] The use of water-dispersible polyisocyanates as a crosslinking component of 2K WPU-s for floor coating applications is to some extent a newer technology that is growing in popularity. It has gained some favour over polyaziridine crosslinkers due to reduced toxicological concerns; however, they are still of concern for allergic reactions, skin irritation and asthma.[9,19,29-32] In Figure 3.1 a typical formulation employed in 2K WPU-s is shown.

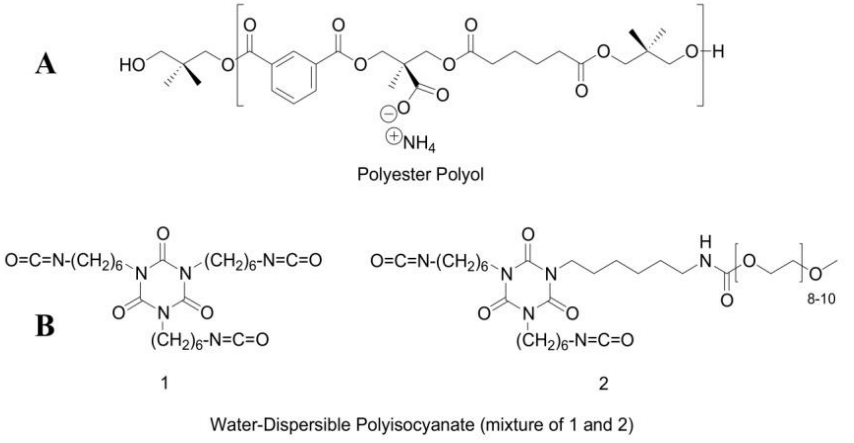

Figure 3.1. Commonly employed A and B compounds in waterborne 2K-WPU-s.

However, water-dispersible polyisocyanates are known to be difficult to incorporate into waterborne dispersions due to their high degree of hydrophobicity and viscosity, usually requiring them to be diluted. Water-dispersible polyisocyanates also have a shorter pot life than polyaziridines – close to 4 h for optimal performance – after this time the resulting dispersion becomes unusable either due to unacceptable performance, appearance or application properties. Furthermore, the above-described reaction of the polyisocyanate with water can result in foam generation and gas entrapment in the finished coating.[29]

A few options exist to incorporate functional groups into waterborne polyurethanes that can crosslink at room temperature upon application and have the potential to provide a self curable system.[8,24,33-35] One of the recently employed strategies is the use of the sol–gel process to prepare highly intermingled organic–inorganic hybrid polymer networks. This strategy is of current scientific interest since it offers the possibility of tailoring the properties of the materials by variation of the relative composition of the inorganic and organic phases.[13,28,36-39] Depending on the desired application, polymers with different mechanical properties can be obtained because of their versatility in the formulation variables. Additionally, because of the hybrid character, they present superior thermal, abrasion and weathering resistance than traditional polymers.[13,28,40-41]

The basic idea behind the development of inorganic–organic hybrid materials is the combination of inorganic and organic moieties in a molecular scale to achieve a synergetic combination of the properties of each of the constituents. Modification of the kind and proportions of the organic and inorganic components allows a deliberate tailoring of properties, combining those of the inorganic and organic components. Therefore, hybrid inorganic–organic materials produce scratch and abrasive-resistant hard nanocomposite coatings with unique property combinations of the inorganic counterpart (hardness, brittleness, UV radiation and thermal stability and solvent resistance) and the organic counterpart (soft, flexible and with good mechanical properties) while maintaining optical transparency.[23,28,36,41-42]

Among the coating materials, silica is a very interesting candidate since it can be used in a high number of applications ranging from paints and magnetic fluids to high-quality

paper coatings. The nanostructure, degree of organization and properties of hybrid materials depend on the chemical nature and ratio of the components. Therefore, the tailored design of products includes the tuning of the nature, extent and accessibility of the inner interfaces.[43-47]

The Sol-Gel process involves inorganic precursors (a metal salt or an organometallic compound) that undergo various reactions resulting in the formation of a three-dimensional molecular network. The reaction is generally divided into two steps: hydrolysis of metal alkoxides to produce hydroxyl groups in the presence of stoichiometric water (usually in the presence of acid or base catalysts), followed by polycondensation of the resulting hydroxyl groups and residual alkoxyl groups to form a three-dimensional network (Figure 3.2).[23,43]

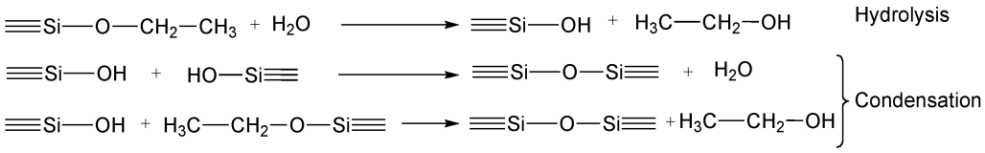

Figure 3.2. Schematic representation of the Sol-Gel process.

Factors such as the nature of the alkyl group, solvent, temperature, water to alkoxide molar ratio, acid or base catalysts, etc. are known to affect the hydrolysis reaction. For example, in the presence of a base catalyst, the rate of condensation is fast compared to hydrolysis and results in the formation of dense, colloidal particles, while using an acid catalyst the rate of condensation is slow compared to hydrolysis, generating many silanol groups on the silica surface.[43]

In recent publications[33-35,48] polyurethane prepolymer dispersions have been reacted with alkoxysilane compounds in order to get a moisture curable PU. Silylated PU dispersions are generally composed of urethane backbones containing condensable final groups. During the water evaporation process, these terminal groups can undergo crosslinking reactions to form a stable siloxane linked network, which results in properties improvement of pure PU-s. In addition, the incorporation of small inorganic domains in the nanoscale gives rise to a synergetic combination of the properties of each

constituent.[8,23-24,35,48-49] In Figure 3.3 a schematic representation of the Sol-Gel crosslinking of alkoxysilane end-capped polymers is shown.

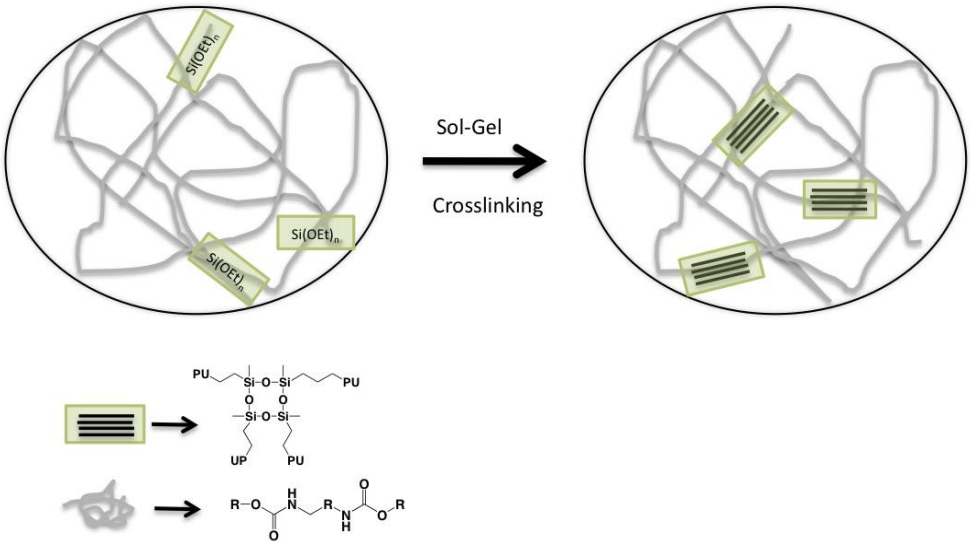

Figure 3.3. Sol-Gel curing process of WPU functionalized with alkoxysilane end-groups.

Following this approach, in this work room temperature self-curable waterborne polyurethane hybrid dispersions were obtained employing (3-aminopropyl) triethoxysilane (APTES) at different concentrations.

Nevertheless, in some cases the insertion of large amounts of alkoxysilane is not appropriate in terms of dispersion stability, mechanical, adhesion or transport properties. Therefore, inorganic moieties need to be inserted separately employing different polymerization techniques.[15-17,25-26,28,41,50-56]

The insertion of inorganic moieties into organic materials can be carried out following different routes. The ones selected in this work were the followings: a) direct blending of organic materials with inorganic nanoparticles and b) Sol-Gel nanocoating of WPU particles with tetraethoxysilane (TEOS).[45-47,57-58] In Figure 3.4 the two employed strategies are summarized. In the case of nanocoating covalently bonded polyurethane silica nanostructures and non-covalently bonded nanostructures were synthesized.

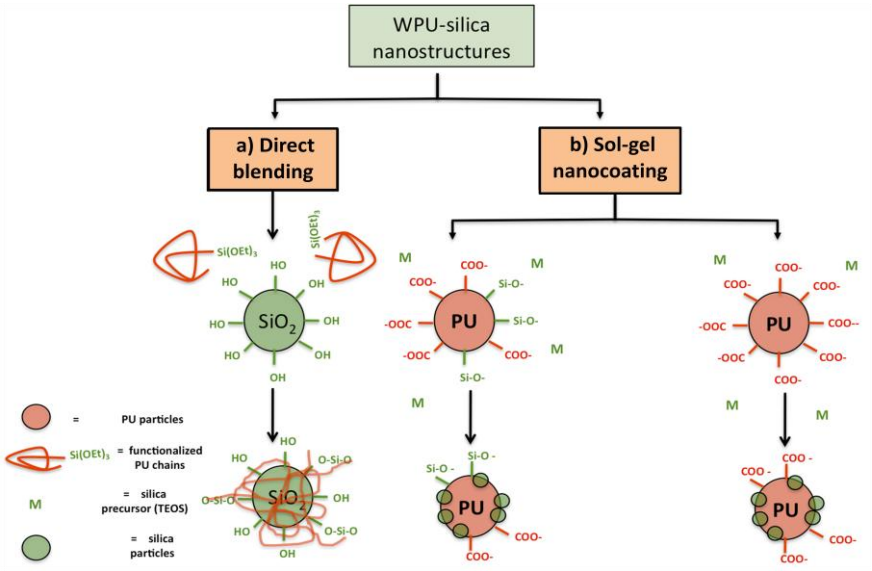

Figure 3.4. Different WPU/silica nanostructures synthesized in this work.

2. EXPERIMENTAL PART

2.1. Materials

2.1.1. Curing agent

In order to improve the compatibility of the organic phase towards the inorganic domains an amine type organosilane compound was incorporated into the polyurethane backbone. This compound is capable of curing at room temperature. As amine groups have higher reactivity towards the isocyanate than alcohol groups their reactions with isocyanate are almost instantaneous and do not require any catalyst. Therefore, amine type curing agents ensure the insertion of alkoxy groups, which are able to cure at room temperature. In this thesis the coupling agent employed was the (3-Aminopropyl)triethoxysilane (APTES). This compound was purchased from Aldrich and was characterized by ^{1}H-NMR (Figure 3.5) and FTIR before use.

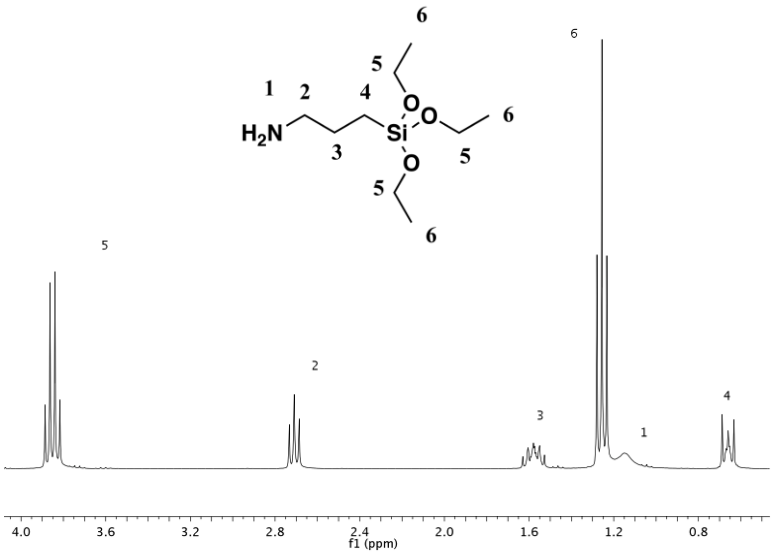

Figure 3.5. Structure and ^{1}H-NMR spectrum of APTES.

2.1.2. Pre-formed Silica materials

As already mentioned, the main challenge of this work was to obtain a good compatiblity between the organic and inorganic phases in order to promote a synergism effect in the final hybrid. In this thesis, silica from different sources was selected as the inorganic phase in order to study their effect on the colloidal features and films homogenity.

2.1.2.1. CAB-O-SIL

CAB-O-SIL M-5 untreated fumed silica is a synthetic, amorphous, silicon dioxide that is generally regarded as unique in industry because of its unusual particle characteristics. It has a small particle size (≈ 10 nm), which trend to aggregate forming particles of 200-300 nm. It has an enormous BET surface area (200$m^2.g^{-1}$) and its chain-forming tendency set it apart in a class of its own. CAB-O-SIL fumed silica is a light, fluffy white powder that it is used in many and great variety of applications. In Figure 3.6 a typical TEM image of CAB-O-SIL is shown. As observed in the ^{29}Si-NMR of spectrum (Figure 3.6) CAB-O-SIL is mainly composed by silicon atoms linked to three (Q_3) and four (Q_4) siloxane groups (see Annex I.)

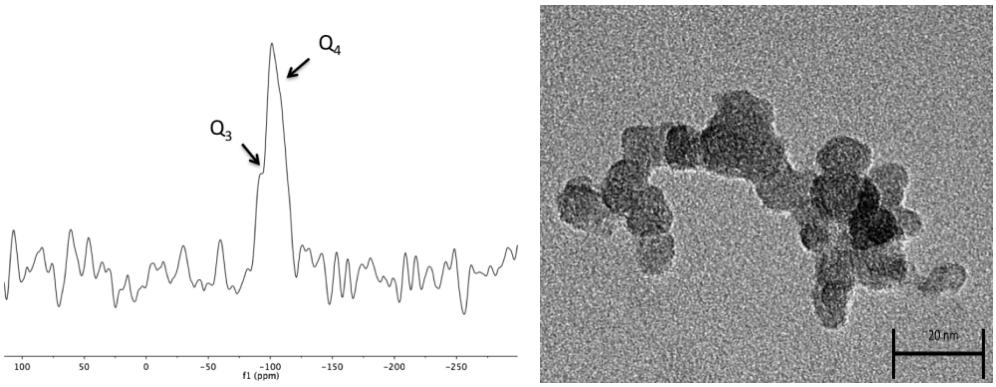

Figure 3.6. ^{29}Si-NMR spectrum and TEM image of commercial CAB-O-SIL.

2.1.2.2. KLEBOSOL

Klebosol colloidal silica are stable water suspensions of independent (or non-agglomerated) particles (SiO_2). A liquid-phase process is used to make silica particles grow, which are non-porous and spherical, resulting in a highly stable and homogeneous suspension. In this thesis 30 wt. % solid, 80 nm particle size (narrow) and 50 $m^2.g^{-1}$ surface area Klebosol was employed. Figure 3.7 shows a typical TEM image of Klebosol particles.

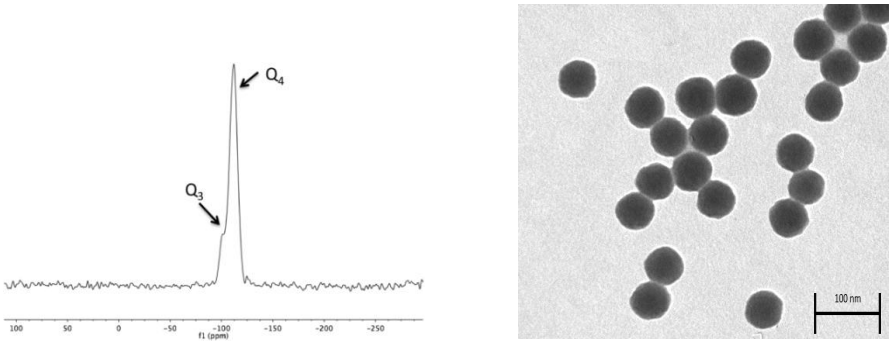

Figure 3.7. ^{29}Si-NMR spectrum and TEM image of commercial KLEBOSOL.

It is important to take into account that the reactivity of silica increases with the number of active sites, which is directly related to the specific surface area, which in terms exhibits an inversely proportional relationship with respect to particle size. Therefore, reactivity is improved in formulations containing smaller particle sizes. As shown Klebosol is also composed mainly by Q_3 and Q_4 structures, indicative of highly condensed silica nanostructures.

2.1.3. Inorganic precursor: Tetraethoxysilane (TEOS)

TEOS was employed as the inorganic precursor (Figure 3.8).

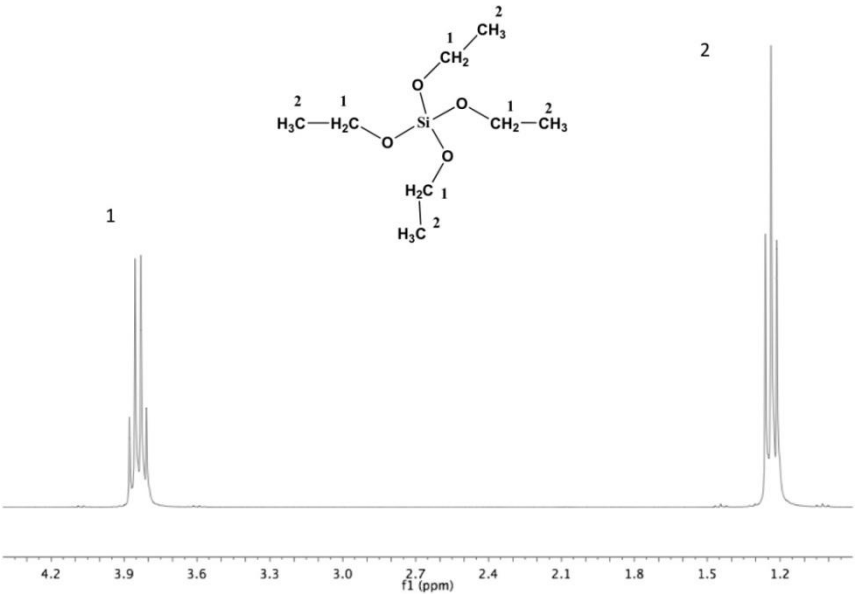

Figure 3.8. ^{1}H-NMR spectrum and chemical structure of TEOS.

This compound is one of the most employed inorganic precursors in order to form in-situ silica spheres. Its polymerization is highly dependent on external features such as temperature, water content and so on. Figure 3.8 shows the structure of TEOS and its ^{1}H-NMR spectrum.

2.2. Synthesis of alkoxysilane end-capped waterborne polyurethane dispersions using APTES

The preparation of the WPU hybrids was carried out in the same equipment as that of WPU-s. The process was divided into three main steps: 1) preparation of the polyurethane prepolymer, 2) functionalization of the prepolymer and 3) emulsification. In the preparation of the polyurethane prepolymer two sub-steps were carried out: In the first one the less reactive diols (DMPA+PBAD) were made react with the isocyanate, while in the second one the majority of the unreacted isocyanate groups reacted with the chain extender (BD), leaving some unreacted isocyanate groups.

In the functionalization step APTES reacted with the remaining free isocyanate groups, giving rise to an alkoxysilane-capped polyurethane. Finally, in the last step the dispersion process was carried out achieving the final self-curable water polyurethane dispersion (Scheme 3.1).

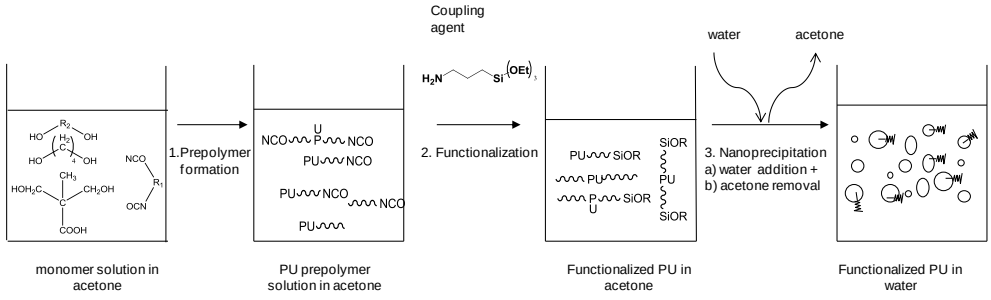

Scheme 3.1. Polymerization process for obtaining functionalized PU nanostructures.

2.2.1. Synthesis of the polyurethane pre-polymer

Polyol (PBAD) 45 g (45 mmol), internal emulsifier (DMPA) 3 g (22 mmol) and TEA 3 g (30 mmol), were fed into the flask reactor together with 400 ppm of DBTDA and 70 g of acetone. When the reaction temperature reached 60 °C, IPDI 25 g (113 mmol) was added drop wise at 1 mL.min^{-1}. The reaction was carried out for 3 hours and the isocyanate end-capped polyurethane prepolymer was obtained. Afterwards, the appropriate amount of

chain extender BD, to leave some unreacted isocyanate groups, was added. This second step was carried out for an additional 3 hours.

2.2.2. Functionalization of PU-s with the aminosilane

The reaction temperature was dropped to 25 °C and the desired amount of APTES, in order to complete the reaction, was introduced. The reaction was carried out for an additional hour, and it was periodically monitored by FTIR. The reaction was stopped when the infrared absorbance of the NCO groups (around 2260 cm^{-1}) was negligible.

2.2.3. Emulsification process

After PU-s functionalization, the temperature of the reactor was maintained at 25 °C and the mechanical stirring was raised to 400 rpm to help the dispersion process. Water (180 g) was added drop wise to the reactor at 3 $mL.min^{-1}$. After water addition, the stirring was kept at the same rate for an additional 30 minutes. Finally, acetone was removed using distillation equipment. The resulting dispersion contained 30-35 wt. % of solids. Scheme 3.2 shows the polymerization process of functionalized and non-functionalized polyurethanes.

2.3. Addition of inorganic moieties to waterborne polyurethanes

Two different strategies were followed in order to obtain the waterborne polyurethane/silica hybrid dispersions.

2.3.1. Direct blending

Waterborne polyurethane silica dispersions were obtained by means of the previously described "acetone-process". The preparation of polyurethane/silica dispersions, using CAB-O-SIL and Klebosol as inorganic filler, was divided into three main steps: a) synthesis of the functionalized polyurethane, b) addition of pre-formed silica and c) emulsification.

2.3.1.1. Addition of pre-formed silica

Pre-formed silica was added after concluding the polymerization process in acetone and before the water addition process. The polyurethane acetone ratio was kept at 60 wt. % in all cases. Preformed silica was added at this point and the stirring was raised to 400 rpm and maintained for 30 min. in order to promote the covalent linkage between the alkoxy groups coming form the functionalized PUs and the sylanol groups of the silica surface, before the emulsification process. CAB-O-SIL and Klebosol preformed silica were employed for both series of polyurethanes (PBAD and PPG based WPU-s) at two different concentrations in order to obtain systems containing 5 and 10 wt. % of preformed silica. Moreover, a small amount of distilled water was added (7g) to promote the hydrolysis of the alkoxy groups (in the case of KLEBOSOL the water content was adjusted taking into account that the silica particles were in aqueous medium). Table 3.1 shows the reagents amount used during the synthesis.

Name	f-WPU (g)	SiO_2 (g)	H_2O (g)
f-WPU+5 wt. % KLEBOSOL	30	1.5	3.5
f-WPU+10 wt. % KLEBOSOL	30	3.0	-
f-WPU+5 wt. % CAB-O-SIL	30	1.5	7.0
f-WPU+10 wt. % CAB-O-SIL	30	3.0	7.0

Table 3.1. Reagent amounts employed in the synthesis of different WPU/silica dispersions.

2.3.1.2. Emulsification process

Subsequently, water was added dropwise to the reactor (55-60 g) at 3 $mL.min^{-1}$ and afterwards, the stirring was kept at 400 rpm for an additional 30 minutes. Finally, acetone was removed using distillation equipment. The resulting dispersion had 30 wt. % of solids.

2.3.2. Sol-Gel nanocoating

Two types of organic inorganic structures were formed: the one so called WPU (without APTES) and the one called f-WPU (with 9.7 wt. % of APTES). The synthesis of WPU-s and f-WPU-s was carried out as described in the previous section. TEOS was added after the emulsification step was concluded. The whole polymerization is detailed in Scheme 3.2.

2.3.2.1. TEOS Sol-Gel process in the presence of WPU-s and f-WPU-s

TEOS was added to the polyurethane dispersion for obtaining polyurethane/silica nanostructures.

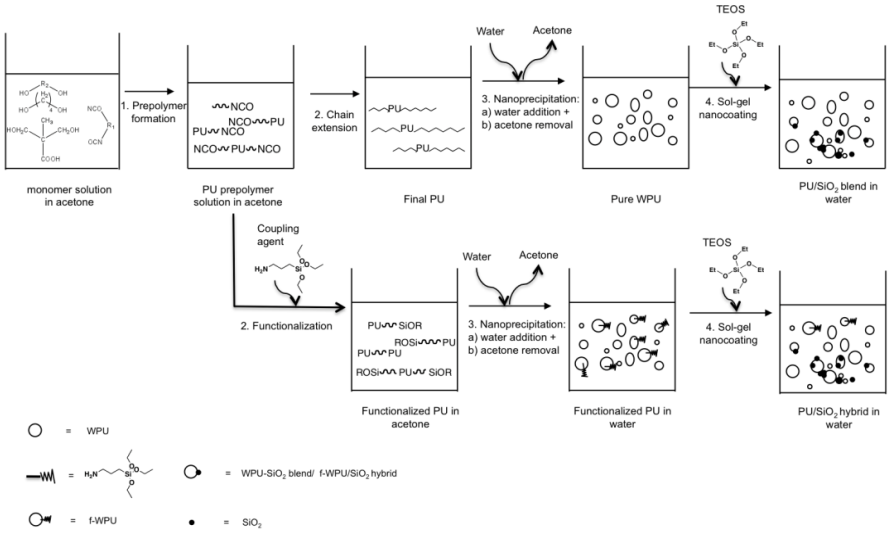

Scheme 3.2. Detailed polymerization process of WPU/silica and f-WPU/silica nanostructures obtained by the nanocoating process.

First of all, the solid content of the polyurethane dispersion was adjusted to 25 wt. % and an aliquot of 40 g of the dispersion was charged into the reactor. The different reaction conditions are shown in Table 3.2. The effect of the nature of the catalyst employed during the synthesis of polyurethane, Sol-Gel process temperature, TEOS concentration and TEOS addition method (one shot or drop wise at 0.70 $mL.h^{-1}$) on the Sol-Gel process was studied. Furthermore the DMPA content was also varied (using 0.20, 0.30 and 0.40 $mmol.g^{-1}_{pol}$) in order to study the effect of the starting particle size on the final dispersion

characteristics. All the samples were filtered and the coagulum content was determined gravimetrically after drying it.

Sample	Sol-Gel T (°C)	[TEOS] wt. %	Catalyst type	Polymerization Process	Stability	DMPA (mmol. g^{-1}_{pol})
WPU-0	75	0	DBTDA	-	Stable	0.3
WPU-1	25	13.1	DBTDA	Batch	Unstable	0.3
WPU-2	50	13.1	DBTDA	Batch	Stable	0.3
WPU-3	75	13.1	DBTDA	Batch	Stable	0.3
WPU-4	50	6.1	DBTDA	Batch	Stable	0.3
WPU-5	50	21.1	DBTDA	Batch	Unstable	0.3
WPU-6	50	13.1	$Zr(acac)_4$	Batch	Unstable	0.3
WPU-7	75	13.1	$Zr(acac)_4$	Batch	Unstable	0.3
WPU-8	75	6.1	DBTDA	Semi-Batch	Stable	0.3
WPU-9	75	13.1	DBTDA	Semi-Batch	Stable	0.3
WPU-10	75	21.1	DBTDA	Semi-Batch	Unstable	0.3
f-WPU-0	75	0	DBTDA	-	Stable	0.3
f-WPU-1	75	6.1	DBTDA	Semi-Batch	Stable	0.3
f-WPU-2	75	13.1	DBTDA	Semi-Batch	Stable	0.3
f-WPU-3	75	21.1	DBTDA	Semi-Batch	Stable	0.3
f-WPU-4	75	0	DBTDA	-	Stable	0.4
f-WPU-5	75	21.1	DBTDA	Semi-batch	Stable	0.4
f-WPU-6	75	0	DBTDA	-	Stable	0.2
f-WPU-7	75	21.1	DBTDA	Semi-batch	Stable	0.2

Table 3.2. Reagent amount and experimental conditions employed in the nanocoating process.

3. RESULTS

3.1. Characterization of alkoxysilane end-capped WPU-s

3.1.1. Chemical characterization of the different alkoxysilane end capped WPU-s

Most of the results shown in this chapter correspond to those obtained with PBAD based WPU systems. However, in the case of PPG based WPU-s the same trend was observed. According to this, the results of PPG based systems are only shown when they differ from those obtained with PBAD.

The silanized WPU-s synthesized using six different APTES concentrations (Table 3.3) were characterized by means of FTIR and NMR spectroscopies in order to evidence APTES insertion.

APTES (wt. %)	PBAD (mmol)	IPDI (mmol)	DMPA (mmol)	TEA (mmol)	APTES (mmol)	BD (mmol)
0	45	113	22	30	0	46
5.0	45	113	22	30	19	37
7.5	45	113	22	30	29	32
9.7	45	113	22	30	38	27
14.0	45	113	22	30	57	18
18.4	45	113	22	30	82	5

Table 3.3. Amount of reagents employed in the different reactions.

Figure 3.9 shows the infrared spectra of five of the systems synthesized. The presence of APTES can be confirmed by the appearance of a new band centred at 1100 cm^{-1}, attributable to Si-O-C stretching vibrations of alkoxy groups, and its insertion into the polymer chains by the shoulder at 1650 cm^{-1} and the broadening of the amide II band at 1550 cm^{-1}. These two new bands, whose intensities increase with APTES concentration, can be assigned to the carbonyl stretching and N-H bending vibrations of urea groups,

generated as a consequence of the reaction between isocyanate and APTES amine groups.

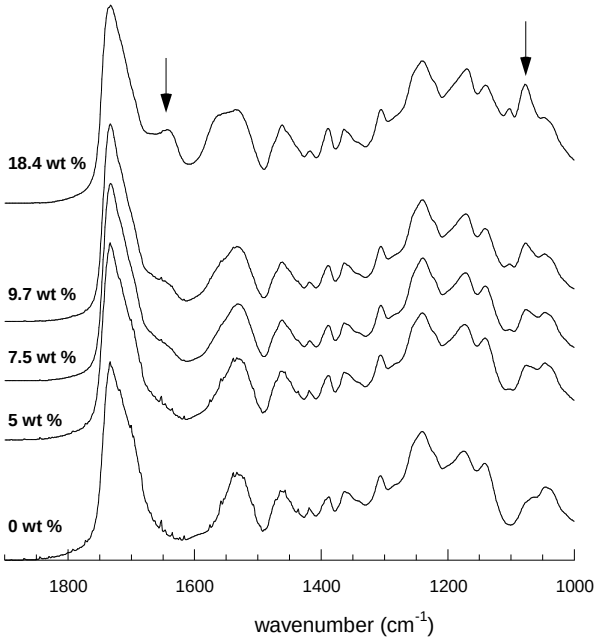

Figure 3.9. Scale expanded FTIR spectra of PBAD based polyurethanes with different APTES content.

As demonstrated in Figure 3.9, FTIR spectroscopy is a useful technique in order to obtain qualitative data about the insertion of the alkoxysilane into the polyurethane chains. Figure 3.10 shows the ^{1}H-NMR spectra of the polyurethanes obtained using different initial APTES concentrations.

As shown in Figure 3.10, the relative area of the signals at 0.6, 3.2 and 3.7 ppm (marked with an arrow in the 18.4 wt. % spectrum) increases with the alkoxysilane concentration. These signals can be assigned to the methylene groups linked to the silicon atom (Si-CH_2), to siloxane (Si-O-CH_2) and to urea groups (NHCONH-CH_2) respectively. The first two ones confirm the presence of alkoxysilane groups. In addition, the signal assigned to the methylene groups linked to urea groups (whose position shifts from 2.7 ppm in the pure

APTES to 3.2 ppm in the inserted APTES) confirms the chemical linkage between the polyurethane and the alkoxysilane.

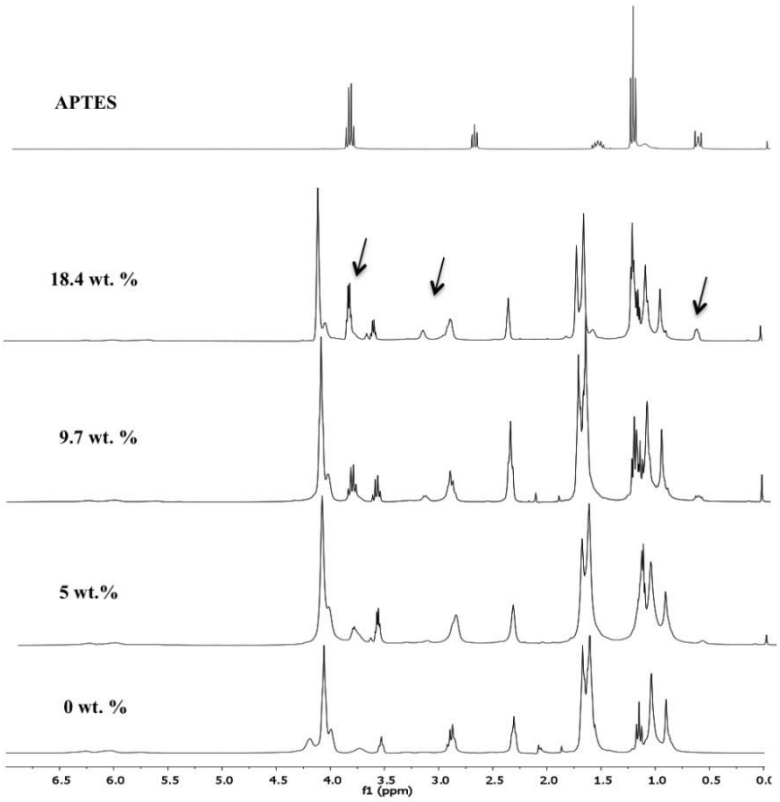

Figure 3. 10. ^{1}H NMR spectra of APTES and PU-s obtained with different initial APTES concentrations.

During the polymerization and functionalization processes, the final alkoxysilane groups can undergo condensation reactions. In order to make sure that this reaction did not occur before water addition, ^{29}Si-NMR studies were carried out to ascertain the exact structure of the silanized PU-s.

In Figure 3.11, the ^{29}Si spectrum of 9.7 wt. % APTES containing polyurethane is presented (all the functionalized polyurethanes showed the same signals). The main peak of the spectrum at -46 ppm is assigned to silicon atoms linked to three ethoxy groups and therefore without siloxane linkage (T_0) (the ^{29}Si-NMR nomenclature is explained in the

Annex I). Although some low signals attributable to hydrolyzed (Si-OH) and partially condensed alkoxy groups at -44 ppm and -53 ppm respectively are observed, the relative intensity of the T_0 signal suggests that the majority of the ethoxysilane groups are not condensed.

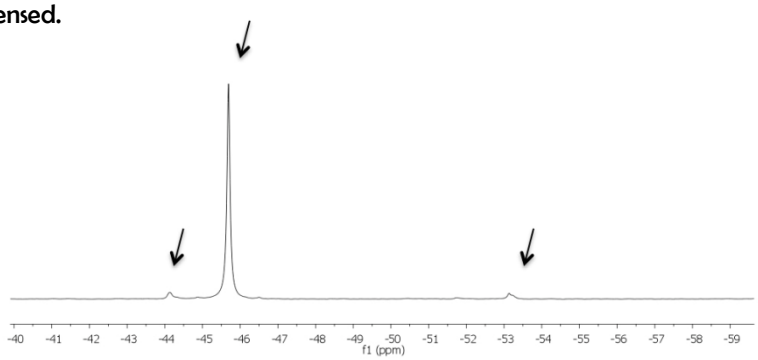

Figure 3.11. ^{29}Si NMR spectrum of a polyurethane functionalized with 9.7 wt. % of APTES.

Finally, elemental analysis measurements were carried out in order to quantify alkoxysilane incorporation in the polymer chains. These results are summarized in Table 3.4.

Si wt. %	5.0 wt. % APTES	9.7 wt. % APTES	18.4 wt. % APTES
Theoretical	0.6	1.3	2.4
Experimental	0.6	1.2	2.3

Table 3.4. Elemental analysis of four different polyurethanes.

The theoretical and experimental values are equal confirming the quantitative insertion of the curing agent into the polymer chains.

3.1.2. Effect of coupling agent (APTES) and internal emulsifier (–COOH) on the emulsification process

3.1.2.1. Effect of coupling agent (APTES) concentration

The presence of alkoxysilane end groups can change the particle size and the emulsion stability. In order to study this effect the final particle size after emulsification was

determined by DLS as a function of APTES concentration. In Figure 3.12 the final particle size as a function of the APTES concentration for PBAD and PPG based polyurethanes is depicted.

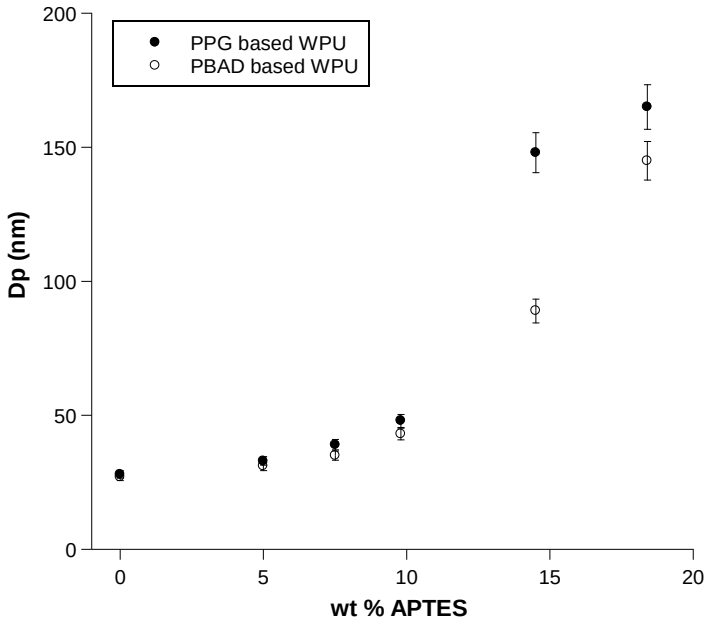

Figure 3.12. Particle size variation of silanized WPU dispersions for different curing agent concentrations.

As can be seen, at low APTES contents the mean particle size increases slightly with APTES concentration. However, this increase is much more pronounced at APTES concentrations above 10 wt. %.

It should bear in mind that as the curing agent content increases, the number of urea groups in the polymer chain increases and therefore the polymer becomes a polyurethane-polyurea system. Due to the less hydrophilic character of urea groups compared with urethane groups, at the same amount of functionalized diol, larger particle sizes are obtained, as previously reported by Song et al.[59] In addition, the higher number of Si(OEt) groups as we increase the alkoxysilane concentration, favours their

condensation at high pH, considerably affecting the particle size and the dispersion stability.

However, it was stated elsewhere[8,33,35,60] that the particle size of the dispersions is not affected by silylation. This was attributed to the small amount of APTES employed in the prepolymer preparation. Our results at low APTES concentration follow this behaviour and suggest that the small increase in particle size is due to the presence of a higher content of urea groups. Nevertheless, the large particle size increase observed at high APTES concentrations suggests that the condensation of alkoxysilane groups takes place during the phase inversion process, considerably affecting the particle size. Finally, the PPG based WPU-s present higher particle size values probably due to the lower affinity of PPG towards water.

3.1.2.2. Effect of the internal emulsifier (–COOH) content

As we described in the previous chapter the -COOH content has a great effect in terms of particle size and dispersion viscosity. Thus, working at large -COOH concentrations promotes the formation of smaller particle sizes whose stability and film formation characteristics are better with the counterpoint of an important increase of the dispersion viscosity, which can promote particle aggregation and instability.

In order to investigate the effect of –COOH content on the emulsification process, the synthesis of APTES (9.7 wt. %) containing WPU-s at different concentrations of acid groups (0.20 $mmol.g^{-1}_{pol}$, 0.30 $mmol.g^{-1}_{pol}$ and 0.40 $mmol.g^{-1}_{pol}$) was carried out. In Figure 3.13 the effect of COOH content on the final particle size for the system containing 9.7 wt. % APTES is shown. The system is compared with the pure polyurethane (without APTES).

As observed in both systems the particle size decreases with the COOH concentration. However, when using 9.7 wt. % of APTES for a given COOH concentration, the particle size is higher than the obtained without APTES. This result evidences that APTES promotes particle aggregation, probably due to the condensation reaction of alkoxysilane groups during the phase inversion.

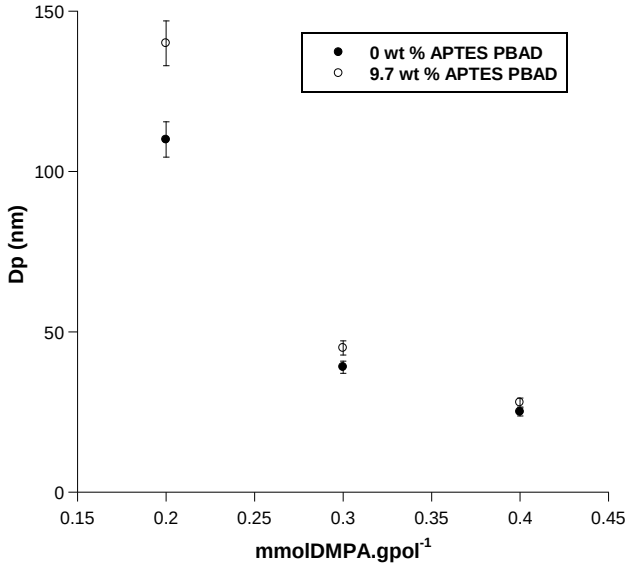

Figure 3.13. Particle size variation of silanized WPU dispersions for a system containing 9.7 wt. % APTES and pure polyurethane at diferent COOH concentrations.

3.1.3. Morphology of functionalized polyurethane particles

3.1.3.1. Effect of APTES content in the particle morphology

The morphology of the polyurethane dispersions was followed by TEM. The experimental conditions for sample preparation are depicted in Annex I. Figure 3.14 shows the photographs of the pure polyurethane and the polyurethane functionalized with 9.7 wt. % of APTES. For the pure polyurethane (left), the particle size distribution is broad. Although the mean particle size is around 30 nm, larger (100-200 nm) and smaller particles (5-10 nm) can be detected.

The sample containing 9.7 wt. % of APTES shows a narrower particle size distribution, more homogeneous than that of the pure polyurethane. The same stands true for the samples obtained with 5 and 7.5 wt. % APTES (images not shown).

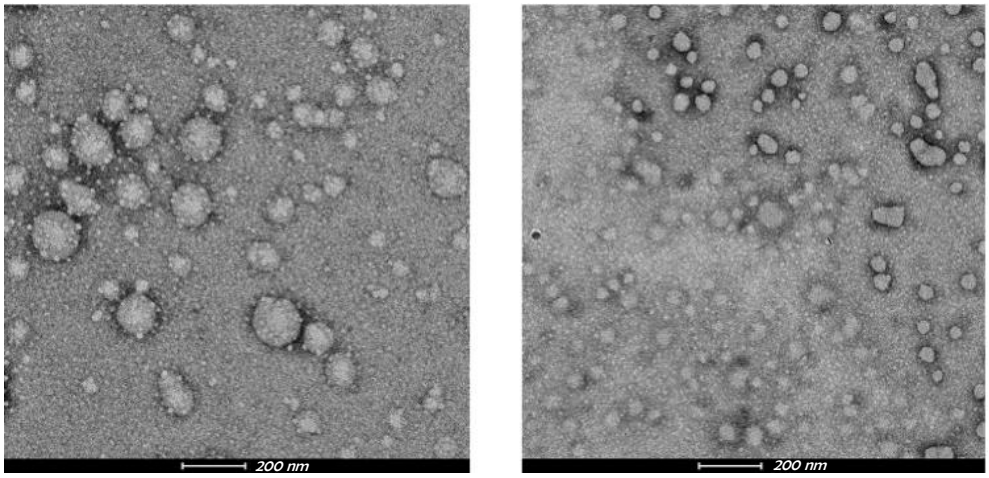

Figure 3.14. TEM images of diluted samples of pure polyurethane (left) and of 9.7 wt. % APTES-containing polyurethane (right) particles stained with PTA.

However, the inorganic domains cannot be detected by this technique, which is probably due to their small size. This fact confirms, in a certain way, that at low alkoxysilane concentrations the aggregation of the silica is negligible. On the contrary, when higher APTES concentrations (14 and 18.4 wt. %) are employed, this trend changes as can be observed in Figure 3.15.

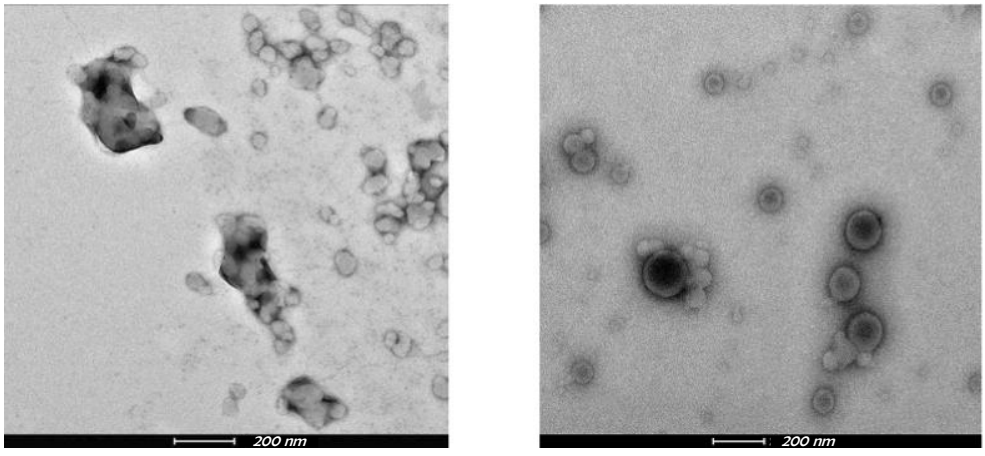

Figure 3.15. TEM images of diluted polyurethane samples containing 14 and 18.4 wt. % APTES, (left and right respectively) without PTA.

The high concentration of alkoxy groups significantly affects the morphology of the particles obtained. Due to the larger number of hydrolysable alkoxy groups, the condensation reaction can take place during the phase inversion process, creating inorganic-rich domains (Figure 3.15).

Thus, the system containing 14 wt. % of APTES presents hybrid morphologies where the inorganic domains can be easily identified as black zones, mainly located at the particle surface or entrapped within the hybrid aggregates. In the case of the system with 18.4 wt. % of alkoxysilane, core-shell type structures are obtained where the inorganic domains are mainly situated inside the PU particles. In our opinion, in these two last cases, the high concentration of APTES promotes the phase separation between the organic and inorganic domains, and therefore APTES concentration not only affects the particle size but also the particle morphology.

3.1.4. Effect of –COOH content in the morphology

The effect of the –COOH content was also studied by TEM. Figure 3.16 shows the photographs of the polyurethanes with 9.7 wt. % APTES containing 0.30 $mmol.g^{-1}_{pol}$ and 0.20 $mmol.g^{-1}_{pol}$ COOH (the image of the system with 0.40 $mmol.g^{-1}_{pol}$ is similar to the one containing 0.30 $mmol.g^{-1}_{pol}$).

As can be seen the morphology of these two systems is totally different. Thus, the system containing 0.20 $mmol.g^{-1}_{pol}$ COOH displays a core-shell type morphology, similar to the one observed for the system containing 18.4 wt. % APTES. In our opinion, the low concentration of –COOH reduces considerably the number of particles. This reduction increases the number of alkoxysilane groups per particle enhancing the partial condensation between alkoxysilane end-groups in the particles. As a consequence, larger inorganic domains are obtained in the case of polyurethanes containing 0.20 $mmol.g^{-1}_{pol}$ of DPMA than in the other two cases at higher concentrations.

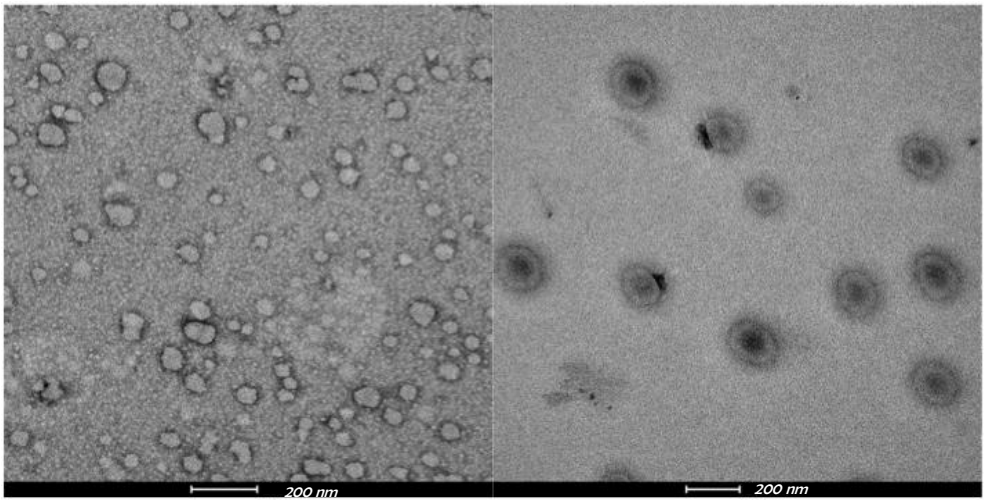

Figure 3.16. TEM images of diluted polyurethane samples containing 9.7 wt. % APTES and 0.30 mmol.g$^{-1}_{pol}$ (left) and 0.20 mmol.g$^{-1}_{pol}$ (right).

3.1.5. Particle surface characterization

The variation of the zeta potential as a function of pH for all the PU aqueous dispersions was determined to characterize the particle surface composition (Figure 3.17). The experimental conditions for carrying out the zeta potential measurements are depicted in Annex I. As can be observed, using low APTES concentrations (5-9.7 wt. %) the values of the zeta potential, in the whole pH range, are very close to those obtained for colloidal silica. This result suggests that in this range of concentration, silanol groups are located on the surface of the polyurethane particles, which exhibit consequently the same behaviour as colloidal silica. However, when 18.4 wt. % of APTES is employed, the zeta potential in the whole pH range is closer to that of the pure polyurethane dispersion. This result indicates that at this concentration, the surface of the particles is mainly covered by carboxylate groups present in the polyurethane chains. Therefore, at high APTES concentrations, most of the alkoxy groups condense during the phase inversion process reducing the expected number of silanol groups distributed on the surface. Therefore, the silanized PU dispersion has in this case almost the same isoelectric point (the point where the z potential is 0) as the pure PU. These results are in good agreement to those obtained by TEM.

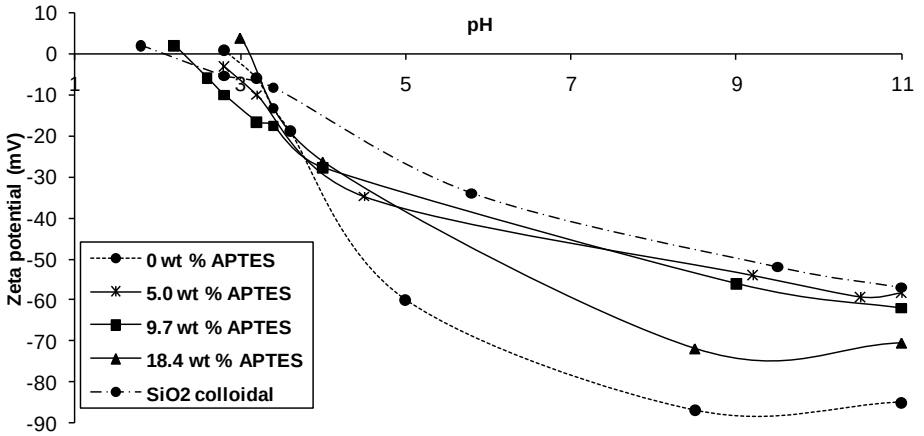

Figure 3.17. Zeta potential vs. pH of colloidal silica and different PU dispersions.

3.1.6. Curing process of the alkoxysilane end-capped PU dispersions

FTIR spectra of the sample containing 18.4 wt. % of APTES, before (when it is in acetone) and after curing at room temperature, are shown in Figure 3.18.

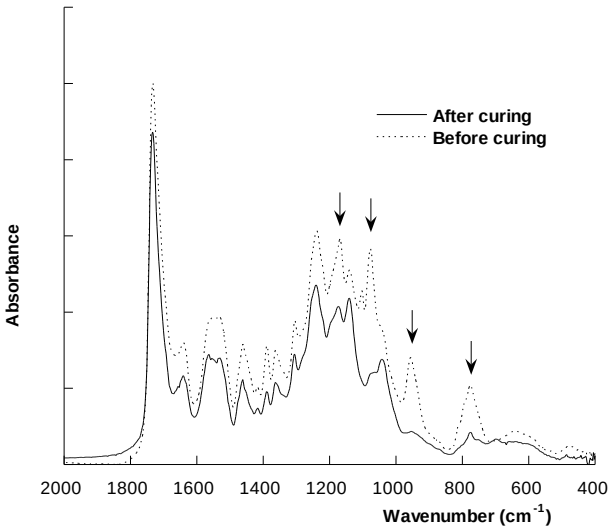

Figure 3.18. Scale expanded FTIR spectra of polyurethanes containing 18.4 wt. % of APTES obtained before and after curing for 48 hours at room temperature.

Absorptions related to the alkoxysilane groups are ≈1170 cm^{-1} (Si-O-C rocking), ≈1100cm^{-1} (νa(C-C+C-O)), ≈960 cm^{-1} (δ(CCH_3)) and ≈790 cm^{-1} (ν(Si-O+C-O)). These absorptions can be clearly seen in the spectrum obtained before curing. However, when the curing reaction takes place, the alkoxysilane groups undergo hydrolysis and condensation reactions, giving rise to a decrease in the intensity of the band corresponding to the alkoxysilane groups and an increase in the intensity of the bands of silica (≈1066 cm^{-1} νa(Si-O-Si)).

Moreover, ^{29}Si NMR studies were carried out to determine the structure of the alkoxy groups in the final polyurethane films after drying at room temperature for a minimum of 48 hours. In Figure 3.19, the ^{29}Si solid-state NMR spectra of four PU films cured with different curing agent concentrations are represented.

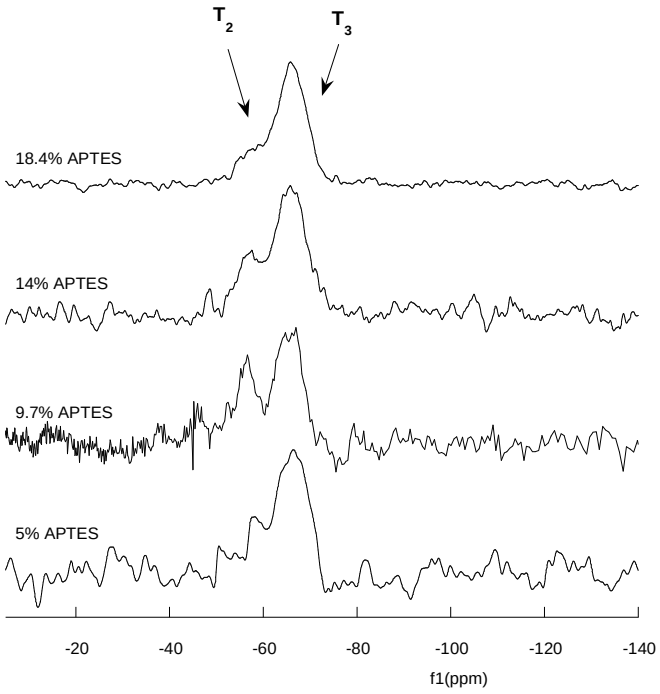

Figure 3. 19. ^{29}Si solid-state NMR spectra of polyurethanes functionalized with different APTES concentrations and cured at room temperature.

Two signals are observed in all the ^{29}Si NMR spectra at approximately -55 and -66 ppm. They represent silicon atoms with two (T_2) and three (T_3) siloxane linkages, respectively, while there is no evidence of any signal associated to T_1 or T_0 structures indicating that the condensation reactions have been almost completed. However, as the APTES concentration increases, the contribution of T_3 type structures increases, suggesting that the condensation degree is enhanced at high APTES concentrations.

Finally, in order to determine the degree of crosslinking, the gel content was calculated as a function of APTES content, curing temperature and soft segment nature.

Five different dispersions based on PBAD were self-cured at two different temperatures for 48 hours. Afterwards the gel content was quantified determining the soluble part of each of them. The gel content is defined as the fraction of polymer that is not soluble in a good solvent (in this case THF) at reflux temperature. In this work the gel content was determined by Soxhlet extraction following this expression:

Gel content = 100(weight after extraction)/(weight before extraction) (Figure 3.20)*

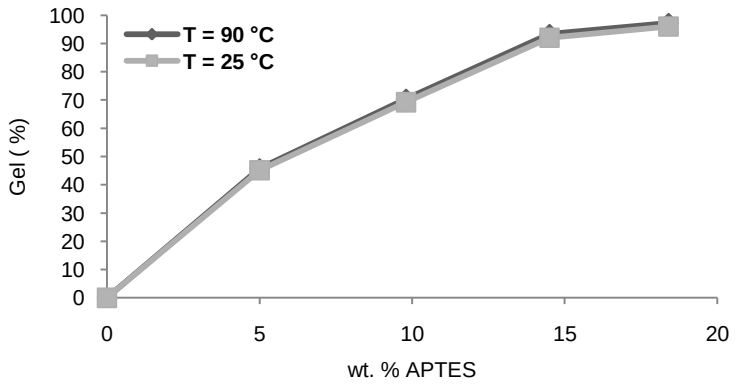

Figure 3.20. Gel content for different dispersions dried at two different temperatures for 48h.

As observed, the gel content considerably increases with the APTES concentration, reaching a plateau at concentrations above 14 wt. % of APTES where the gel content is almost 100 %. This result is expectable due to the higher ability of the system to crosslink as the APTES concentration is increased. Furthermore, at the same APTES concentration

the gel content does not change with the drying temperature. This result confirms that the functionalized polyurethanes are self-curable at room temperature, as has been previously stated for similar systems.[22,59] A similar behaviour was observed in the case of PPG based systems.

3.2. Addition of different inorganic moieties to waterborne polyurethanes

As mentioned through this manuscript two different strategies were employed in order to insert inorganic moieties into the waterborne polyurethanes. In the first one the inorganic compound was just blended with the PU whereas in the second, TEOS was added with the purpose of promoting the covalent linkages with the polymer backbone through the alkoxysilane precursor.

3.2.1. Direct blending

3.2.1.1. Effect of preformed silica in the emulsification process

Pre-formed silica was added before the water addition process for both polyurethane systems (PBAD and PPG based WPU-s). The formed silica was added at this step because being the polyurethane chains in solution, the reaction between the alkoxysilane end-groups of polyurethane chains and silanol groups on the surface of silica particles could take place easier. The effect of pre-formed silica on the final mean particle size (Dp), polydispersity index (P.I.) and dispersion stability is shown (Table 3.5) for the system based on PBAD (the same tendency was observed in the case of PPG).

As shown in Table 3.5, there is an important effect of preformed silica on the final dispersion characteristics. The mean particle size increases sharply as the CAB-O-SIL and Klebosol content is increased. This increase is more pronounced in the case of CAB-O-SIL, probably due to the ability of this type of silica to aggregate forming large particles ($>$ 1μm). As a consequence, these dispersions trend to sediment in a short period of time although they can be redispersed by shaking. In the case of KLEBOSOL, similar behaviour

was observed. Moreover, in all the cases the P.I. increases considerably, probably due to the addition of the inorganic particles of different size and the formation of large aggregates.

Silica content	Dp (nm)	P.I.	Stability
0	45±2	0.18	STABLE
5 wt. % CAB-O-SIL	96±5	0.35	STABLE
10 wt. % CAB-O-SIL	168±12	0.59	PARTIAL-SEDIMENTATION
5 wt. % KLEBOSOL	49±4	0.33	STABLE
10 wt. % KLEBOSOL	79±10	0.44	PARTIAL-SEDIMENTATION

Table 3.5. Particle size, polidispersity index and dispersion stability for functionalized WPU-s containing different CAB-O-SIL and KLEBOSOL concentrations.

In addition, TEM images of the dispersions were obtained to have a more accurate idea about the dispersion characteristics. Figure 3.21 shows the TEM images of the dispersion containing 10 wt. % of CAB-O-SIL. Silica trends to aggregate forming in some cases large aggregates (right) and in other cases smaller silica domains (left).

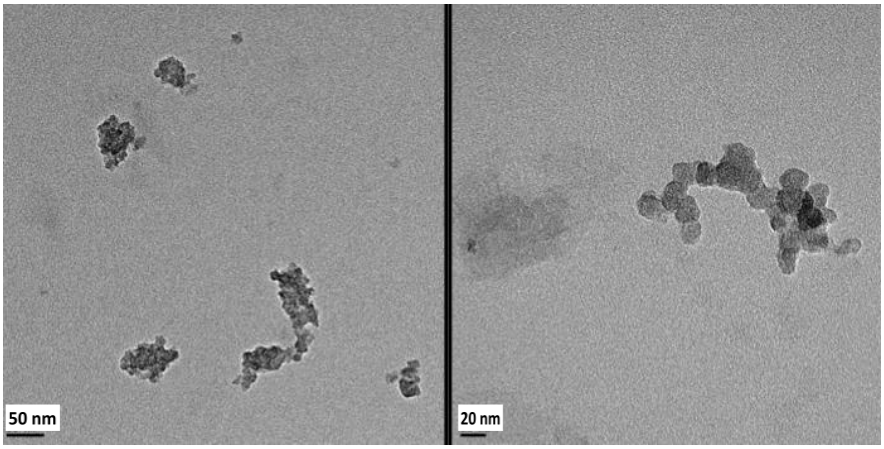

Figure 3.21. TEM images of dispersions with 10 wt. % CAB-O-SIL.

This result fits with the high P.I. determined by light scattering because different particles sizes can be obtained depending on the length of the aggregates.

Moreover, dispersions containing 10 wt % of KLEBOSOL were analyzed by TEM. As shown in Figure 3.22. only KLEBOSOL particles are observed in the image, where no silica aggregates can be evidenced.

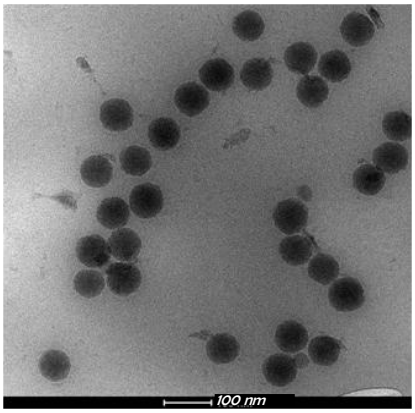

Figure 3.22. TEM images of dispersions containing 10 wt. % KLEBOSOL.

2.3.2.2. Effect of pre-formed silica on the final films

The morphology of the final hybrid films obtained after drying at room temperature the dispersions containing 10 wt % of CAB-O-SIL and KLEBOSOL respectively is studied in this section.

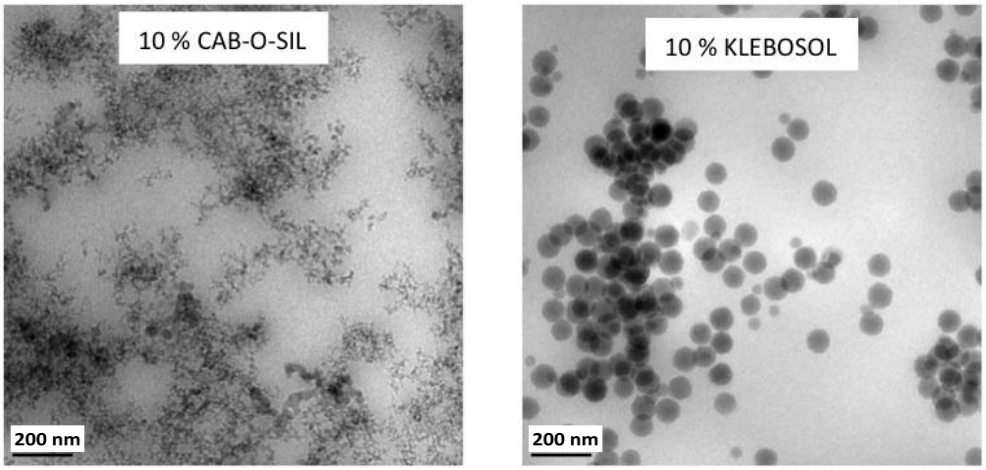

Figure 3.23. TEM images of films dried at room temperature containing 10 wt % of CAB-O-SIL and KLEBOSOL.

TEM images of the films obtained using both commercial silica systems are shown in Figure 3.23. As can be seen, the homogeneity of the films obtained by physical blending is fairly poor.

3.2.2. Sol-Gel nanocoating

All the studies reported in this section were obtained using PBAD as soft segment.

3.2.2.1. Preliminary study for TEOS Sol-Gel process in the presence of WPU particles

During the achievement of PU/silica hybrid dispersions using TEOS as inorganic precursor, ethanol is liberated as a consequence of the Sol-Gel reaction. The quantity of the released ethanol can be determined by means of Gas Liquid Chromatography (GC). In a simple way, if the ethanol amount can be related to the condensation rate, then it is possible to compare the conversion degree of the different systems. The procedure to calculate the conversion is depicted in Annex I.

Figure 3.24 shows the conversion (%) measured by GC as a function of time for the systems polymerized at different temperatures 25 °C (WPU-1) , 50 °C (WPU-2) and 75 °C (WPU-3).

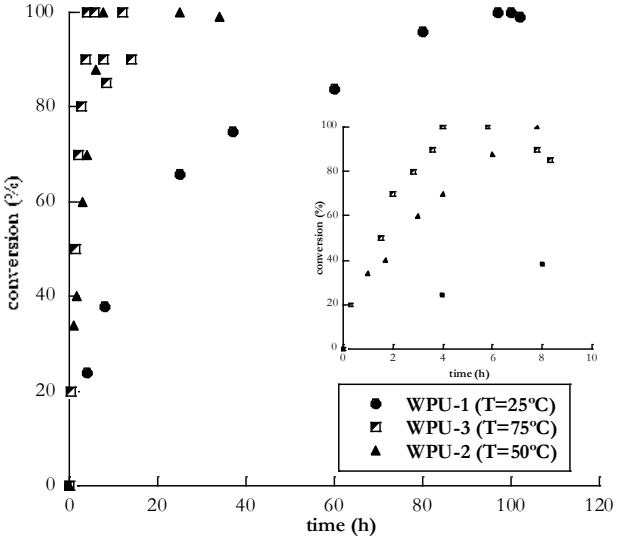

Figure 3.24. Conversion (%) as a function of time for systems WPU-1, WPU-2 and WPU-3 polymerized at three different temperatures.

The condensation rate increases with polymerization temperature and the maximum conversion is observed at shorter times. When TEOS was polymerized at room temperature in the presence of WPU particles, the maximum conversion was obtained at 95 hours although the dispersion was unstable. However, employing higher temperatures stable dispersions were obtained and the maximum conversion time was reduced considerably (8 and 4 hours at 50 °C and 75 °C respectively). Finally, the decrease of the conversion observed at 75 °C after 5 hours can be attributed to ethanol evaporation during the experiment.

In addition, in order to study the effect of the reaction temperature on the condensation degree, solid ^{29}Si NMR spectra of the dried products (WPU-1, WPU-2 and WPU-3) were registered (Figure 3.25).

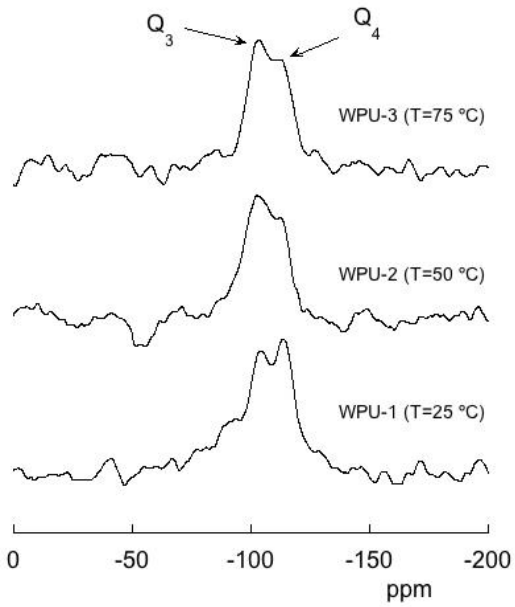

Figure 3.25. CPMAS ^{29}Si-NMR scale expanded spectra of WPU-1, WPU-2 and WPU-3.

Using the Qn notation for describing the chemical environment around Si atom, Q_3 (around -100 ppm) and Q_4 (around -110 ppm) species are observed. It should be taken into account that the relaxation time of Q_4 structures is different to the other species and therefore the condensation grade of Q_4 containing structures can not be determined using CP-MAS[61]. However, this technique allows us to compare the condensation grade of

different systems provided the experiment is carried out at under the same conditions. As shown in Figure 3.25 more condensed structures are obtained when TEOS is polymerized at low temperatures. This result was not expected because, as described in the previous section, the condensation rate increases with temperature. In our opinion, at high temperatures the TEOS polymerization rate was so high that the inorganic network could entrapped some unreacted silanol groups, and as a consequence, total condensation was not achieved and mainly Q_3 structures were obtained.

Another parameter affecting the polymerization rate is the initial TEOS concentration. In order to study this parameter the evolution of the conversion with time for samples containing 6.1 wt. % TEOS (WPU-2), 13.1 wt. % TEOS (WPU-4) and 21.1 wt. % TEOS (WPU-5) is compared (Figure 3.26).

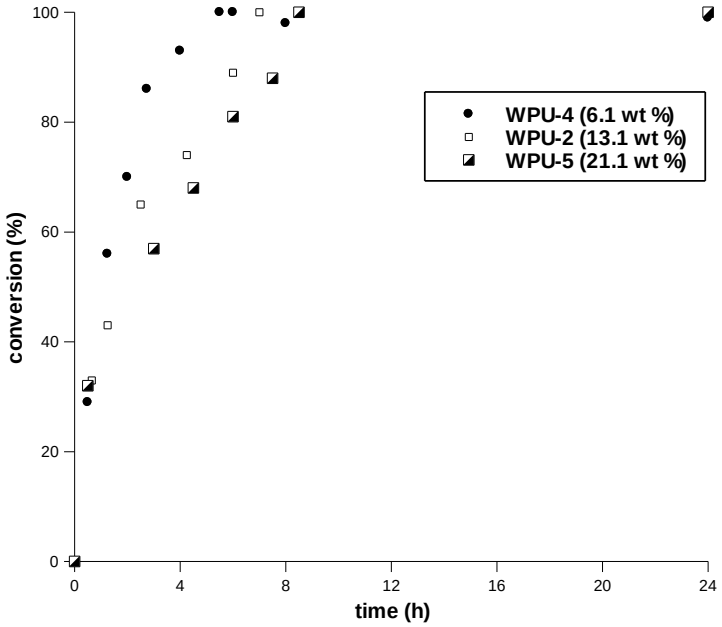

Figure 3.26. Conversion (%) vs. time for the systems WPU-2, WPU-4 and WPU-5 at 50°C.

As can be seen, as TEOS concentration increases the time to reach the maximum conversion increases (5, 7 and 10 hours for 6.1, 13.1 and 21.1 wt. % of TEOS respectively). As TEOS concentration is raised, the condensation rate slows down and the stability of the samples is reduced. We suggest that this occurs because at high TEOS concentrations the

viscosity of the system increases abruptly probably due to the tendency of the alkoxy silane compounds to form gels in water.

^{29}Si NMR spectra of WPU-4 and WPU-5 were similar to the spectrum of WPU-2 shown in Figure 3.25. Therefore, the TEOS concentration did not affect the condensation grade.

In addition to the reaction temperature and TEOS initial concentration, the effect of catalyst chemical nature was also studied. Although the catalytic effect of tin compounds on the Sol-Gel process has been reported in literature[62], there are no references about the effect of $Zr(acac)_4$. In order to investigate the catalytic effect of both organocatalytic compounds WPU-2, WPU-3, WPU-6 and WPU-7 were employed. In Figure 3.27 the Sol-Gel process conversion (%) measured by GC as a function of time for both catalysts at two different temperatures is shown.

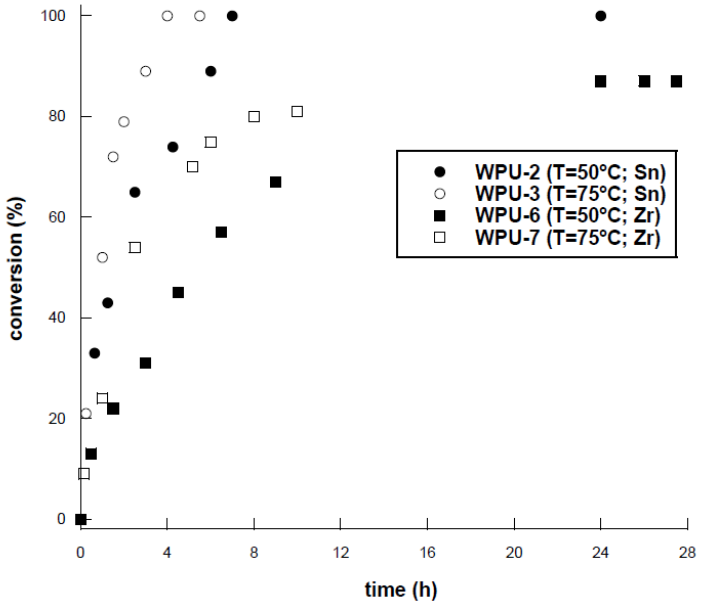

Figure 3.27. Conversion as a function of time for WPU-2, WPU-3, WPU-6 and WPU-7.

As can be observed in Figure 3.27 the catalyst has a great effect on TEOS polymerization process. When zirconium catalyst was employed, the polymerization rate was considerably reduced and total conversion was not achieved (80-85 %). Furthermore the systems polymerized in the presence of zirconium were unstable. In our opinion the

zirconium catalyst did not activate the Sol-Gel reaction, reducing the condensation rate comparing to tin catalyst. In addition, the lower condensation rate promotes TEOS evaporation before completing the Sol-Gel process, reducing the maximum conversion at both temperatures.

The effect of the catalyst employed was also studied by ^{29}Si NMR, by means of two samples obtained under the same experimental conditions but with different catalyst WPU-3 (with DBTDA) and WPU-7 (with $Zr(acac)_4$) (Figure 3.28).

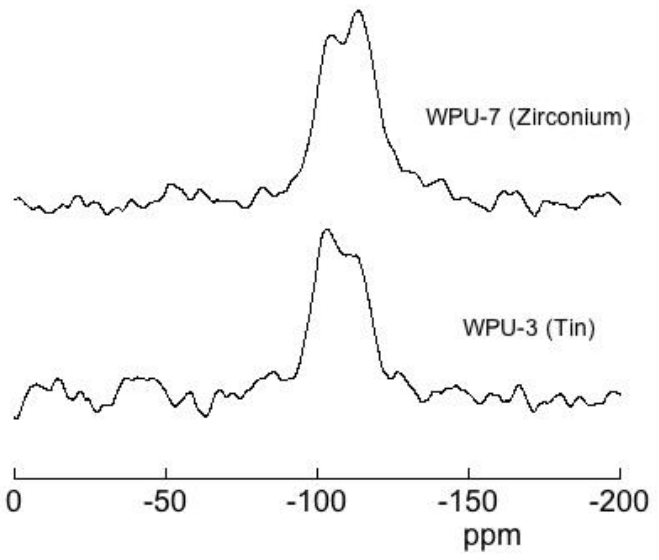

Figure 3.28. CPMAS ^{29}Si-NMR scale expanded spectra of WPU-3 and WPU-7.

As shown in Figure 3.28 more condensed structures are observed when TEOS was polymerized with zirconium catalyst. Although the condensation rate was lower, the same behaviour was observed when studying the effect of temperature, obtaining higher condensed structures at lower condensation rates. This fact was attributed to the unreacted silanol groups trapped inside the inorganic network. Similar results were observed for samples WPU-2 (DBTDA at 50 °C) and WPU-6 ($Zr(acac)_4$ at 50 °C).

All the experiments, shown so far, were performed adding TEOS under batch conditions. In order to promote the deposition of TEOS onto the surface of the WPU particles some experiments were carried out adding TEOS dropwise at 0.7 $mL.h^{-1}$ (semi-batch). For this

purpose the ^{29}Si-NMR spectra of samples obtained from experiments WPU-3 (batch) and WPU-8 (semi-batch) were compared (Figure 3.29).

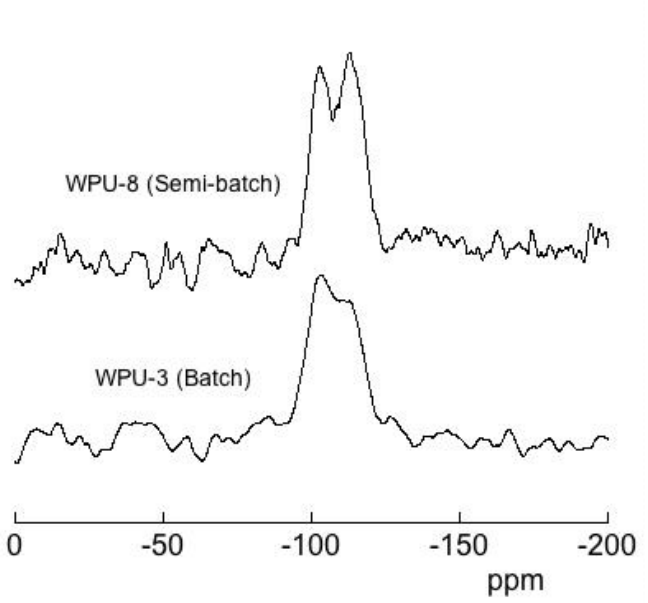

Figure 3.29. CPMAS ^{29}Si-NMR scale expanded spectra of samples WPU-3 and WPU-8.

Under semi-continuous polymerization conditions higher conversion grades were obtained. In our opinion this fact occurs because during the whole polymerization process TEOS concentration is low, avoiding the trapping of silanol groups in the inorganic network.

Therefore, it can be concluded that in order to obtain large condensation graded stable dispersions, low TEOS concentration and high condensation rate are required. According to these results, the best experimental conditions that fulfill these requirements are the following: tin catalyst and high condensation temperatures (75 °C).

3.2.2.2. Synthesis of WPU/f-WPU silica nanostructures

Using the best conditions established in the previous section, different amounts of TEOS were polymerized in the presence of non-functionalized (WPU) and functionalized (f-WPU) polyurethane particles. The particle size distribution together with the stability

of non-functionalized and functionalized final dispersions were studied by means of DLS and Turbiscan (Table 3.6). A description of the experimental conditions used in the synthesis of all samples is summarized in Table 3.2.

Sample	SiO_2 The. wt. %	SiO_2 Exp. Wt. %	Dp (nm)	P.I.	Coagulum wt. %	Stability
WPU-0	0.0	0.0 ± 0.3	29±1	0.15	0	Stable
WPU-8	2.0	1.6 ± 0.2	42±3	0.19	2±1	Stable
WPU-9	4.2	3.7 ± 0.1	58±5	0.33	6±1	Stable
WPU-10	7.2	6.6 ± 0.3	61±10	0.43	8±1	Non Stable
f-WPU-0	2.8	2.4 ±0.2	42±1	0.12	0	Stable
f-WPU-1	4.8	4.3 ± 0.3	50±2	0.17	< 1	Stable
f-WPU-2	6.0	6.1 ± 0.1	63±2	0.22	2±2	Stable
f-WPU-3	10.0	10.0 ± 0.1	98±4	0.25	5±1	Stable

Table 3.6. Theoretical and experimental silica content, particle size, polidispersity index, coagulum weight and dispersion stability, for non-functionalized (WPU) and functionalized (f-WPU) samples.

All the non-functionalized samples were stable except the one containing the largest TEOS concentration, whereas, in the case of functionalized samples all dispersions were stable. In our opinion this fact occurs because presumably the functionalized polyurethane particles have a higher affinity towards TEOS than non functionalized particles.

In addition, the increase of TEOS amount makes the coagulum content together with particle size and polydispersity index increase for both type of systems. This increase in the particle size can not be explained assuming that TEOS is totally covering the polyurethane particles. Following the expression proposed by Bourgeat Lami et al.[58] the increase in the diameter of the coated particles for all the cases must be close to 1 nm. Therefore in our opinion silica generated from TEOS promotes particle aggregation increasing the mean particle size, polydispersity index as well as coagulum size.

The silica content of the final products was experimentally determined from the residual weight value after TGA analysis and compared with the theoretical one assuming total

conversion. As observed in Table 3.6, the theoretical and experimental values are identical.

In Figure 3.30 FTIR spectra of WPU-0 and 21.1 wt. % of TEOS (WPU-10) on the left and two functionalized systems without TEOS (f-WPU-0) and with 21.1 wt. % of TEOS (f-WPU-3) on the right, are shown.

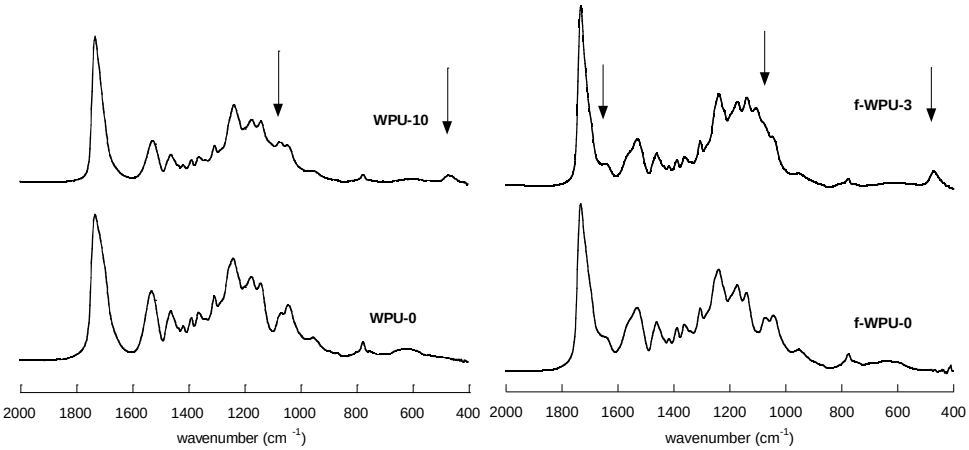

Figure 3.30. Scale expanded infrared spectra of samples WPU-0 and WPU-10 (left) and f-WPU-0 and f-WPU-3 (right) cured films.

The increase of silica bands at 1066 cm^{-1} and 470 cm^{-1} νa (Si–O–Si), confirms that the polymerization reaction of TEOS in the presence of WPU particles takes place. The only difference observed between both types of systems is the presence of a shoulder at 1650 cm^{-1} in the functionalized systems, assigned to the carbonyl stretching of urea groups, generated as a consequence of the insertion of the coupling agent.

In order to know the structure of Si atoms present in the final products ^{29}Si-NMR studies were carried out. In Figure 3.31 ^{29}Si-NMR spectra of the f-WPU-0 and f-WPU-3 (before and after TEOS addition) are shown.

Using the Tn notation for describing the chemical environment around Si atom, T_2 (around -55 ppm) and T_3 (around -66 ppm) species were observed before TEOS addition. After TEOS addition Q_3 (around -100 ppm) and Q4 (around -110 ppm)

structures were observed together with the previously mentioned T structures. Moreover, the intensity of T_2 structures decreased, probably due to the reaction between the two inorganic precursors.

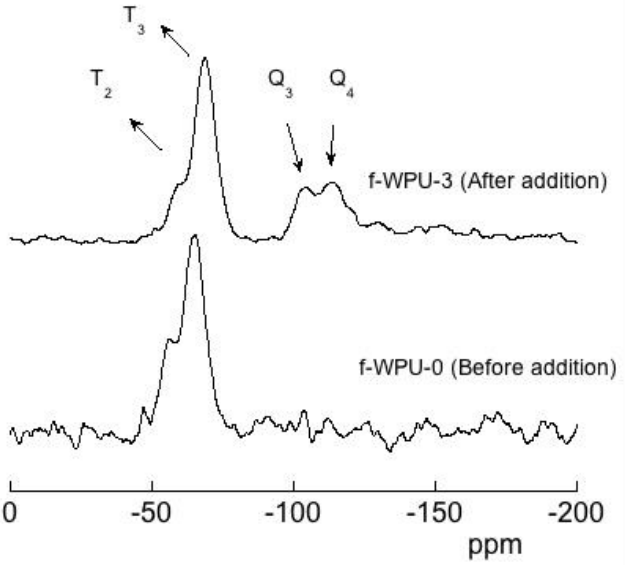

Figure 3.31. CPMAS ^{29}Si-NMR scale expanded spectra of samples f-WPU-0 and f-WPU-3.

3.2.2.3. Comparison between nanostructures obtained using functionalized polyurethane particles with different DMPA contents

In order to establish the influence of PU particle size on TEOS polymerization, three systems were polymerized starting from functionalized polyurethanes particles (9.7 wt. % APTES) and containing 0.20 mmol.DMPA.g^{-1}_{pol} (f-WPU-7), 0.30 mmol.DMPA.g^{-1}_{pol} (f-WPU-3) and 0.40 mmol.DMPA.g^{-1}_{pol} respectively. As previously stated, varying the DMPA content, the particle size can be fixed. In Figure 3.32 the particle size variation during the polymerization process is shown.

The systems containing 0.30 mmol.DMPA.g^{-1}_{pol} and 0.40 mmol.DMPA.g^{-1}_{pol} show an important increase in the particle size due to the particle aggregation. However, in the case of 0.20 mmol.DMPA.g^{-1}_{pol} particle size remains constant as a function of time indicating that TEOS did not create any particle aggregation. In our opinion this

behaviour can be attributed to the lower viscosity of this system comparing with the other two.

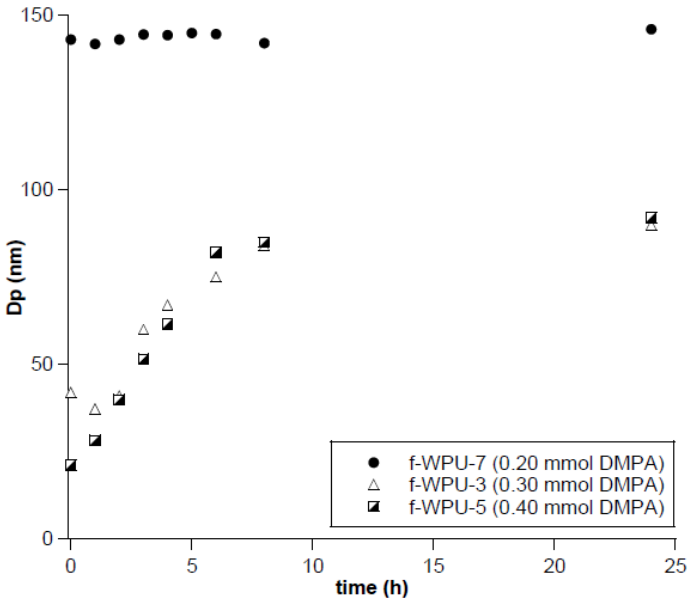

Figure 3.32. Particle size variation during the polymerization process of TEOS using different DMPA concentrations.

TEM images of dispersions before and after TEOS addition are shown in Figure 3.33. The dispersions were studied without PTA, in order to facilitate the detection of silica domains. Before TEOS addition, the dispersion containing 0.20 mmol.DMPA.g^{-1}_{pol} displays core-shell type morphology due to the lower content of acid groups. After TEOS addition isolated silica particles are distributed in the dispersion. It should be stress that there is not any interaction between the two types of silica.

However, the systems containing 0.30 and 0.40 mmol.DMPA.g^{-1}_{pol} before TEOS addition present a homogeneous morphology and after TEOS addition the silica domains are located on the surface of the functionalized polyurethane particles. In our opinion, the number of remaining alkoxy groups increases with DMPA content promoting their interaction with those of TEOS.

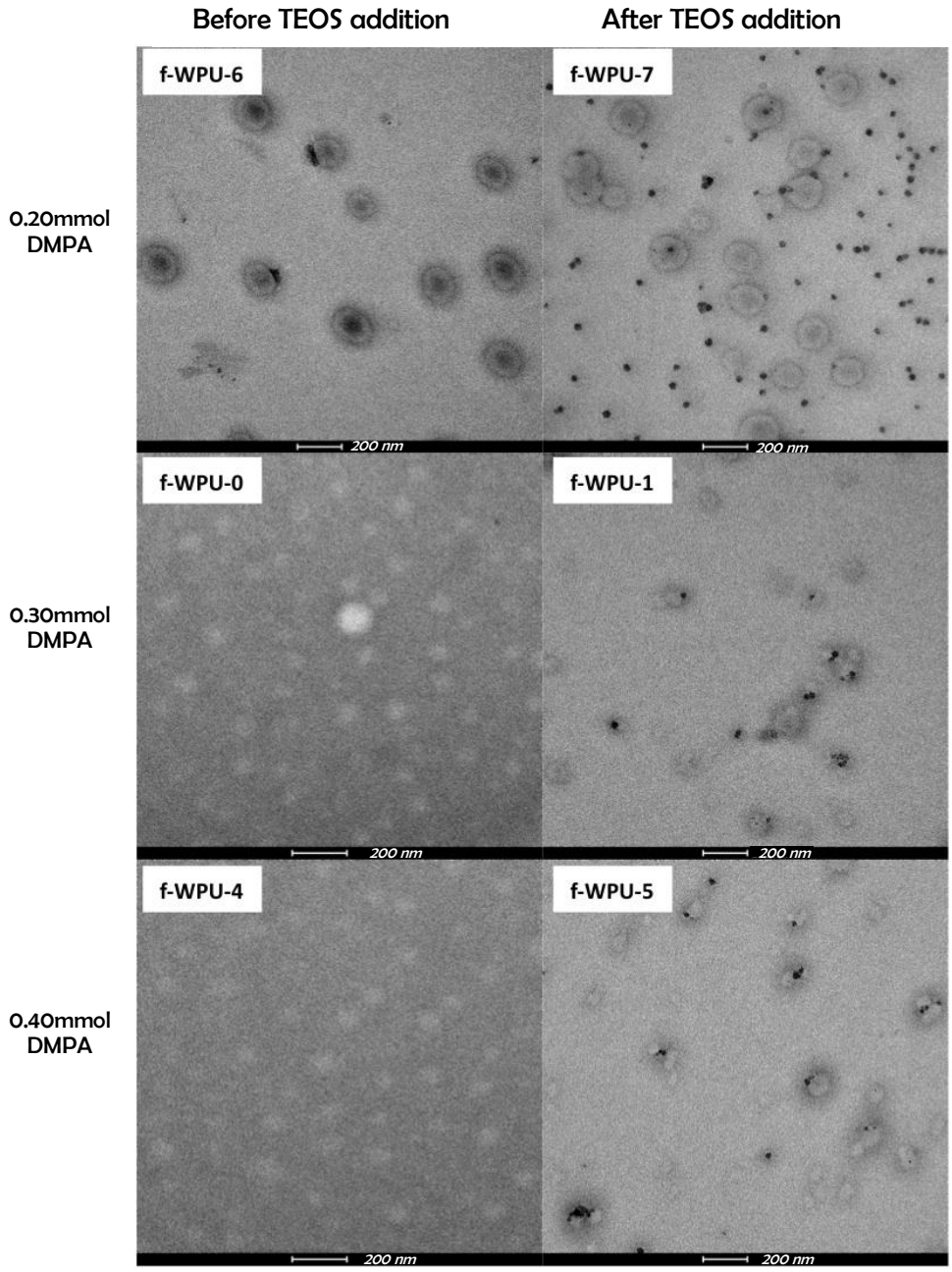

Figure 3.33. TEM images of functionalized dispersions with different DMPA contents.

3.2.2.4. Comparison between nanostructures obtained using functionalized and non-functionalized polyurethane particles.

The morphology of the final hybrid films obtained after curing the different dispersions at room temperature is studied in the following section.TEM images of the films obtained using functionalized and non functionalized particles with the same DMPA content (0.30 mmol.DMPA.g^{-1}_{pol}) are shown in Figure 3.34.

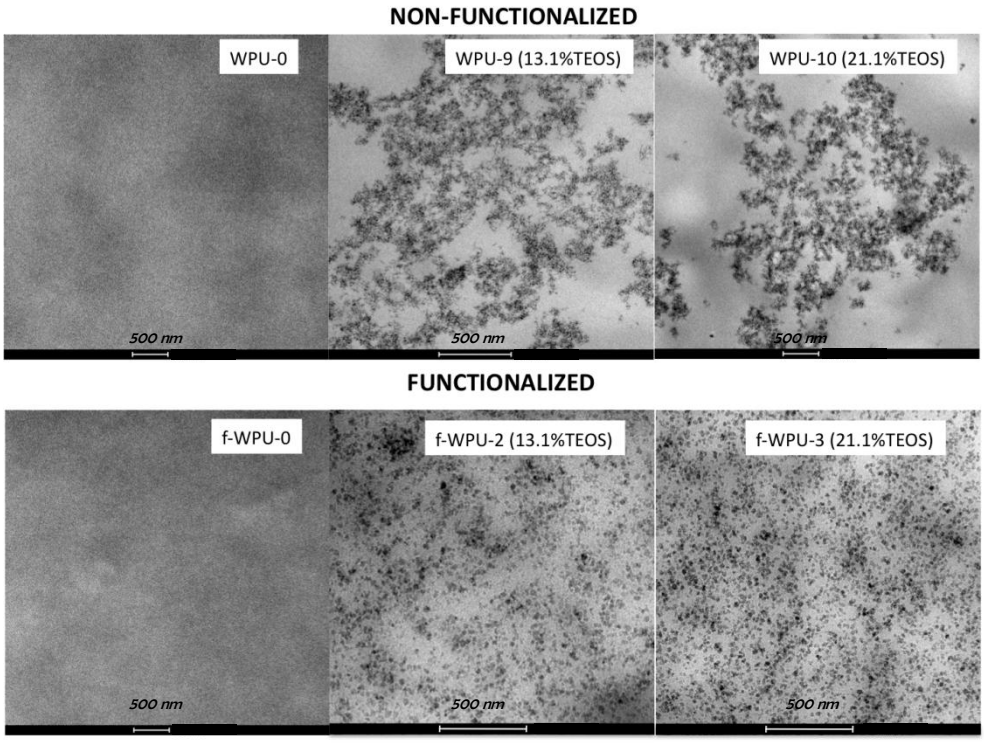

Figure 3.34. TEM images of cured functionalized and non-functionalized films.

Before TEOS addition the functionalized and non-functionalized films were completely homogeneous. This result was predictable for the non functionalized particles because the system does not contain any inorganic domains. However, the films obtained from functionalized particles show also a homogeneous morphology that can be explained considering that the silica domains are too small to be detected by TEM.

After TEOS addition, nanometric silica particles are observed in TEM images regardeless the functionalization. It is important to remark that in the samples obtained from non functionalized polyurethane particles, the silica is aggregated and its distribution is not homogeneous. However, the silica distribution in the polyurethane matrix is considerably enhanced when the polyurethane particles were previously functionalized with the aminosilane type precursor.

4. CONCLUSIONS

Polyurethane dispersions containing covalently bonded alkoxysilane end groups were successfully obtained by means of the acetone process using different concentrations of APTES. The quantitative incorporation of the alkoxysilane groups into the polyurethane chains was confirmed by means of FTIR, ^{1}H-NMR and elemental analyses.

The effect of the curing agent concentration on the particle size and morphology was also investigated. According to DLS results, the final particle size of the dispersions increased with APTES concentration, especially for high concentrations. Moreover, at low APTES concentrations, no silica domains could be detected by TEM. However, for APTES concentrations higher than 9.7 wt. %, the polyurethane particles contained inorganic-rich domains, confirming the partial condensation of alkoxy groups during the emulsification process, promoting their aggregation.

The zeta potential measurements demonstrated that the highest number of silanol groups on the particle surface was obtained when using 9.7 wt. % of APTES, supporting TEM observations.

All the dispersions were able to cure at room temperature because of the condensation of alkoxysilane end groups during the drying process, giving rise to a covalently linked organic/inorganic hybrid films. ^{29}Si NMR and FTIR measurements obtained before and after curing the dispersions at room temperature confirmed that crosslinking occurred during the drying process, and not during the polymerization.

The addition of commercial silica (CAB-O-SIL and Klebosol) increased particle size and distribution of polyurethane dispersions in relation to those of the original particles.

In the case of polyurethane/silica nanostructures obtained by TEOS Sol-Gel process, the stability of the dispersion was dependent on TEOS concentration; at large TEOS concentration stable dispersions could only be obtained using functionalized particles. In all cases the particle size increased with TEOS concentration.

In addition, the DMPA content has a large effect on the initial particle size (or the starting particle morphology) which has a great effect on TEOS deposition onto the surface of polyurethane particles. Large DMPA contents promoted the formation of silica on the particle surface.

Polyurethane/silica nanostructures obtained by the physical blending of functionalized polyurethanes and CAB-O-SIL and KLEBOSOL silica gave rise to non homogeneous final films.

The resulting films from the APTES containing systems showed a homogeneous morphology according to TEM results. The effect of the addition of TEOS was totally different for functionalized and non-functionalized systems, giving rise to more homogeneous hybrid systems in the first case.

5. BIBLIOGRAPHY

1 Frisch, K. 60 years of polyurethanes. (Kresta JE (Detroit) 1998).

2 Segura, D. M., Nurse, A. D., McCourt, A., Phelps, R. & Segura, A. in Handbook of adhesives and sealants Vol. 1 (ed Cognard Philippe) 101-162 (Elsevier Science Ltd, 2005).

3 Barni, A. & Levi, M. Aqueous polyurethane dispersions: A comparative study of polymerization processes. Journal of Applied Polymer Science 88, 716-723 (2003).

4 Chinwanitcharoen, C., Kanoh, S., Yamada, T., Hayashi, S. & Sugano, S. Preparation of aqueous dispersible polyurethane: Effect of acetone on the particle size and storage stability of polyurethane emulsion. Journal of Applied Polymer Science 91, 3455-3461 (2004).

5 Yang, J. E., Kong, J. S., Park, S. W., Lee, D. J. & Kim, H. D. Preparation and properties of waterborne polyurethane–urea anionomers. I. The influence of the degree of neutralization and counterion. Journal of Applied Polymer Science 86, 2375-2383 (2002).

6 Dieterich, D. Aqueous emulsions, dispersions and solutions of polyurethanes; synthesis and properties. Progress in Organic Coatings 9, 281-340 (1981).

7 Polyurethanes for high performance coatings V. Focus on Powder Coatings 2008, 7-8 (2008).

8 Subramani, S., Lee, J. M., Cheong, I. W. & Kim, J. H. Synthesis and characterization of water-borne crosslinked silylated polyurethane dispersions. Journal of Applied Polymer Science 98, 620-631 (2005).

9 Otts, D. B. & Urban, M. W. Heterogeneous crosslinking of waterborne two-component polyurethanes (WB 2K-PUR); stratification processes and the role of water. Polymer 46, 2699-2709 (2005).

10 Coogan, R. G. Post-crosslinking of water-borne urethanes. Progress in Organic Coatings 32, 51-63 (1997).

11 Fink, J. K. in Reactive polymers fundamentals and applications 69-138 (William Andrew Publishing, 2005).

12 Blank, W. J. & Tramontano, V. J. Properties of crosslinked polyurethane dispersions. Progress in Organic Coatings 27, 1-15 (1996).

13 Chattopadhyay, D. K. & Webster, D. C. Thermal stability and flame retardancy of polyurethanes. Progress in Polymer Science 34, 1068-1133 (2009).

14 Madbouly, S. A. & Otaigbe, J. U. Recent advances in synthesis, characterization and rheological properties of polyurethanes and POSS/polyurethane nanocomposites dispersions and films. Progress in Polymer Science 34, 1283-1332 (2009).

15 Chen, Y., Zhou, S., Yang, H. & Wu, L. Structure and properties of polyurethane/nanosilica composites. Journal of Applied Polymer Science 95, 1032-1039 (2005).

16 Lai, S. M., Wang, C. K. & Shen, H. F. Properties and preparation of thermoplastic polyurethane/silica hybrid using sol–gel process. Journal of Applied Polymer Science 97, 1316-1325 (2005).

17 Yang, C. H., Liu, F. J., Liu, Y.-P. & Liao, W. T. Hybrids of colloidal silica and waterborne polyurethane. Journal of Colloid and Interface Science 302, 123-132 (2006).

18 http://www.bayermaterialsciencenafta.com/processing/cas/1k-waterborne/index.html.

19 http://www.bayermaterialsciencenafta.com/processing/cas/2k-waterborne/index.html.

20 Rolf Gertzmann, C. I., Peter Schmitt,. Waterborne polyurethane coatings for wood floors - the next generation. Bayer MaterialScience LLC (2007).

21 Gironès, J. Pimenta, M.T.B., Vilaseca, F., de Carvalho, A.J.F., Mutjé, P. & Curvelet A.A.S. Blocked isocyanates as coupling agents for cellulose-based composites. Carbohydrate Polymers 68, 537-543 (2007).

22 Kim, B. K. Aqueous polyurethane dispersions. Colloid and Polymer Science 274, 599-611 (1996).

23 Rekondo, A., Fernández-Berridi, M. J. & Irusta, L. Synthesis of silanized polyether urethane hybrid systems. Study of the curing process through hydrogen bonding interactions. European Polymer Journal 42, 2069-2080 (2006).

24 Subramani, S., Cheong, I. W. & Kim, J. H. Synthesis and characterizations of silylated polyurethane from methyl ethyl ketoxime-blocked polyurethane dispersion. European Polymer Journal 40, 2745-2755 (2004).

25 Torró-Palau, A. M., Fernández-García, J. C., César Orgilés-Barceló, A. & Martín-Martínez, J. M. Characterization of polyurethanes containing different silicas. International Journal of Adhesion and Adhesives 21, 1-9 (2001).

26 Park, N. H., Lee, J. W. & Suh, K. D. In situ polyurethane/silica composite formation via a Sol-Gel process. Journal of Applied Polymer Science 84, 2327-2334 (2002).

27 Pajerski, A. & Ahrens, G. in Paint & Coatings Industry "1K polyurethane dispersion for conventional 2K applications" (2009).

28 Chattopadhyay, D. K. & Raju, K. V. S. N. Structural engineering of polyurethane coatings for high performance applications. Progress in Polymer Science 32, 352-418 (2007).

29 Pajerski, A. & Ahrens, G. www.lubrizol.com/1K-Polyurethane-Dispersion-Conventional-2K-Applications.pdf (2009).

30 Otts, D. B., Pereira, K. J., Jarret, W. L. & Urban, M. W. Dynamic colloidal processes in waterborne two-component polyurethanes and their effects on solution and film morphology. Polymer 46, 4776-4788 (2005).

31 Huybrechts, J. T. & Tanghe, L. M. 2.1 VOC solvent borne 2K clear coats based on star oligoethers. Progress in Organic Coatings 58, 217-226 (2007).

32 Yahkind, A. L., Paquet Jr, D. A., Parekh, D. V., Stine, C. L. & van der Ven, L. G. J. Polyols based on isocyanates and melamines and their applications in 1K and 2K coatings. Progress in Organic Coatings 67, 137-145 (2010).

33 Subramani, S., Lee, J. Y., Choi, S. W. & Kim, J. H. Waterborne trifunctionalsilane-terminated polyurethane nanocomposite with silane-modified clay. Journal of Polymer Science Part B: Polymer Physics 45, 2747-2761 (2007).

34 Subramani, S., Choi, S. W., Lee, J. Y. & Kim, J. H. Aqueous dispersion of novel silylated (polyurethane-acrylic hybrid/clay) nanocomposite. Polymer 48, 4691-4703 (2007).

35 Subramani, S., Lee, J. M., Lee, J. Y. & Kim, J. H. Synthesis and properties of room temperature curable trimethoxysilane-terminated polyurethane and their dispersions. Polymers for Advanced Technologies 18, 601-609 (2007).

36 Castelvetro, V. & De Vita, C. Nanostructured hybrid materials from aqueous polymer dispersions. Advances in Colloid and Interface Science 108-109, 167-185 (2004).

37 Han, Y. H., Taylor, A., Mantle, M. D. & Knowles, K. M. Sol-Gel derived organic-inorganic hybrid materials. Journal of Non-Crystalline Solids 353, 313-320 (2007).

38 Chattopadhyay, D. K. & Webster, D. C. Hybrid coatings from novel silane-modified glycidyl carbamate resins and amine crosslinkers. Progress in Organic Coatings 66, 73-85 (2009).

39 Chattopadhyay, D. K., Zakula, A. D. & Webster, D. C. Organic-inorganic hybrid coatings prepared from glycidyl carbamate resin, 3-aminopropyl trimethoxy silane and tetraethoxyorthosilicate. Progress in Organic Coatings 64, 128-137 (2009).

40 Cho, J. W. & Lee, S. H. Influence of silica on shape memory effect and mechanical properties of polyurethane-silica hybrids. European Polymer Journal 40, 1343-1348 (2004).

41 Yeh, J. M., Yao, C. T., Hsieh, C. F., Yang, H. C. & Wu, C. P. Preparation and properties of amino-terminated anionic waterborne-polyurethane-silica hybrid materials through a Sol-Gel process in the absence of an external catalyst. European Polymer Journal 44, 2777-2783 (2008).

42 Rekondo, A., Fernández-Berridi, M. J. & Irusta, L. Photooxidation and stabilization of silanised poly(ether-urethane) hybrid systems. Polymer Degradation and Stability 92, 2173-2180 (2007).

43 Brinker, C. J. & Scherer, G. W. Sol-Gel Science: The physics and chemistry of Sol-Gel processing. (Elsevier Editor, 1990).

44 Livage, J., Coradin, T. & Roux, C. Bioactive Sol-Gel hybrids. (Wiley-VCH Verlag GmbH & Co. KGaA, 2005).

45 Bourgeat-Lami, E. in Encyclopedia of nanoscience and nanotechnology Vol. 8 (ed Singh Nalwa Hayri) (American Scientific Publishers, 2004).

46 Bourgeat-Lami, E. Organic-inorganic nanostructured colloids. Journal of Nanoscience and Nanotechnology 2, 1-24 (2002).

47 Bourgeat-Lami, E., Herrera, N., Putaux, J.L., Perro, A., Reculusa, S., Ravaine, S. & Duguet E. Designing organic/inorganic colloids by heterophase polymerization. Macromolecular Symposia 248, 213-226 (2007).

48 Jeon, H. T., Jang, M. K., Kim, B. K. & Kim, K. H. Synthesis and characterizations of waterborne polyurethane-silica hybrids using Sol-Gel process. Colloids and Surfaces A: Physicochemical and Engineering Aspects 302, 559-567 (2007).

49 Wang, H., Shen, Y., Fei, G., Li, X. & Liang, Y. Micromorphology and phase behaviour of cationic polyurethane segmented copolymer modified with hydroxysilane. Journal of Colloid and Interface Science 324, 36-41 (2008).

50 Zou, H., Wu, S. & Shen, J. Polymer/Silica nanocomposites: preparation, characterization, properties, and applications. Chemical Reviews 108, 3893-3957 (2008).

51 Chen, G., Zhou, S., Gu, G. & Wu, L. Modification of colloidal silica on the mechanical properties of acrylic based polyurethane/silica composites. Colloids and Surfaces A: Physicochemical and Engineering Aspects 296, 29-36 (2007).

52 Chen, Y., Zhou, S., Yang, H., Gu, G. & Wu, L. Preparation and characterization of nanocomposite polyurethane. Journal of Colloid and Interface Science 279, 370-378 (2004).

53 Chen, J. J., Zhu, C. F., Deng, H. T., Qin, Z. N. & Bai, Y. Q. Preparation and characterization of the waterborne polyurethane modified with nanosilica. Journal of Polymer Research 16, 375-380 (2009).

54 Rehab, A. & Salahuddin, N. Nanocomposite materials based on polyurethane intercalated into montmorillonite clay. Materials Science and Engineering: A 399, 368-376 (2005).

55 Cao, X., James Lee, L., Widya, T. & Macosko, C. Polyurethane/clay nanocomposites foams: processing, structure and properties. Polymer 46, 775-783 (2005).

56 Chen, X., You, B., Zhou, S. & Wu, L. Surface and interface characterization of polyester-based polyurethane/nano-silica composites. Surface and Interface Analysis 35, 369-374 (2003).

57 Bourgeat-Lami, E. & Duget, E. in Functional Coatings: by polymer encapsulation (ed Swapan Kumar Ghosh) Ch. 4, 85-152 (Wyley VCH, 2006).

58 Tissot, I., Novat, C., Lefebvre, F. & Bourgeat-Lami, E. Hybrid latex particles coated with silica. Macromolecules 34, 5737-5739 (2001).

59 Song, C., Yuan, Q. & Wang, D. Effect of the content of urea groups on the particle size in water-borne polyurethane or polyurethane/polyacrylate dispersions. Colloid and Polymer Science 282, 642-645 (2004).

60 Xiaojuan, L., Xiaorui, L., Lei, W. & Yiding, S. Synthesis and characterizations of waterborne polyurethane modified with 3-aminopropyltriethoxysilane. Polymer Bulletin 65, 45-57 (2010).

61 Baccile, N., Laurent, G., Bonhomme, C., Innocenzi, P. & Babonneau, F. Solid-State NMR Characterization of the surfactant–silica interface in templated silicas: acidic versus basic conditions. Chemistry of Materials 19, 1343-1354 (2007).

62 Canevali, C., Chiodini, N., Marazzoni, F., Padovani, J., Paleari, A., Scotti, R. & Spinolo, G. Substitutional tin-doped silica glasses: an infrared study of the Sol-Gel transition. Journal of Non-Crystalline Solids 293-295, 32-38 (2001).

CHAPTER IV: MECHANICAL, THERMAL ADHESION AND TRANSPORT PROPERTIES OF WPU-s

CHAPTER IV: MECHANICAL, THERMAL, ADHESION AND TRANSPORT PROPERTIES OF WPU

1. INTRODUCTION

As mentioned through this thesis, the main application of the synthesized organic-inorganic hybrids is centred in the world of coatings, adhesives and sealants. Waterborne polyurethane hybrids are well positioned to find an increasing usage as adhesives, coating and sealants due to a variety of reasons.[1-5] Polyurethanes themselves offer good adhesion to a number of substrates such as concrete, wood, plastic and glass due to their elasticity and structural properties. Furthermore, the release of VOC-s to the atmosphere in these systems is considerably reduced compared to conventionally employed solvent-based systems.[6-11]

However, some inferior properties of waterborne polyurethanes such as low mechanical strength, solvent and chemical resistance restrict to some extent their utility for high performance applications. Therefore, it is important to modify WPU-s with inorganic moieties in order to improve the mentioned properties. These "new" systems are increasing their use due to the synergetic effect between the organic and inorganic phases.[12-27] This synergetic effect can only be observed when good compatibility between phases is achieved.[28-32]

It is obvious that depending on the application (pressure sensitive adhesive, hot melt, sealant or coating) the final product characteristics must be different and also the strategy to follow during the synthesis process. Accordingly, it is important to determine their thermal, mechanical and adhesion properties and their performance as a function of temperature. In addition, if these systems are going to be applied as coatings, the measurements of their permeability response are important data.

In this final chapter the main properties of the synthesized waterborne polyurethanes are described and the effect of APTES concentration, soft-segment nature and silica content is investigated. In addition, covalently linked hybrids are compared with nanostructured blends.[8,11,20-21,23,26-27,33-49]

2. THERMAL PROPERTIES: DIFFERENTIAL SCANNING CALORIMETRY (DSC)

2.1. Introduction

DSC is a widely employed technique in order to determine the thermal properties of polyurethane hybrids. One of the characteristics of segmented polyurethanes is that the hard and soft segments trend to separate in phases, giving rise to two glass transition temperatures,[50-51] corresponding to the soft and hard segment respectively. Due to their different nature, the Tg of the soft segment is below the Tg of the hard one.[52-54]

2.2. Experimental part

Samples were dried at 21 ± 2 °C and at 50 ± 5 wt. % relative humidity for at least one week before performing the DSC tests. The experimental conditions are depicted in Annex I.

2.3. Results and discussion

DSC thermograms of all the synthesized polyurethanes were recorded in order to determine the glass transition temperature (Tg) of both segments and the melting temperature (Tm) in the semicrystalline systems. The effect of different variables such as APTES content, soft segment nature and silica content (coming from various sources) in the final products characteristics was studied.

2.3.1. Effect of APTES

The DSC thermograms for polyurethanes based on PPG and PBAD containing different APTES concentrations are shown in Figure 4.1. In the case of PBAD based WPU-s, there is an endothermic transition around 45 °C in the DSC thermograms of 0 and 5 wt. % of APTES containing systems that can be atributted to the melting process of the soft segment. However, this peak disappears at APTES concentrations higher than 9.7 wt. %.

This result can be explained upon the basis that the crosslinking degree increases with APTES concentration, reducing the chain mobility and therefore limiting the capacity of the soft segments to crystallize. This behaviour has also been reported in literature for similar systems.[43,55]

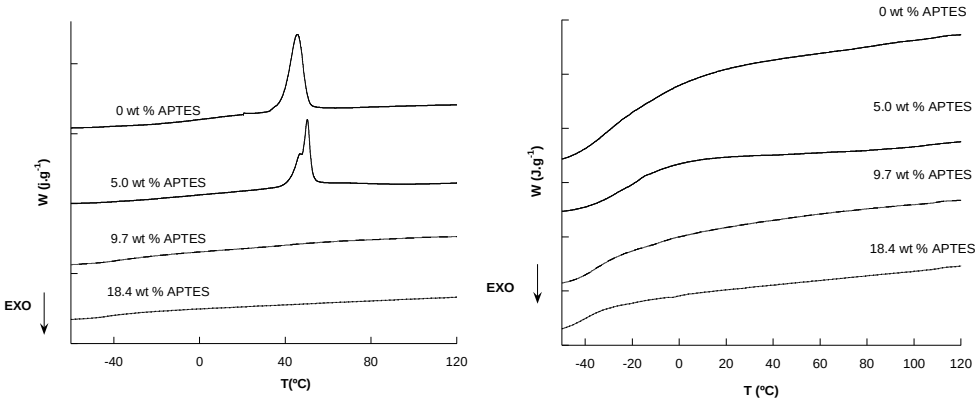

Figure 4.1. DSC thermograms of both series of WPU-s (PBAD based WPU-s on the left and PPG based WPU-s on the right) for different APTES concentrations.

PBAD based systems also show a transition around -40 °C that can be attributed to the glass transition temperature of the soft segments (Tg_s). Taking into account that the Tg of pure PBAD is around -72 °C, when this segment is incorporated in the PU chain, this value shifts towards higher values,[51] as a consequence of its chemical linkage with the hard segments, restricting their movement and increasing the Tgs value.

Tgs values for the systems containing different APTES concentrations are shown in Table 4.1. As can be observed, the Tgs for the systems containing PBAD decrease slightly with the APTES concentration. This result is not easy to explain because taking into account that the crosslinking degree increases with APTES, Tgs should expect to increase. However, bearing in mind that APTES is linked to the polyurethane chains via reaction with IPDI, end-chained urethane and urea groups are forced to come closer during the curing process. As a consequence, the curing process promotes phase separation between segments and thus the Tgs can decrease with APTES concentration.

Finally, in the thermograms of the systems containing 9.7 and 18.4 wt. % of APTES a second glass transition can be hardly detected at about 60°C. This transition is probably

due to the motion of the hard segment (Tg_h) indicating that the synthesized polyurethanes show a phase separated morphology.

Name	PBAD-WPU-s			PPG-WPU-s
	Tgs (°C)	Tm (°C)	ΔH_f ($J.g^{-1}$)	Tgs (°C)
0 wt. % APTES	-30	45	26	-29
5.0 wt. % APTES	-35	47	17	-33
9.7 wt. % APTES	-37	-	-	-35
14.0 wt. % APTES	-39	-	-	-38
18.4 wt. % APTES	-41	-	-	-40

Table 4.1. DSC results of polyurethanes containing different APTES concentrations.

The thermograms of the systems based on PPG are shown in Figure 4.1 (right) and the values of the transitions are shown in Table 4.1. In this case, there is not any melting endothermic peak, which confirms that the PPG based systems are amorphous. Moreover, a glass transition at about -40 °C is observed in all the thermograms which can be assigned to Tg of the soft segments. The value of this transition is in all the systems higher than that of pure PPG and decreases with APTES concentration due to the higher phase separation of these systems, although the Tgh of the separated hard segement are not observed.

2.3.2. Effect of the addition of silica

Table 4.2 summarizes the DSC results obtained for functionalized polyurethanes (9.7 wt. % APTES) containing different types of silica.

In all the cases the Tg of the systems does not change with the introduction of inorganic domains. This means that the interactions between the nanoparticles and the polymeric matrix are poor.

It should be mentioned that the two systems based on PBAD which contain CAB-O-SIL present a melting transition centered at 50 °C. This result can be explained taking into

account that CAB-O-SIL can act as a nucleating agent increasing the crystallinity of the PBAD based WPU-s, as reported previously in literature.[56]

Silica content and origin	PBAD-WPU-s			PPG-WPU-s
	Tg (°C)	Tm (°C)	AH_f ($J.g^{-1}$)	Tg (°C)
0	-37	-	-	-35
2 wt. % SiO_2 (in-situ)	-36	-	-	-35
4 wt. % SiO_2 (in-situ)	-36	-	-	-34
8 wt. % SiO_2 (in-situ)	-34	-	-	-33
5 wt. % KLEBOSOL	-38	-	-	-37
10 wt. % KLEBOSOL	-36	-	-	-36
5 wt. % CAB-O-SIL	-37	51	12	-35
10 wt. % CAB-O-SIL	-38	50	2	-36

Table 4.2. DSC results of different functionalized WPU/silica nanostructures.

3. THERMO-MECHANICAL PROPERTIES: DYNAMIC MECHANICAL THERMAL ANALYSIS (DMTA)

3.1. Introduction

The dynamic mechanical and thermal analyzer (DMTA) is an excellent tool to study the relaxation behaviour, change in loss or storage modulus and glass transition temperature (Tg) of polymeric materials.[57]

DMTA is useful for studying the viscoeslastic behaviour of polymers as a function of temperature. In this technique, a sinusoidal stress is applied to the sample and the strain in the material is measured. For an "ideal" elastic solid the resulting strain and stress are perfectly in phase. However, for an "ideal" viscous liquid, there is a 90 degree phase lag

of strain respect to stress. In the case of viscoelastic polymers, some phase lag (δ) occurs during DMTA test.

Polymes can be characterized by means of the *storage modulus (E´)* and the *loss modulus (E´´).* The storage modulus measures the stored energy and is related to the elasticity of the material, while the loss modulus measures the energy dissipated heat, related to the viscosity of the material. The phase angle *tan* δ is defined as:

$\tan \delta = E'' / E'$

At the glass transition, the storage modulus decreases dramatically, the loss modulus increases and tan δ shows a maximum.

3.2. Results and discussion

The effect of different variables such as APTES content, soft segment nature or silica content (coming from different sources) on the final products characteristics were studied.

3.2.1. Effect of APTES content

DMTA curves of pure WPU-s and different functionalized WPU-s films for both series of polyurethanes (PBAD and PPG) containing different amounts of APTES are shown in Figure 4.2.

As observed, DMTA results for both series of polyurethanes (PPG and the PBAD based systems) follow the same tendency. It is important to point out that the increase of APTES concentration reduces the maximum value of tan δ, moving from values close to 0.8-0.9 for low APTES concentrations (5 wt. %) to values of about 0.3 when large APTES concentrations are used, indicating that the material is composed of more rigid domains. The stiffness can be related to a larger crosslinking degree and to the inclusion of inorganic rigid domains into the polyurethane backbone.

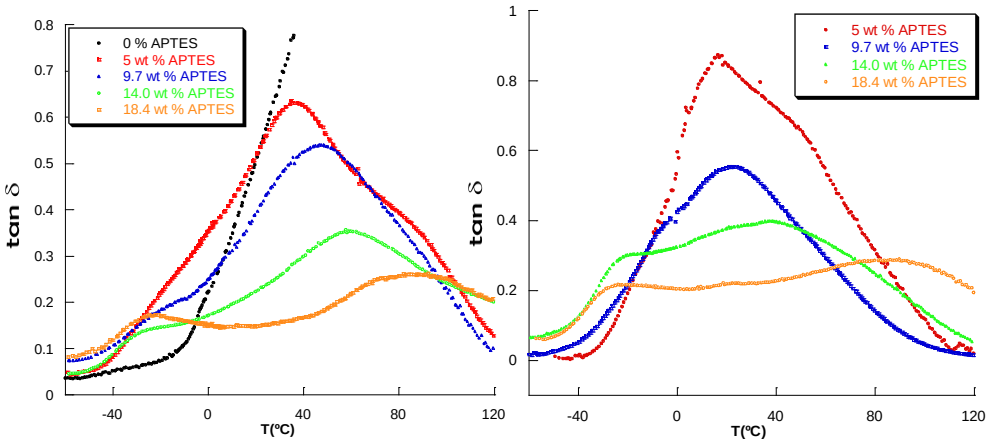

Figure 4.2. DMTA results of PBAD (left) and PPG (right) based WPU-s as a function of APTES concentration.

In addition, tan δ shows two peaks in all the systems. One of them located at temperatures below 0º C and the other at higher temperatures, which can be related to the glass transition temperatures of soft (Tg_s) and hard segments (Tg_h) respectively[57]. If we consider the DMTA graph obtained for the PBAD based systems, it is evident that the peak assigned to the hard segment glass transition (Tg_h) shifts towards higher values with APTES concentration, while the Tg of the soft segment moves to lower values. This fact proves that as APTES increases the difference between the Tgs of the two segments also increases, indicating that APTES promotes the phase separation of both types of segments[50].

The same conclusions have been obtained by DSC. In fact, DSC and DMTA are complementary techniques in order to determine the thermal transitions of segmented polyurethane hybrids. In the case of DSC, the glass transition of the soft segments can be determined, whereas the DMTA allows the determination of the glass transition of the hard segments.

4. MECHANICAL PROPERTIES

4.1. Introduction

Due to the great versatility of polyurethane properties, these materials can respond appropriately to the required mechanical properties of adhesives and sealants as a function of the chosen applications.

Generally, adhesives are rigid materials with low flexibility and large resistance to stress and shear stress,[11,60] whereas, in the case of sealants these properties change as a function of their workplace. For instance, a material that is used for the junctions of buildings must be flexible to withstand the contraction and contraction movements created by temperature changes. Nevertheless, when large weights and stresses must be withstood, a material with high modulus and low flexibility is the desired one.

The organic-inorganic hybrids have attracted significant interest because of the efficient combination of properties of both type of compounds. In general, the presence of micro-size hard particles introduces stress concentrations, rendering the resulting composite more brittle than the polymer itself. However, when nanoparticles are used, enhanced mechanical properties (tensile strength) can be observed when the nanoparticles are uniformly distributed in the polymer matrix. In nanocomposites, the local stress can be more easily transferred into the tougher particles with the result that the matrix appears to be amenable to a larger local plastic deformation. Thus, in some especial cases, the inorganic component can enhance the tensile strength and the modulus without extensively decreasing the deformation at break.

4.2. Experimental part

Samples were dried at 21 ± 2 °C and at 50 ± 5 % relative humidity for at least one week before performing the mechanical tests. The samples were dried in a Teflon mold. Specimens for tensile tests were die cut following the standard ASTM D638 type V (Figure 4.3).

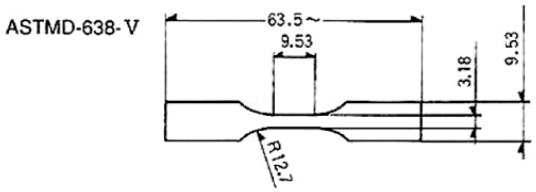

Figure 4.3. Image of the specimen employed for stress-strain tests.

Tensile tests were carried out using an Instron 5569 machine, at 23 ± 2 °C and at 50 ± 5 % relative humidity. Tensile strength (σ) and ductility, measured by means of the elongation at break (ε(%)), were determined from the load-displacement curves at a cross-head speed of 25 $mm.min^{-1}$. Five tensile specimens were tested.

4.3. Results of Tensile Test

4.3.1. Effect of APTES

PPG/PBAD based WPU-s were tested in order to obtain the stress-strain curves as a function of APTES concentration. As previously mentioned, APTES increases the crosslinking density of the final film considerably, affecting the characteristics of the final product. In Figure 4.4 the stress-strain curves of PPG based WPU-s with different APTES concentrations are shown.

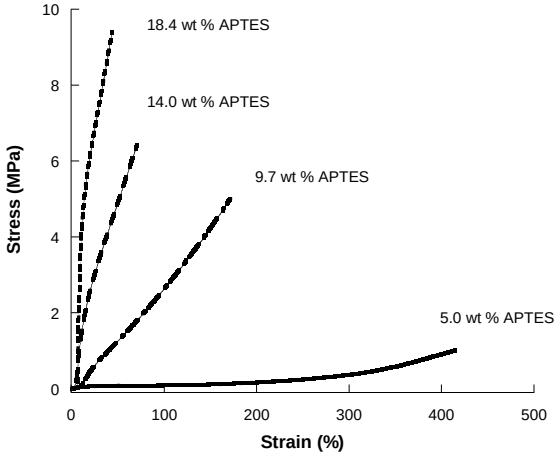

Figure 4.4. Stress-strain data of PPG based WPU-s as a function of APTES concentration.

As can be seen, there is clearly different behaviour according to APTES content. Thus, at low APTES content the system behaves as a flexible material whereas at high APTES content the material is quite rigid. Therefore, the modulus increases and the strain decreases as a function of APTES concentration.

Table 4.3, summarizes the values of elongation at break, modulus and tensile strength in all the studied systems. As shown, the tensile strength increases from 1 to 10 MPa as APTES increases from 5 wt. % to 18.4 wt. %. However, the deformation at break decreases from 400 to 35. The larger crosslinking density as APTES content increases makes the systems more rigid, thus reducing the elongation and increasing the modulus.[43] Therefore the tensile strength also increases with the curing degree.

Name	Strain (%)	Modulus (MPa)	Tensile strength (MPa)
5.0 wt. % APTES	401 ± 10	< 1	1.5 ± 0.2
9.7 wt. % APTES	175 ± 5	6 ± 1	5.0 ± 0.1
14.0 wt. % APTES	64 ± 1	22 ± 2	6.4 ± 0.3
18.4 wt. % APTES	34 ± 4	124 ± 9	9.9 ± 0.5

Table 4.3. Strain, tensile strength and modulus values of PPG based WPU-s as a function of APTES concentration.

In the case of PBAD based systems a different tendency in the stress strain curves with different APTES concentrations is observed (Figure 4.5). The results are summarized in Table 4.4.

Name	Strain (%)	Modulus (MPa)	Tensile strength (MPa)
0 wt. % APTES	84 ± 8	102 ± 15	< 0.5
5.0 wt. % APTES	125 ± 10	36 ± 7	2.0 ± 0.3
7.5 wt. % APTES	300 ± 7	22 ± 6	21 ± 1
9.7 wt. % APTES	295 ± 12	25 ± 7	23 ± 2
14.0 wt. % APTES	60 ± 5	143 ± 10	9.5 ± 0.8

Table 4.4. Strain, tensile strength and modulus values of PBAD based WPU-s as a function of APTES concentration.

The material containing 5 wt. % of APTES presents a slight increase in the strain (from 84 to 125) and in the tensile strength (from less than 1 to 2) with respect to the pure WPU, together with a sharp decrease in the modulus (from 102 to 36) (Table 4.4). Nevertheless, the materials containing 7.5 and 9.7 wt. % of APTES present a sharp increase in the strain (from 84 to ≈300), and the tensile strength (from less than 1 to ≈20), together with an important decrease in the modulus (from 102 to ≈20).

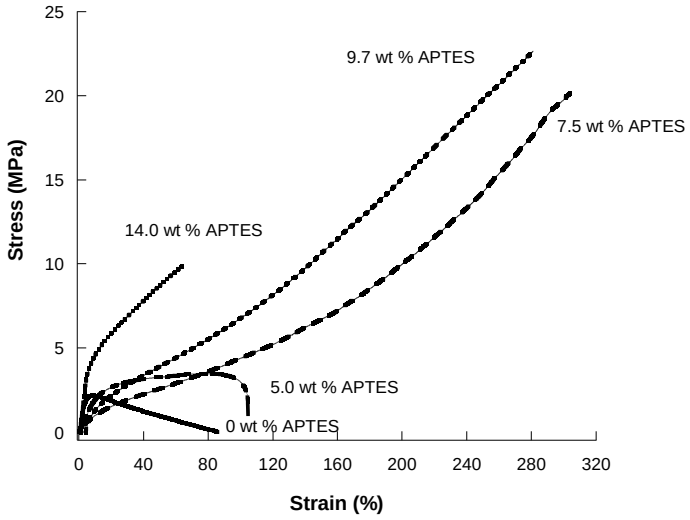

Figure 4.5. Stress-strain data of PBAD based WPU-s as a function of APTES concentration.

As previously reported, the system without APTES is semi-crystalline, whereas the systems containing APTES concentrations higher than 5 wt. % are amorphous. Considering the two semi-crystalline systems (0 and 5 wt. % of APTES), the higher tensile strength and the lower modulus of the system containing 5 wt. % APTES can be related to a lower crystallinity degree.

In the amorphous systems, the tensile strength decreases and the modulus increases with the APTES concentration, due to the higher crosslinking degree of the systems. In this case, the system containing 18.4 wt. % could not be evaluated because of the difficulty in the preparation of appropriate specimens.

4.3.2. Effect of the addition of silica

The effect of the addition of silica to the 9.7 wt. % functionalized WPU-s on the mechanical properties is shown in Figures 4.6, 4.7 and 4.8.

As can be observed, the deformation at break decreases with silica for all systems regardless of its origin. This effect is well established in the literature[47,61-66], because the insertion of rigid zones into the polyurethane backbone reduces the elongation at break. However, the systems containing SiO_2 from the addition of TEOS experiment a higher decrease compared with the other two types of systems. In PPG based systems, if we compare the data obtained for a fixed SiO_2 content (5 wt. %) the deformation at break values go from 160 for CAB-O-SIL, 120 for Klebosol down to 80 for TEOS containing systems. At first glance it could be argued that a non homogeneous distribution of silica in the PU matrix was responsible for this fact. However, according to Figures 3.23 and 3.34 only the systems containing TEOS show good silica distribution. Therefore, in our opinion the observed decrease of the elongation at break should correspond to the higher crosslinking degree of TEOS containing samples. Silanol groups generated during the TEOS Sol-Gel process can react with those groups of APTES increasing the functionality of the inorganic precursors and leading to a more crosslinked network. Similar behaviour is observed for those systems based on PBAD.

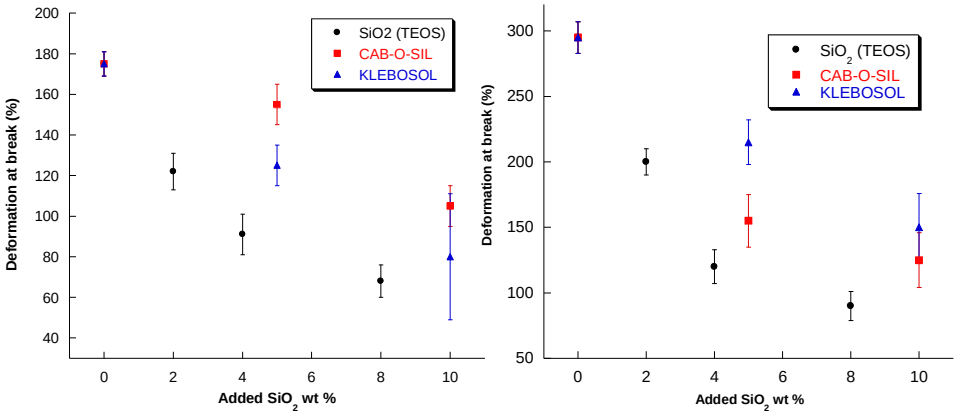

Figure 4.6. The effect of different inorganic moieties on the deformation at break for PPG (left) and PBAD (right) based WPU-s containing 9.7 wt. % of APTES.

The dependence of the modulus as a function of the silica content is depicted in Figure 4.7. For all cases, a slight increase in the modulus as a function of silica content is observed. For PPG based WPU-s, there is a clear jump in the modulus value at 10 wt. % of added silica for the case of physical blends (data not measured for TEOS containing systems). This behaviour has also been reported in the literature[65] where it is stated that a certain number of nanosilica particles is required to reinforce the polymeric matrix. According to our results this value is about 10 wt. % of silica.

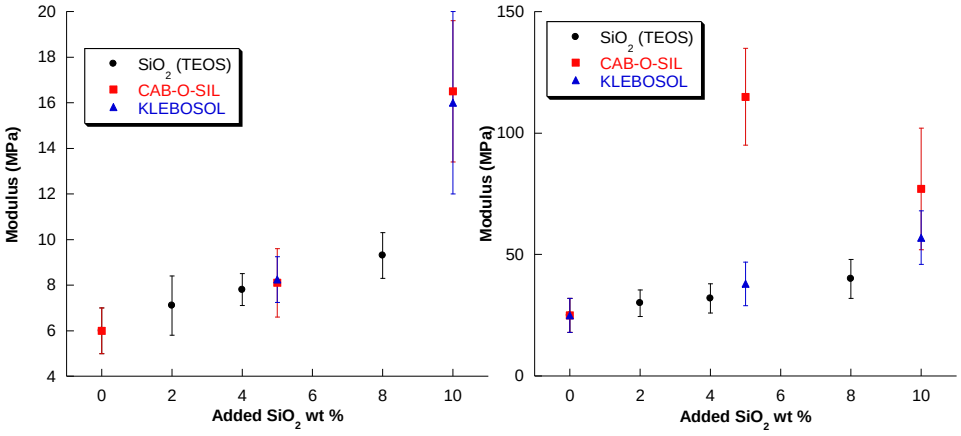

Figure 4.7. The effect of different inorganic moieties on the modulus of PPG (left) and PBAD (right) based WPU-s containing 9.7 wt. % of APTES.

For PBAD based systems a slight increase in the modulus with the silica content is also observed. However, in this case, it seems that the quantity of silica employed is not enough to reinforce the polymeric matrix. In addition, the system containing 5 wt. % of CAB-O-SIL shows an unexpected high modulus value. The fact that this system is semicrystalline, according to DSC results, (Table 4.2) could explain this behaviour.

In Figure 4.8 the effect of both the origin and nature of silica on the tensile strength for 9.7 wt. % APTES based on both WPU-s (PPG and PBAD) is shown. As can be seen all the systems experiment a clear reduction in the tensile strength value. These results indicate that the addition of more silica does not reinforce the material and in fact increases its fragility.

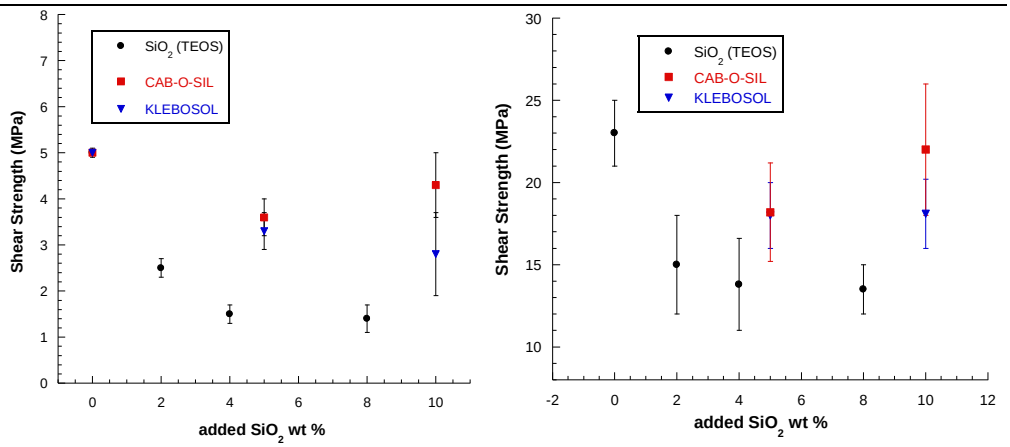

Figure 4.8. The effect of different inorganic moieties on the shear strength of PPG (left) and PBAD (right) based WPU-s containing 9.7 wt. % of APTES.

5. ADHESION PROPERTIES

5.1. Introduction

The first issue studying adhesion properties is to define what adhesion means as there are many different definitions in literature. In a simple way adhesion can be defined as the work required separating two interfaces that are adhered.[11,67] Nevertheless, in order to carry out a quantitative study this definition presents many disadvantages. Therefore, in the literature adhesion is related with the strength required to debond a coating or film from a substrate. The adhesion strength can be determined by many different standard test methods (Lap Shear Test, Peeling Test, Pull Test, Scratch Test....) all of them presenting advantages and disadvantages.[68-69]

Peel and Lap Shear Tests were selected in this study taking into account the nature and the possible applications of the polyurethanes. Before carrying out the adhesion measurements, an experiment was defined in order to determine the best experimental conditions (temperature of adhesion, time of exposure before adhesion...) to obtain a good adhesion between the different substrates.

5.2. Experimental part

5.2.1. Experiment design

In a conventional experiment, one or more process variables (or factors) are deliberately changed in order to observe the effect that these variables have on one or more response parameters. The (statistical) design of experiments (DOE) is an efficient procedure for planning experiments so that the data obtained can be analyzed to render valid conclusions. DOE begins by determining the objectives of an experiment and selecting the process factors for the study before carrying it out. Well chosen experimental designs maximize the amount of "information" that can be extracted for a given amount of experimental effort.

In this work a full factorial design with two levels of two variables (time before adhering the substrates and temperature of adhesion) was used and the analysis of variance (ANOVA) was used to interpret the data. The shear strength obtained after a Lap Shear Test was used in this study as the response dependent variable. As the temperature of adhesion is an important variable at the point for the utilization of an adhesive, it is necessary to know the temperature the adhesive has the best performance. Moreover, the film formation time before adhering the substrates is another important factor that has to be taken into consideration when determining the lifetime of an adhesive before performing the adhesion test. These two factors are connected between them making study at unison necessary.

In this work PBAD based f-WPU was selected (containing 9.7 wt. % of APTES) because previous experiments had shown that this starting material is the most appropriate for adhesion applications.

5.2.2. Lap Shear Test

Lap Shear Test is commonly employed in order to determine the holding power ability of a tape to remain adhered under a load applied parallel to the surface of the tape. It gives an idea of the cohesive strength of the adhesive. The polyurethane adhesive was applied onto the faces of two metallic panels that were clamped to the jaws of an Instron Tensile Tester. The adhesion values were obtained from pulling the panels following the ASTM D3163 standard.

The Lap Shear Test representation is shown in Figure 4.9.

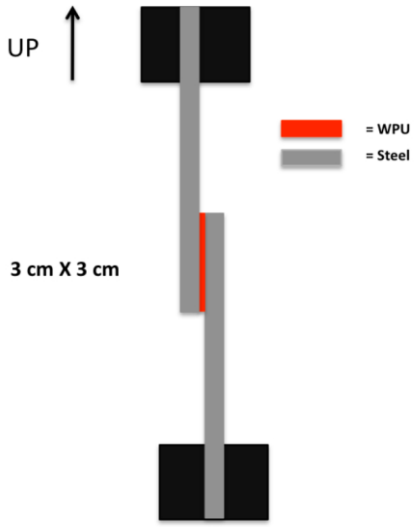

Figure 4.9. Schematic representation of the Lap Shear Test.

The procedure used to perform the Lap Shear Test was as follows:

- 30 wt. % of the polyurethane dispersion was applied using a roller applicator of 200 μm onto a 3 X 10 cm metallic panel.

- The samples were prepared at two different experimental conditions; one drying the films at room temperature for 10 minutes and adhering the two metallic panels at a

pressure of 10 MPa at room temperature for 15 minutes to improve the contact. The second one drying the films at room temperature for 120 minutes and adhering the two metallic panels at a pressure of 10 MPa at 90 °C for 15 minutes to improve the contact.

- The samples were kept at room temperature for 14 days before the measurements.

- The test was carried out at 300 $mm.min^{-1}$ until total debonding after clamping both metallic panels.

5.2.3. Peel Test

Peel resistance is a measure of the force required to peel away a strip of tape from a rigid surface at a specific angle and speed. There are several different combinations of speeds and angles for testing the peel of a polyurethane adhesive. In this work the tests were performed using a 180° angle and a rate of 300 $mm.min^{-1}$.

The adhesive was applied between a standard metallic panel and a PET film. The free end of the PET film was doubled back and clamped to the upper jaw of an Instron Tensile Tester. The adhesion value is the average pull value obtained during peeling of the tape and it is expressed in MPa (initial peel values are disregarded). Apart from measuring the peel resistance of the adhesive, the method allows the evaluation of the kind of failure that occurs (adhesive or cohesive) by observing the remaining residue. In this case the experiments were carried out following ASTM D-903 standard.

The procedure used to perform the 180° Peel Test was as follows:

- 30 wt. % of the polyurethane dispersion was applied using a roller applicator of 200 μm onto a 3 X 10 cm metallic panel.

- After drying the sample for 10 minutes at room temperature, the film of PET was adhered at a pressure of 10 MPa at room temperature for 15 minutes to improve the contact.

- The samples were kept at room temperature for 14 days before the measurement.

- The Peeling Test was carried out at 300 mm.min^{-1} until total debonding.

Figure 4.10 shows a schematic representation of the experiment.

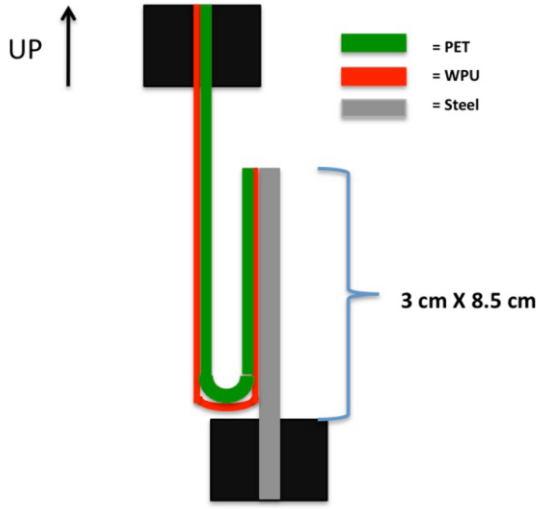

Figure 4.10. Schematic representation of the 180° Peel Test.

5.2.4. Shear Adhesion Failure Temperature (SAFT)

SAFT refers to the upper temperature limit at which an adhesive is able to support a certain amount of weight. This adhesion test gives a value that can be related with the maximum usage temperature of an adhesive. The polyurethane sample was applied between a standard metallic panel and a PET film. Tests were performed in a SAFT oven containing three metal panels where 12 samples can be clamped. Usually, 4 samples for each dispersion were tested in order to check the reproducibility. When failure of the adhesive occurred, the standard weights fell onto the sensors and the counter of the corresponding sample stopped. The oven was connected to a computer where the time and the temperature of failure were registered. Figure 4.11 shows a schematic representation of the measurement apparatus.

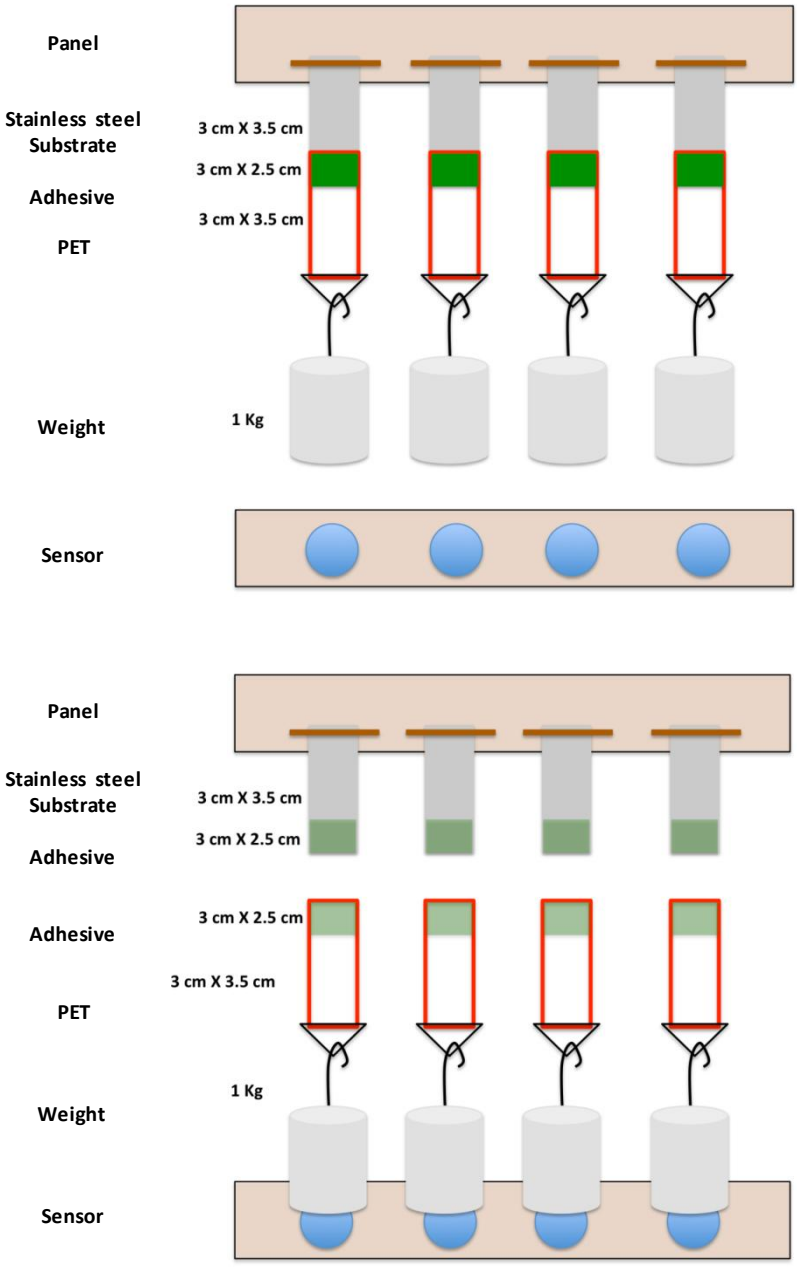

Figure 4.11. Schematic representation of SAFT experiment.

The procedure used to perform the SAFT test was as follows:

- 30 wt. % of the polyurethane dispersion was applied using a roller applicator of 200 μm onto a 3 X 10 cm metallic panel.

- After drying the sample for 10 minutes at room temperature, the film of PET was adhered at a pressure of 10 MPa at room temperature for 15 minutes to improve the contact.

- The samples were kept at room temperature for 13 days before measuring.

- A high temperature resistance tape (a siliconed polyester tape) was further attached to the surface of the film in order to reinforce it without affecting the adhesion test.

- The samples were kept at 30 °C for 1 day for equilibrating.

- Standard weights (1 Kg) were positioned and the counter was turned on until failure.

The image at the top shows the starting point of the measurement and the one at the bottom the final point after adhesion failure. SAFT was measured using a temperature ramp of 1 °C.min^{-1} from 30 °C to 210 °C (maximum temperature allowed in the oven).

5.3. Results and discussion

5.3.1. Experiment design

It is clear that for room temperature self-curable adhesives, as the one synthesized in this work, the time between performing the adhesion and carrying out the adhesion measurement has an important effect on the adhesion strength. According to this, some preliminary experiments were carried out in order to determine the time to obtain the maximum adhesion strength.

In Figure 4.12, the shear strength obtained in the Lap Shear Test as a function of the adhesion time for a WPU based on PBAD containing 9.7 wt. % of APTES is shown. The

adhesion was performed at two temperatures (35 and 105 °C) for 15 minutes and the samples were kept at room temperature for different times after the adhesion.

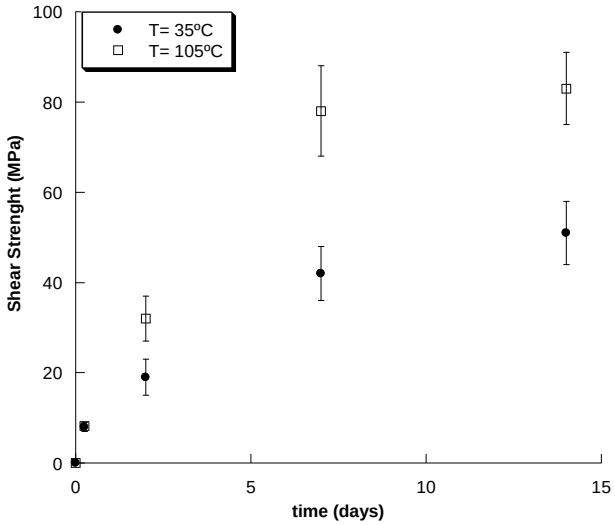

Figure 4.12. Effect of time on adhesion strength at two different temperatures.

As can be seen the shear strength values obtained at both temperatures, increase with time, achieving a plateau after seven days of performing the adhesion process. As a result, all the subsequent experiments were carried out 14 days after performing the adhesion.

After this experiment, the effect of the film formation time and the adhesion temperature for the shear strength in a WPU based on PBAD containing 9.7 wt. % of APTES was studied using the DOE methodology. The rest of the variables such as the pressure and time of adhesion at the punching machine (10 MPa and 15 min respectively) or the time gap between the adhesion and measurement (14 days) were kept constant.

Table 4.5 summarizes the shear strength values obtained at different experimental conditions. The symbol -, + and 0 indicates the lowest, the highest and the central value of the variables respectively.

	Pattern	Temperature (°C)	Time (min)	Shear strength (MPa)
1	-+	35	144	42.9
2	++	105	144	109.7
3	--	35	10	66.4
4	+-	105	10	81.0
5	00	70	77	74.5

Table 4.5. Shear strength values obtained at different experimental conditions.

Using the Anova methodology, the following equation can be determined from the experiment results (using the codified data -1, 0, +1 for the low, mid and high variable levels respectively).

$$Shear\ strength = 73.5 + 14.68.\ T(^{o}C) + 2.93.\ t(min) + 18.73.\ T(^{o}C).\ t(min) \pm Exp.\ error$$

Table 4.6 displays the regression coefficients (Estimate), the standard error of the parameter, t Ratio (parameter estimate divided by standard error), probability (the probability of a greater absolute t-value occurring just by chance if the parameter has no effect in the model) for all terms in the regression model. The terms with t ratio higher than 50 are statistically significant, so the variable temperature of adhesion and the correlation between temperature of adhesion and time of exposure before adhesion are the most important terms. Thus, the largest shear strength is obtained when the adhesion process is performed at high temperatures and at a longer film formation time.

Term	Estimate	Standard error	t Ratio	Prob > t
T (°C)	14.68	0.28	52.43	0.0121
Exposure time	2.93	0.28	10.46	0.0607
T(°C) Exposure time	18.73	0.28	66.89	0.0095

Table 4.6. Values obtained from the experiment design varying the exposure time and temperature.

The main idea is that when performing the adhesion at high temperatures, long film formation times must be kept. However, when performing the adhesion at low temperatures an opposite effect is observed. Moreover, in this last case the obtained adhesion values are lower than those obtained at high temperatures. In our opinion at low adhesion temperatures, short film formation times are needed in order to avoid polymer chain stiffness before adhering both panels.

Taking into account the experimental design results, long drying times (2 h) have been selected when the adhesion is carried out at high temperatures (90 °C) and short drying times (10 min) when the adhesion is carried out at room temperature.

5.3.2. Effect of APTES concentration on the Lap Shear Test

In order to examine the effect of APTES concentration on the Lap Shear Test two different experiments were carried out for both systems (PBAD and PPG). In Figure 4.13 the shear strength as a function of APTES content for PPG and PBAD based WPU-s adhered at room temperature is shown.

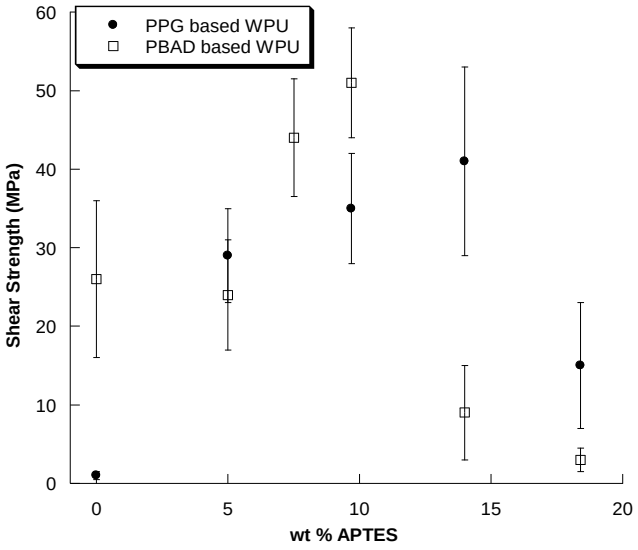

Figure 4.13. Shear strength vs. APTES content for WPU-s based on PPG and PBAD adhered at room temperature.

As shown in Figure 4.13, the adhesion strength of the IPDI/PPG sample considerably increases with APTES concentration up to a value at about 14 wt. % APTES, where it sharply decreases. According to literature results,[55] this behaviour can be explained upon the basis that at high APTES content the system becomes too rigid to keep its adhesive properties. In the case of PBAD based samples, the trend of the shear strength vs. APTES content is similar to the previously described system. However, the sample with 5 wt. % of APTES displays lower shear strength than that of the system without APTES. Once again, this anomalous behaviour can be assigned to the crystallinity of the system. At concentrations above 5 wt. %, the system becomes amorphous, showing then the same trend as IPDI/PPG, increasing the maximum adhesion strength up to a value where it becomes so rigid that it loses all its adhesive properties.

Figure 4.14 shows the shear strength as a function of APTES content for PPG and PBAD based WPU-s adhered at 90 °C.

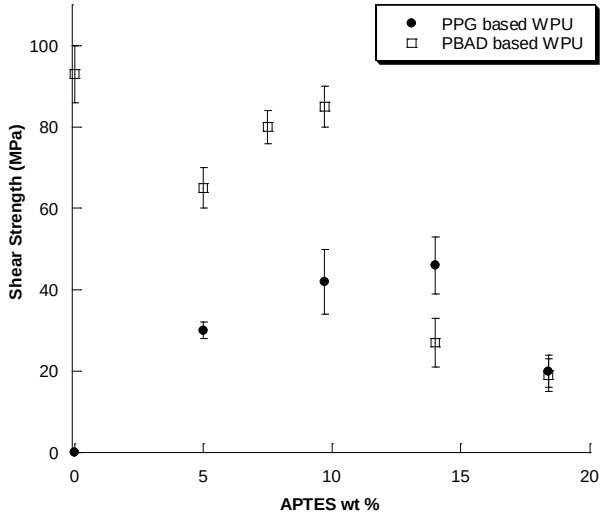

Figure 4.14. Shear strength vs. APTES content for systems based on PPG and PBAD at 90 °C.

As can be seen, in both cases the trend of the shear strength vs. APTES content is similar to that observed when the adhesion was performed at 25 °C. However, it must be pointed out that the values for PBAD systems are much higher than in the previous test. These results can be explained for the samples with no APTES and low APTES content

taking into account the crystallinity of the material. When the adhesion is performed at 90 °C, the polymer melts enhancing the contact between the substrate and the adhesive. However, there is not a clear explanation for the observed behaviour at high APTES contents, as the resulting systems are totally amorphous at room temperature. In our opinion this performance can be related to the higher viscosity of PBAD systems compared to the PPG ones. Considering that PBAD based WPU-s are more viscous than the PPG based ones, the adhesion at high temperatures promotes the chain mobility, improving the contact with the substrate and as a consequence improving the shear strength.

In the systems based on PPG the shear strength shows the same behaviour as that observed when the adhesion is performed at room temperature.

5.3.3. Effect of pre-formed and in-situ formed silica in Lap Shear Test

Different amounts of silica were added to the 9.7 wt. % APTES containing systems and their shear strength was determined (Figure 4.15).

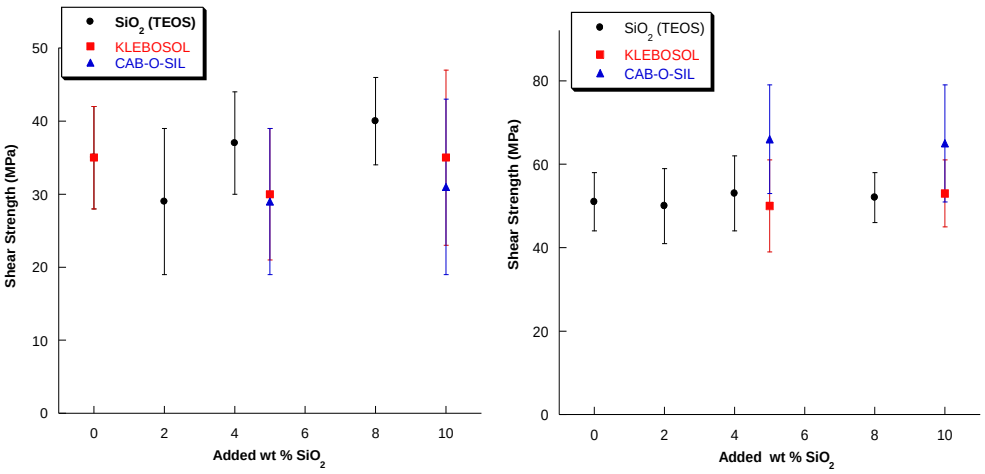

Figure 4.15. Shear strength vs. silica content and nature for (PPG (left) and PBAD (right) based systems carried out at room temperature.

As observed in Figure 4.15 it is clear that neither the type nor the content of silica have an effect on the shear strength in both types of systems (PPG and PBDA), as the adhesion values are quite similar for all of them taking into consideration experimental error. The addition of extra silica from different sources does not improve the adhesion strength probably because the amount of silica already present in the system (APTES) is the maximum for improving the adhesion strength.[70-73]

5.3.4. Peel Test

In order to examine the effect of APTES concentration on the final peel adhesion properties several tests were carried out for both systems and the results are shown in Figure 4.16.

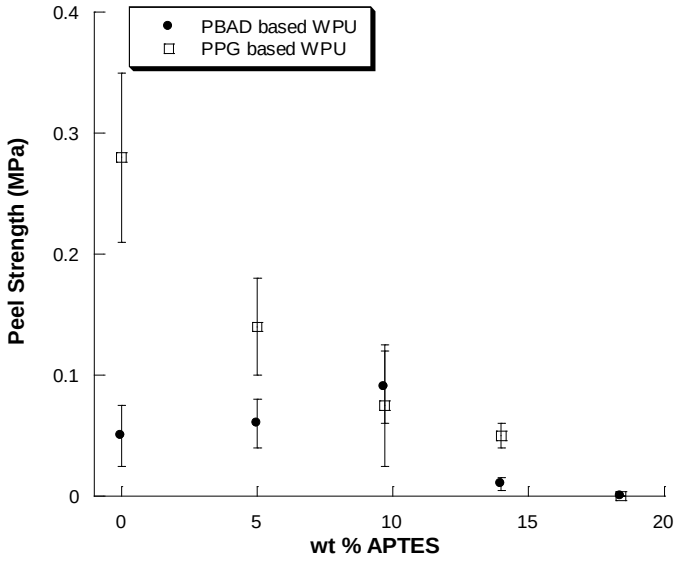

Figure 4.16. Peel Test results of PPG and PBAD based WPU-s as a function of APTES concentration.

It must be pointed out that the obtained peel adhesion values for all the systems are low. In all cases the adhesion failure was adhesive to PET. Moreover it is clearly observed that in the case of PPG based WPU-s the adhesion strength decreases with APTES content as

expected, due to the decrease of the elasticity of the system, reducing the peel adhesion capacity.

In contrast, in the case of the PBAD based WPU-s the adhesion strength increases slightly up to a value and then sharply decreases. In this case, the increase can be justified by the decrease of the cristallinity. However, once the system becomes amorphous the increase of APTES reduces the flexibility of the system and therefore the peel adhesion capacity.

Finally, in the case of pre-formed silica and TEOS (data not shown) no significant differences were observed obtaining similar values in all cases.

5.3.5. Shear Adhesion Failure Temperature (SAFT) Test

As mentioned, the SAFT test gives information about the maximum utilization temperature of an adhesive. All the adhesion measurements described so far were performed at room temperature. However, it is important to determine the upper temperature limit at which an adhesive is able to support a certain weight. In Figure 4.17 the temperature limit for supporting 1 kg of weight as a function of APTES for both series of polyurethanes is shown.

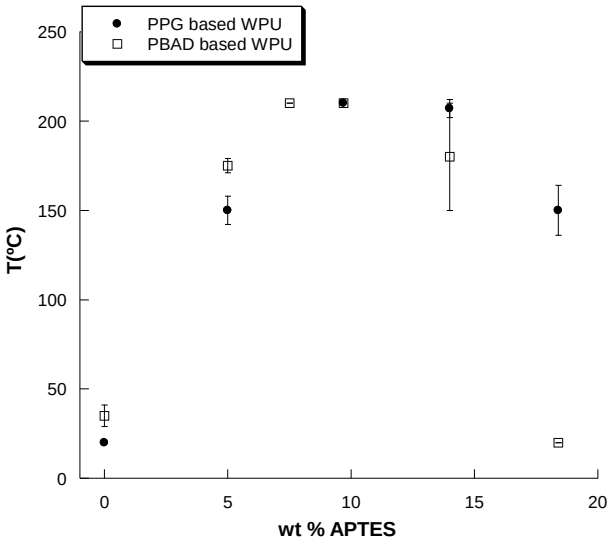

Figure 4.17. SAFT results of PPG and PBAD based WPU-s as a function of APTES concentration.

The maximum service temperature increases with APTES content up to a point where it starts to decrease. Accordingly, both systems present an optimum window of maximum service temperature between 5 and 15 wt. % of APTES. Therefore it can be considered that a certain degree of crosslinking is needed to increase the temperature resistance of the adhesive. However, large crosslinking degrees make the adhesive so rigid that it is unable to adhere to the substrate.

In fact, the systems containing 9.7 wt. % of APTES (for PBAD and PPG) were able to last at least a minimum of 12 hours at 210 °C.

6. TRANSPORT PROPERTIES

6.1. Introduction

All polymers are permeable to gases and vapors to a different extent. Permeability is a physical property of great importance in a variety of industrial and biomedical applications of polymers. Examples of these applications include: filtration, the separation of gas and liquid mixtures, water desalination, food packaging, protective coatings (e.g., paints and varnishes), controlled drug release and biomedical devices.[24,53,74-77]

Membranes can be classified in two main groups: porous and non porous or dense membranes. On the one hand, in the porous membranes, well defined pores are presented and the gases or vapors can go through them if their size is smaller than that of the pores. On the other hand, in the non porous membranes, gases or vapours permeate through membranes when a pressure differential is established between the two opposite membrane interfaces. The permeation of gases through nonporous membranes is generally described in terms of a "solution-diffusion" mechanism.[38-39,78]

According to this mechanism, gas permeation is a complex process consisting of the following sequence of events: (1) solution (absorption) of the gas at the exposed interface of the membrane with the higher pressure; (2) molecular ("random walk") diffusion of

the gas in and through the membrane; and (3) release of the gas from solution (desorption) at the opposite interface (exposed to a lower pressure). The term permeation is accordingly used here to describe the overall mass transport of the penetrant gas across the membrane.[78]

One option to improve the intrinsic permeability of polymers is the addition of inorganic materials, as these materials are considered impenetrable for gas molecules.[79] However, a poor interfacial adhesion between the organic and the inorganic moieties can generate holes facilitating the permeation of gases through the organic-inorganic membrane. Therefore, it is crucial to obtain a good compatibility between the organic/inorganic moieties in order to improve the permeability.[80]

In this section a variety of membranes were prepared by casting the dispersion onto a Teflon moulded employing PBAD and PPG based WPU-s containing different APTES concentrations and different silica origin and content. The oxygen permeability of these membranes was studied using a Mocon Oxtran 2/21 permeator (the sample preparation is depicted in Annex I).

6.2. Results and Discussion

In Figure 4.18 the effect of APTES content on the oxygen permeability coefficient is shown for PBAD and PPG based WPU-s. As observed, regardless of APTES concentration the PBAD based systems have lower permeability coefficients than those of PPG based ones. This result can be expected due to the semi-crystalline structure of PBAD based WPU-s compared to PPG based WPU-s and due to the lower polarity of the latter. It has been stated that the permeability coefficient can be related to the polarity of the polyurethane in the sense that the higher the polarity the lower the permeability coefficient.[39,76-77]

In addition, the permeability coefficients of both systems increase with APTES content, reaching a plateau at high APTES concentrations. In our opinion, this result is not consistent with the idea that the insertion of inorganic precursors, able to create inorganic moieties, increases gas tortuosity across the membrane reducing the permeability

coefficient.[24,79] However, according to Merkel et al.[81] the permeability coefficient can also increase as a consequence of the generation of defects in the polymer/filler interphase giving rise to a rapid and non selective diffusion (Knudsen diffusion).

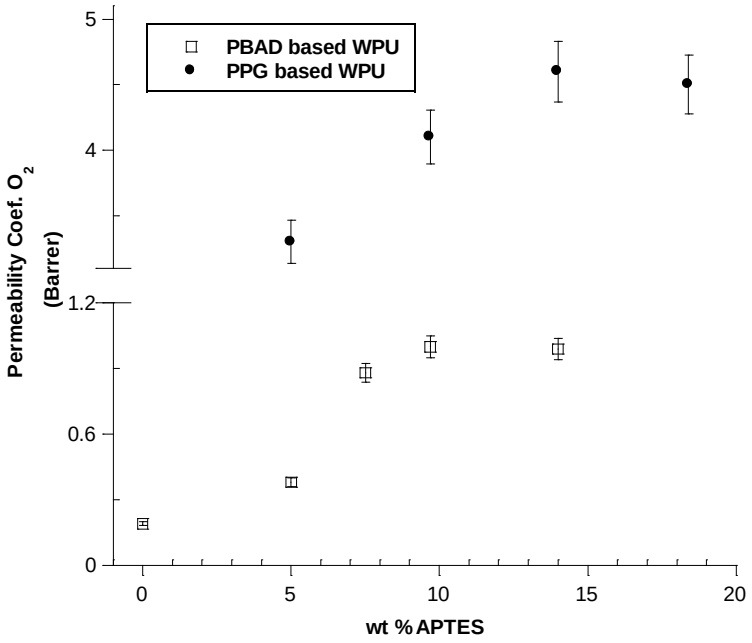

Figure 4.18. Oxygen permeability coefficient value as a function of APTES content for both types of polyurethanes.

In Figure 4.19 the effect of both the origin and content of silica is studied for PPG based WPU-s. As can be observed, the permeability coefficients decrease with silica content regardless of the silica nature in opposition to the data obtained with functionalized polyurethanes.

It seems that the incorporation of tetrafunctional silica makes the permeability decrease while the silica generated from APTES (trifunctional) has the opposite effect. It can be argued that the inorganic domains generated by APTES present uncondensed silica structures, facilitating the gas permeation. However, the introduction of silica via tetrafunctional groups gives rise to more perfect silica domains that increase the tortuosity path through the WPU membrane.

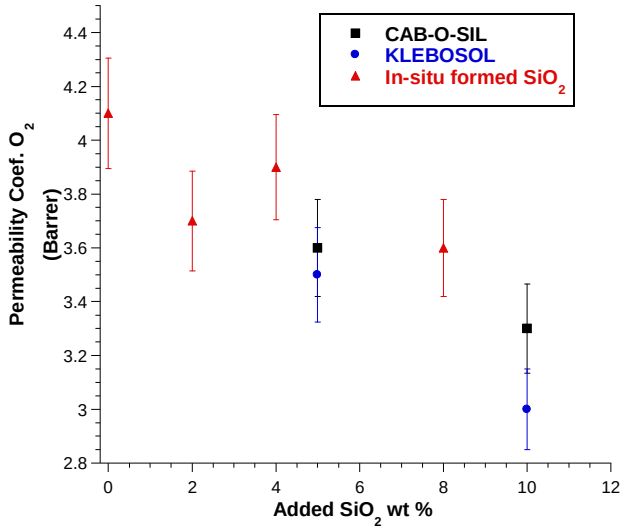

Figure 4.19. Permeability coefficient as a function of silica origin and concentration for PPG based WPU-s (0 point is considered the WPU containing 9.7 wt. % APTES).

In Figure 4.20. the effect of both the origin and content of silica are studied for PBAD based WPU-s with 9.7 wt. % APTES.

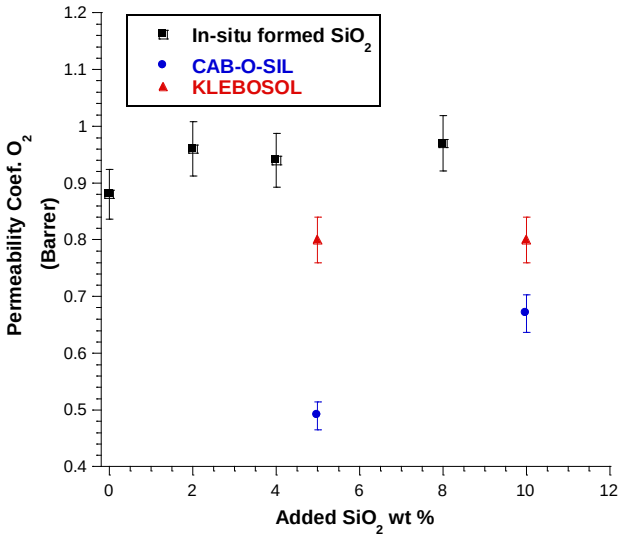

Figure 4.20. The permeability coefficient as a function of silica origin and concentration for PBAD based WPU-s (0 is considered the WPU containing 9.7 wt. % APTES).

The permeability coefficients do not change with the in situ formed silica. Furthermore, for the cases of Klebosol and CAB-O-SIL, the permeability coefficients decrease initially

with silica content up to a value where they keep constant, or increase. This result indicates that in the case of PBAD based WPU-s the improvement in the permeability coefficient is limited. This effect is probably due to the lower value of the permeability in PBAD based systems compared with those of the PPG based systems. The low permeability for CAB-O-SIL containing systems is probably related to the recovery of the PBAD cristallinity according to DSC data.

7. THERMAL DEGRADATION

7.1. Introduction

The widespread use of synthetic polymers has revolutionized the manufacturing industry and the range of products available. However, many synthetic polymers suffer from much greater thermal instability and flammability than traditional materials as the quest for synthetic polymers with good physical properties continues.

The well established TGA technique has been widely used over many decades in studying the thermal behaviour and properties of various types of polymeric materials and evaluating the thermal parameters for their degradation processes.

Although there are many reports in the literature devoted to the study of the maximum usage temperature and thermal degradation of polyurethanes, these studies are scarce in the case of waterborne polyurethanes.

In this work the thermogravimetric technique has been selected to study the thermal degradation of the different series of synthesized polyurethanes with respect to the effect of APTES, soft-segment nature and TEOS content.

7.2. Results and discussion

7.2.1. TGA analysis of WPU-s

Before examining the effect of APTES on the thermal stability of the synthesized systems, the thermogravimetric behaviour of polypropylene glycol and polyadipate based waterborne Polyurethanes was determined and compared with that of their counterparts which do not contain the internal emulsifier (DMPA).

Figure 4.21 shows the thermogram of a PPG based waterborne polyurethane without APTES containing approximately 40 wt. % of rigid segment. As can be seen, the polymer degrades basically in two steps that can be correlated with the decomposition of the rigid (1st step) and the flexible segments respectively. In addition, the percentage of mass loss of the first step coincides with the rigid segment content, corroborating that polyurethane decomposition starts through the rupture of the urethane linkages. In the second step, PPG decomposition takes place almost in one single step, without leaving any residue. This result is in total agreement with that of a polyurethane based on IPDI/PPG/BD with 35 wt. % of rigid segment (Figure 4.21). Although not shown, the same results were obtained for Poly(butylene adipate) based WPU-s. Therefore, we can conclude that the presence of DMPA does not alter the thermal stability of WPU-s.

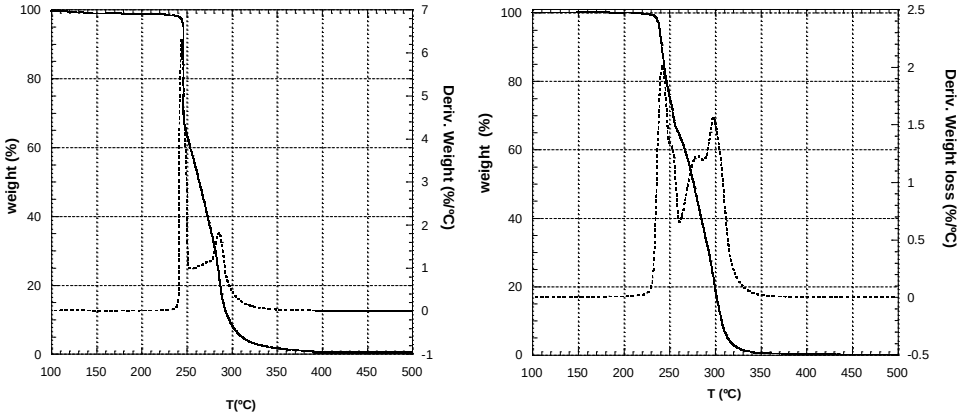

Figure 4.21. TGA and DTG curves of PPG based PU-s with (right) and without (left) DMPA.

7.2.2. Effect of APTES on the thermal stability

In order to examine the effect of APTES on the thermal stability, TGA analysis for waterborne PBAD/IPDI and PPG/IPDI based systems with different APTES contents were carried out. As has been mentioned on several occasions through the manuscript, the incorporation of APTES to the chain end of the polymer makes the system crosslink due to the hydrolysis and condensation reactions of alkoxy groups.

Figure 4.22 displays the thermograms of PPG based systems with different APTES content. As can be seen, the crosslinked films present more complex thermal behaviour than the non-functionalized homonymous.

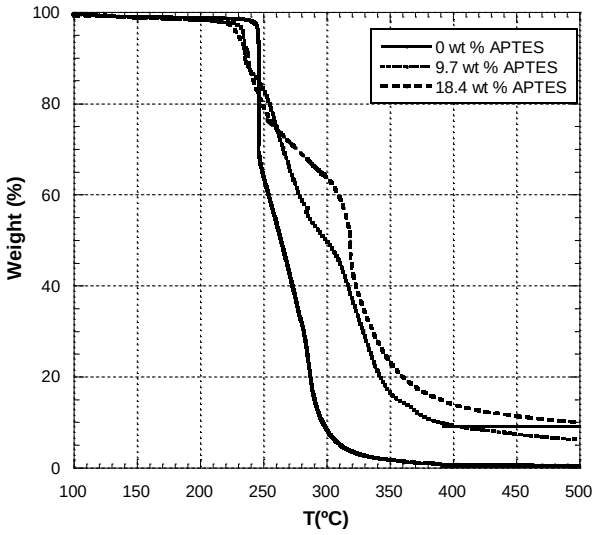

Figure 4.22. TGA curves of PPG based WPU-s containing different APTES concentrations.

Thus, the functionalized systems show a mass loss distributed in several steps. In the first one, where it is known that the degradation of the rigid segment takes place, the observed mass loss is much lower than the rigid content (about 40 wt. %), and in addition, this mass loss decreases with APTES content. In the temperature region between 250 °C and 300 °C, the soft segment of the non-functionalized system decomposes almost completely, while in the two functionalized ones the remaining mass

is about 50 wt. % and 64 wt. % respectively. Between 350 °C and 600 °C a new mass loss step is observed, which must be related to the concentration of APTES rigid segment. After the inclusion of air in the system an additional 3 wt. % mass loss is detected for both functionalized systems, which can be related to the volatilization of organic moieties entrapped in the inorganic network. Finally, a residue of about 3 wt. % and 6 wt. % is observed, which can be associated with the SiO_2 content.

The thermograms of PBAD based systems are shown in Figure 4.23. In this case, both rigid and soft segments decompose in the same temperature range, making it difficult to distinguish the two degradation processes observed for PPG based systems. However, here again the remaining mass at 350 °C increases with APTES concentration. Between 350 and 600 °C there is also a mass loss step that can be related with the organic moieties entrapped in the inorganic network. Finally, the residue content agrees with the content of the inorganic domains.

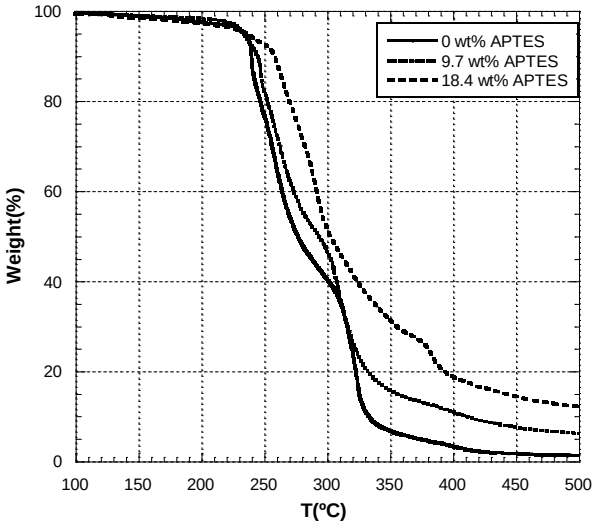

Figure 4.23. TGA curves of PBAD based WPU-s containing different APTES concentrations.

According to these results, it is evident that the presence of APTES modifies the degradation profile of the samples. Although their degradation onset temperature is almost the same, the temperature range where the overall mass loss takes place,

increases with APTES concentration. This result can indicate that the SiO2 network prevents the volatilization of the chain extremes to some extent. In addition, the participation of the chain ends acquires more relevance at high APTES contents because the polymer molecular weight decreases with increasing the functionalization agent. Finally, the residue content is in accordance with the percentage of inorganic domains.

7.2.3. Effect of pre-formed silica and commercial silica

The effect of the "in situ" formed silica on the thermal degradation for both series of WPU-s (PPG and PBAD) was studied (Figure 4.24).

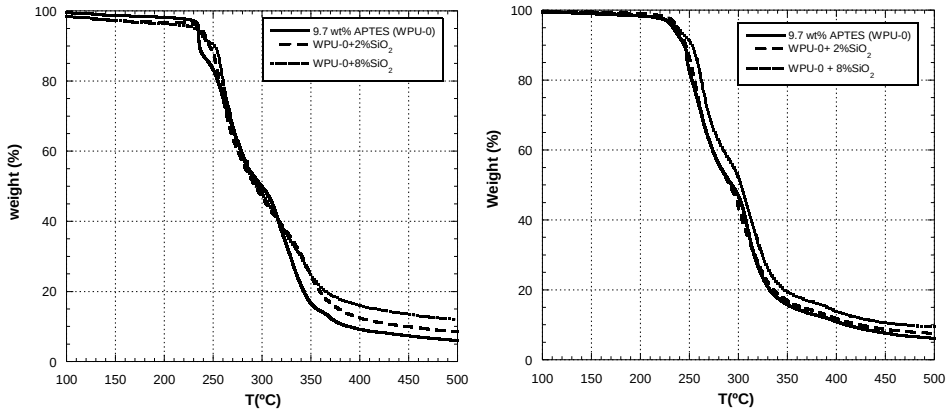

Figure 4.24. TGA curves of PBAD (left) and PPG (right) based WPU-s containing different silica contents.

As observed, there is no improvement in the thermal degradation as a function of silica content. The TGA curves are identical in all cases, observing a higher residue as silica content increases.

8. CONCLUSIONS

In this chapter the main properties and characteristics of synthesized polyurethanes were studied using different experimental techniques such as DSC, DMTA, Stress-Strain measurements, Shear Strength, Lap Shear Test, Peel Test, SAFT test, Oxygen Permeability Test and TGA. The main conclusions from these studies are summarized below:

According to DSC and DMTA experiments, the incorporation of APTES in the systems favours the phase separation between the rigid and flexible segments of WPU-s. Moreover, APTES reduces the relative crystallinity of PBAD WPU-s.

In addition, APTES also has a large effect on the mechanical properties of the films as a consequence of the increase in their crosslinking density. The greater the APTES content the larger the crosslinking density, making the systems more rigid, and reducing the elongation and increasing the modulus. In the case of PBAD based systems, the opposite behaviour is observed in the range of low APTES concentrations as a consequence of a relative crystallinity decrease. Once the systems become amorphous (high APTES content), the same behaviour as that of PPG based systems is observed. However, the addition of preformed and in situ formed silica does not have a pronounced effect on the mechanical properties.

The Lap Shear Tests have demonstrated that all the systems studied show a good adhesion performance both at room and at high temperatures, and the adhesion properties are influenced by APTES content. Thus, the Lap Shear adhesion increases as a function of APTES up to a point where the adhesion capacity disappears due to the rigidity of the material. According to SAFT results both PBAD and PPG based systems present an optimum window of maximum service temperature between 5 and 15 wt. %o APTES.

In relation to TGA experiments it can be concluded that the presence of APTES modifies the degradation mechanisms of both PPG and PBAD based systems. Although the degradation onset temperatures are almost the same as those of the non containing

APTES samples, the temperature at which the overall mass loss takes place clearly increases with the amount of APTES.

The Oxygen Permeability of the films increases with the content of APTES indicating that some defects at the interface of the inorganic domains/polymer can have been generated or/and that silica presents uncondensed structures that facilitate the gas permeation through the films.

9. BIBLIOGRAPHY

1 http://www.bayermaterialsciencenafta.com/processing/cas/1k-waterborne/index.html.

2 http://www.bayermaterialsciencenafta.com/processing/cas/2k-waterborne/index.html.

3 Hepburn, C. Polyurethane elastomers. (Elsevier Applied Science, 1992).

4 Frisch, K. 60 years of polyurethanes. (Kresta JE, 1998).

5 Wojcik, R. T. PU coatings: from raw materials to end-products. (Technomic Publishing, 1998).

6 Rink, H. P. & Mayer, B. Water-based coatings for automotive refinishing. Progress in Organic Coatings 34, 175-180 (1997).

7 http://www.p2pays.org/ref/01/00777/alternat.htm.

8 Cheng, K., Chen, W. Method for the preparation of water-borne polyurethane adhesive. US Patent 6191214 B1 patent (2001).

9 Ai, Z., Deng, R., Zhou, Q., Liao, S. & Zhang, H. High solid content latex: Preparation methods and application. Advances in Colloid and Interface Science 159, 45-59 (2010).

10 Polyurethanes for high performance coatings V. Focus on Powder Coatings 2008, 7-8 (2008).

11 Segura, D. M., Nurse, A. D., McCourt, A., Phelps, R. & Segura, A. in Handbook of adhesives and sealants Vol. 1 (ed Cognard Philippe) 101-162 (Elsevier Science Ltd, 2005).

12 Jena, K. K. & Raju, K. V. S. N. Synthesis and characterization of hyperbranched polyurethane hybrids using tetraethoxysilane (TEOS) as cross-linker. Industrial & Engineering Chemistry Research 47, 9214-9224 (2008).

13 Chen, G., Zhou, S., Gu, G. & Wu, L. Acrylic-based polyurethane/silica hybrids prepared by acid-catalyzed sol–gel process: structure and mechanical properties. Macromolecular Chemistry and Physics 206, 885-892 (2005).

14 Choi, H. Y., Bae, C. Y. & Kim, B. K. Nanoclay reinforced UV curable waterborne polyurethane hybrids. Progress in Organic Coatings 68, 356-362 (2010).

15 Chen, J., Zhou, Y., Nan, Q., Sun Y., Ye, X. & Wang Z. Synthesis, characterization and infrared emissivity study of polyurethane/TiO2 nanocomposites. Applied Surface Science 253, 9154-9158 (2007).

16 Schubert, U., Huesing, N. & Lorenz, A. Hybrid inorganic-organic materials by Sol-Gel processing of organofunctional metal alkoxides. Chemistry of Materials 7, 2010-2027 (1995).

17 Kim, B. K., Seo, J. W. & Jeong, H. M. Morphology and properties of waterborne polyurethane/clay nanocomposites. European Polymer Journal 39, 85-91 (2003).

18 Rekondo, A., Fernández-Berridi, M. J. & Irusta, L. Synthesis of silanized polyether urethane hybrid systems. Study of the curing process through hydrogen bonding interactions. European Polymer Journal 42, 2069-2080 (2006).

19 Florian, P., Jena, K. K., Allauddin, S., Narayan, R. & Raju, K. V. S. N. Preparation and characterization of waterborne hyperbranched polyurethane-urea and their hybrid coatings. Industrial & Engineering Chemistry Research 49, 4517-4527 (2010).

20 Chen, H., Fan, Q., Chen, D. & Yu, X. Synthesis and properties of polyurethane modified with an aminoethylaminopropyl-substituted polydimethylsiloxane. II. Waterborne polyurethanes. Journal of Applied Polymer Science 79, 295-301 (2001).

21 Chen, Y., Zhou, S., Yang, H. & Wu, L. Structure and properties of polyurethane/nanosilica composites. Journal of Applied Polymer Science 95, 1032-1039 (2005).

22 Subramani, S., Lee, J. M., Cheong, I. W. & Kim, J. H. Synthesis and characterization of water-borne crosslinked silylated polyurethane dispersions. Journal of Applied Polymer Science 98, 620-631 (2005).

23 Yang, C. H., Liu, F. J., Liu, Y. P. & Liao, W. T. Hybrids of colloidal silica and waterborne polyurethane. Journal of Colloid and Interface Science 302, 123-132 (2006).

24 Zhou, H., Chen, Y., Fan, H., Shi, H., Luo, Z. & Shi, B. The polyurethane/SiO2 nano-hybrid membrane with temperature sensitivity for water vapor permeation. Journal of Membrane Science 318, 71-78 (2008).

25 Subramani, S., Lee, J. Y., Choi, S. W. & Kim, J. H. Waterborne trifunctional silane-terminated polyurethane nanocomposite with silane-modified clay. Journal of Polymer Science Part B: Polymer Physics 45, 2747-2761 (2007).

26 Chattopadhyay, D. K. & Raju, K. V. S. N. Structural engineering of polyurethane coatings for high performance applications. Progress in Polymer Science 32, 352-418 (2007).

27 Chattopadhyay, D. K. & Webster, D. C. Thermal stability and flame retardancy of polyurethanes. Progress in Polymer Science 34, 1068-1133 (2009).

28 Bourgeat-Lami, E. in Encyclopedia of nanoscience and nanotechnology Vol. 8 (ed Singh Nalwa Hayri) (American Scientific Publishers, 2004).

29 Bourgeat-Lami, E. Organic-inorganic nanostructured colloids. Journal of Nanoscience and Nanotechnology 2, 1-24 (2002).

30 Bourgeat-Lami, E., Herrera, N., Putaux, J.L., Perro, A., Reculusa, S., Ravaine, S. & Duguet E. Designing organic/inorganic colloids by heterophase polymerization. Macromolecular Symposia 248, 213-226 (2007).

31 Caruso, R. A. & Antonietti, M. Sol-gel nanocoating: An approach to the preparation of structured materials. Chemistry of Materials 13, 3272-3282 (2001).

32 Zou, H., Wu, S. & Shen, J. Polymer/silica nanocomposites: preparation, characterization, properties, and applications. Chemical Reviews 108, 3893-3957 (2008).

33 Jeon, H. T., Jang, M. K., Kim, B. K. & Kim, K. H. Synthesis and characterizations of waterborne polyurethane-silica hybrids using Sol-Gel process. Colloids and Surfaces A: Physicochemical and Engineering Aspects 302, 559-567 (2007).

34 Yoon Jang, J., Kuk Jhon, Y., Woo Cheong, I. & Hyun Kim, J. Effect of process variables on molecular weight and mechanical properties of water-based polyurethane dispersion. Colloids and Surfaces A: Physicochemical and Engineering Aspects 196, 135-143 (2002).

35 Zheng, J., Luo, J., Zhou, D., Shen, T., Li, H., Liang, L. & Lu, M. Preparation and properties of non-ionic polyurethane surfactants. Colloids and Surfaces A: Physicochemical and Engineering Aspects 363, 16-21 (2010).

36 Cho, J. W. & Lee, S. H. Influence of silica on shape memory effect and mechanical properties of polyurethane-silica hybrids. European Polymer Journal 40, 1343-1348 (2004).

37 Lai, S. M., Wang, C. K. & Shen, H. F. Properties and preparation of thermoplastic polyurethane/silica hybrid using sol–gel process. Journal of Applied Polymer Science 97, 1316-1325 (2005).

38 Hsieh, K. H., Tsai, C. C. & Chang, D. M. Vapor and gas permeability of polyurethane membranes. Part II. Effect of functional group. Journal of Membrane Science 56, 279-287 (1991).

39 Hsieh, K. H., Tsai, C. C. & Tseng, S. M. Vapor and gas permeability of polyurethane membranes. Part I. Structure-property relationship. Journal of Membrane Science 49, 341-350 (1990).

40 Finnigan, B., Martin, D., Halley, P., Truss, R. & Campbell, K. Morphology and properties of thermoplastic polyurethane nanocomposites incorporating hydrophilic layered silicates. Polymer 45, 2249-2260 (2004).

41 Lee, Y. M., Lee, J. C. & Kim, B. K. Effect of soft segment length on the properties of polyurethane anionomer dispersion. Polymer 35, 1095-1099 (1994).

42 Wen, T. C., Wang, Y. J., Cheng, T. T. & Yang, C. H. The effect of DMPA units on ionic conductivity of PEG-DMPA-IPDI waterborne polyurethane as single-ion electrolytes. Polymer 40, 3979-3988 (1999).

43 Xiaojuan, L., Xiaorui, L., Lei, W. & Yiding, S. Synthesis and characterizations of waterborne polyurethane modified with 3-aminopropyltriethoxysilane. Polymer Bulletin 65, 45-57 (2010).

44 Chattopadhyay, D. K., Mishra, A. K., Sreedhar, B. & Raju, K. V. S. N. Thermal and viscoelastic properties of polyurethane-imide/clay hybrid coatings. Polymer Degradation and Stability 91, 1837-1849 (2006).

45 Modesti, M., Lorenzetti, A., Besco, S., Hrelja, D., Semenzato, S., Bertani, R. & Michelin, R. A. Synergism between flame retardant and modified layered silicate on thermal stability and fire behaviour of polyurethane nanocomposite foams. Polymer Degradation and Stability 93, 2166-2171 (2008).

46 Blank, W. J. & Tramontano, V. J. Properties of crosslinked polyurethane dispersions. Progress in Organic Coatings 27, 1-15 (2006).

47 Chattopadhyay, D. K., Muehlberg, A. J. & Webster, D. C. Organic-inorganic hybrid coatings prepared from glycidyl carbamate resins and amino-functional silanes. Progress in Organic Coatings 63, 405-415 (2008).

48 Czech, Z. & Pelech, R. Thermal decomposition of polyurethane pressure-sensitive adhesives dispersions. Progress in Organic Coatings 67, 72-75 (2010).

49 Król, P., Pielichowska, K. & Byczynski, L. Thermal degradation kinetics of polyurethane-siloxane anionomers. Thermochimica Acta 507-508, 91-98 (2010).

50 Kanapitsas, A., Pissis, P., Gomez-Ribelles, J. L., Monleon-Pradas, M., Privalko, E.G. & Privalko, V.P. Molecular mobility and hydration properties of segmented

polyurethanes with varying structure of soft- and hard-chain segments. Journal of Applied Polymer Science 71, 1209-1221 (1999).

51 Camberlin, Y. & Pascault, J. P. Quantitative DSC evaluation of phase segregation rate in linear segmented polyurethanes and polyurethaneureas. Journal of Polymer Science: Polymer Chemistry Edition 21, 415-423 (1983).

52 Lee, D. K., Tsai, H. B. & Stanford, J. L. Phase separation in segmented polyurethanes derived from mixtures of polyether polyols with different functionality. Journal of Polymer Research 3, 221-225 (1996).

53 Mondal, S. & Hu, J. L. Structural characterization and mass transfer properties of nonporous segmented polyurethane membrane: Influence of hydrophilic and carboxylic group. Journal of Membrane Science 274, 219-226 (2006).

54 Seo, J. W. & Kim, B. K. Preparation and properties of waterborne polyurethane /nanosilica composites. Polymer Bulletin 54, 123-128 (2005).

55 Wang, L., Shen, Y., Lai, X., Li, Z. & Liu, M. Synthesis and properties of crosslinked waterborne polyurethane. Journal of Polymer Research, 1-8 (2010).

56 Jiang X. L., Luo, S. J. & Chen, X. D. Effect of nucleating agents on crystallization kinetics of PET. Express polymer Letters 4, 245-251 (2007)

57 Kwon, J., Rahman, M. & Kim, H. Preparation and properties of crosslinkable waterborne polyurethanes containing aminoplast. Fibers and Polymers 7, 95-104 (2006).

58 Ahn, B. U., Lee, S. K., Lee, S. K., Park, J. H. & Kim, B. K. UV curable polyurethane dispersions from polyisocyanate and organosilane. Progress in Organic Coatings 62, 258-264 (2008).

59 Subramani, S., Lee, J. M., Lee, J. Y. & Kim, J. H. Synthesis and properties of room temperature curable trimethoxysilane-terminated polyurethane and their dispersions. Polymers for Advanced Technologies 18, 601-609 (2007).

60 Burchardt, B. R. & Merz, P. W. Handbook of adhesives and sealants Vol. 2 (ed Cognard Philippe) (Elsevier Science Ltd 2006).

61 Rehab, A. & Salahuddin, N. Nanocomposite materials based on polyurethane intercalated into montmorillonite clay. Materials Science and Engineering: A 399, 368-376 (2005).

62 Lai, S. M. & Liu, S. D. Properties and preparation of thermoplastic polyurethane/silica hybrids using a modified sol–gel process. Polymer Engineering & Science 47, 77-86 (2007).

63 Judeinstein, P. & Sanchez, C. Hybrid organic-inorganic materials: a land of multidisciplinarity. Journal of Materials Chemistry 6, 511-525 (1996).

64 Han, Y. H., Taylor, A., Mantle, M. D. & Knowles, K. M. Sol-Gel derived organic-inorganic hybrid materials. Journal of Non-Crystalline Solids 353, 313-320 (2007).

65 Lai, S. M., Wang, C. K. & Shen H. F. Properties and preparation of thermoplastic polyurethane/silica hybrid using Sol-Gel process. Journal of Applied Polymer Science 97, 1316-1325 (2005).

66 Chen, J. J., Zhu, C. F., Deng, H. T., Qin, Z. N. & Bai, Y. Q. Preparation and characterization of the waterborne polyurethane modified with nanosilica. Journal of Polymer Research 16, 375-380 (2009).

67 Packham, D. E. Handbook of adhesion. Second edn, (John Wiley & Sons, Ltd, 2005).

68 Lacombe, R. Adhesion measurement methods: theory and practice. (Hopewell Junction, 2005).

69 Mittal, K. L. Adhesion measurements of films & coatings. Vol. 2 (VSP, 1995).

70 Torró-Palau, A. M., Fernández-García, J. C., César Orgilés-Barceló, A. & Martín-Martínez, J. M. Characterization of polyurethanes containing different silicas. International Journal of Adhesion and Adhesives 21, 1-9 (2001).

71 Orgilés-Calpena, E., Arán-Aís, F., Torró-Palau, A. M., Orgilés-Barceló, C. & Martín-Martínez, J. M. Influence of the chemical structure of urethane-based thickeners on the properties of waterborne polyurethane adhesives. The Journal of Adhesion 85, 665-689 (2009).

72 Torró-Palau, A., Fernández-García, J. C., Orgilés-barceló, A. C., Pastor-Blas, M. M. & Martín-martínez, J. M. Comparison of the properties of polyurethane adhesives containing fumed silica or sepiolite as filler. The Journal of Adhesion 61, 195-211 (1997).

73 Maciá-Agulló, T. G., Fernández-García, J. C., Pastor-sempere, N., Orgilés-Barceló, A. C. & Martín-Martínez, J. M. Addition of silica to polyurethane adhesives. The Journal of Adhesion 38, 31-53 (1992).

74 Teo, L. S., Chen, C. Y. & Kuo, J. F. The gas transport properties of amine-containing polyurethane and poly(urethane-urea) membranes. Journal of Membrane Science 141, 91-99 (1998).

75 Meng, Q. B., Lee, S. I., Nah, C. & Lee, Y. S. Preparation of waterborne polyurethanes using an amphiphilic diol for breathable waterproof textile coatings. Progress in Organic Coatings 66, 382-386 (2009).

76 Wolinska-Grabczyk, A. & Jankowski, A. Gas transport properties of segmented polyurethanes varying in the kind of soft segments. Separation and Purification Technology 57, 413-417 (2007).

77 Ponangi, R., Pintauro, P. N. & De Kee, D. Free volume analysis of organic vapor diffusion in polyurethane membranes. Journal of Membrane Science 178, 151-164 (2000).

78 Stern, S. A. & Fried, J. R. in Physical properties of polymers handbook (ed James E. Mark) 1033-1047 (Springer, 2007).

79 Vladimirov, V., Betchev, C., Vassiliou, A., Papageorgiou, G. & Bikiaris, D. Dynamic mechanical and morphological studies of isotactic polypropylene/fumed silica nanocomposites with enhanced gas barrier properties. Composites Science and Technology 66, 2935-2944 (2006).

80 Lagaron, J. M., Catalá, R. & Gavara, R. Structural characteristics defining high barrier properties in polymeric materials. Materials Science and Technology 20, 1-7 (2004).

81 Merkel, T.C., Freeman B. D., Spontak, R. J., He, Z., Pinnau, I., Meakin, P. & Hill A. J. Sorption, transport, and structural evidence for enhanced free volume in Poly(4-methyl-2-pentyne)/fumed silica nanocomposite membranes. Chemistry of Materials 15, 109-123 (2003)

CHAPTER V: CONCLUSIONS

CONCLUSIONS

In this chapter the main conclusions of this thesis are summarized.

- The synthesis of water polyurethane dispersions based on isophorone diisocyanate (IPDI) and two different soft segments, polypropylene glycol (PPG) and poly(1,4-butylene adipate) (PBAD), were successfully carried out using 1,4-butanediol (BD) and 2-bis(hydroxymethyl) propionic acid (DMPA) as hard segments. For this purpose two catalysts were employed: the commonly used tin compound (DBTDA) and $Zr(acac)_4$. An important difference in the polymerization mechanism was observed depending on the catalyst employed.

- Polyurethane dispersions were obtained by means of the acetone process and the results showed that a minimum amount of ionic groups (DMPA), as a function of polyurethane initial concentration, is required in order to obtain stable polyurethane dispersions. When the phase inversion process was performed at temperatures higher than 35 °C the particle size increased and the dispersions became unstable and the same effect was observed when acetone was removed at high temperatures. Therefore, low phase inversion and mild evaporation temperatures must be used in order to obtain stable dispersions. These results can be of great interest in the production of different particle size dispersions that can be commercialized as low VOC polyurethane adhesives.

- Polyurethane dispersions based on both PPG and PBAD containing covalently bonded alkoxysilane end groups were also successfully obtained by means of the acetone process using different concentrations of APTES. The quantitative incorporation of the alkoxysilane groups into the polyurethane chains was confirmed by means of FTIR, ^{1}H-NMR and elemental analyses.

- According to DLS results, the final particle size and morphology of the dispersions clearly depend on APTES concentration, especially in the range of high concentrations. From TEM results it can be concluded that totally homogeneous

dispersions are obtained at low APTES concentrations while inorganic-rich domain containing particles are observed when the APTES concentration is higher than 9.7 wt. %.

- ^{29}Si-NMR, FTIR and gel and swelling measurements confirmed that these dispersions are able to cure at room temperature because of the condensation of alkoxysilane end groups during the drying process, giving rise to covalently linked organic/inorganic hybrid films.

- Waterborne polyurethane/silica nanostructures were successfully prepared through the Sol-Gel process using TEOS as the inorganic precursor and the best experimental conditions for the Sol-Gel reaction were established. At large TEOS concentrations stable and homogeneous dispersions could only be obtained using functionalized WPU-s. After drying these dispersions, films with a good distribution of the inorganic domains were only obtained using functionalized WPU-s.

- When polyurethane/silica nanostructures were obtained by physical blending the homogeneity of the dispersions and the corresponding films was considerably reduced compared to that of the systems obtained by the Sol-Gel process.

- The results of the thermal, mechanical, adhesion and transport properties of the synthesized systems demonstrated that the insertion of APTES improves most of the properties of the films. However, it must be pointed out that a good dispersion of the inorganic moieties into the polyurethane matrix does not ensure the improvement of the final properties.

ANNEX I: EXPERIMENTAL TECHNIQUES

ANNEX I: EXPERIMENTAL TECHNIQUES

1. FOURIER TRANSFORM INFRARED SPECTROSCOPY (FTIR)

FTIR was employed to characterize both the reagents employed, and the products obtained in this memory. This technique was also utilized to study the reaction kinetics and mechanism in the synthesis of waterborne polyurethanes.

All the spectra were recorded using a Nicolet 6700 spectrometer at a resolution of 2 cm^{-1}, and a total of 64 interferograms were signal averaged. All the spectra were obtained from solution or dispersion casting onto KBr or KRS-5 windows respectively.

1.1. Characteristic FTIR bands of polyurethanes

In Annex 1.1 the most important bands are summarized.

Position (cm^{-1})	Assignation
3420	Stretching vibration free N-H
3320	Stretching vibration associated N-H
2850-3000	Stretching vibration of R groups
1750-1690	Stretching vibration of C=O groups (free & associated) Amide I
1500-1580	Stretching vibration of C-N + deformation of N-H (Amide II)
1460-1490	Bending vibration CH_3 & CH_2
1375	Bending vibration CH_3
1300	Bending vibration N-H + Stretching vibration C-N (Amide III)
1240	Stretching vibration of C-O-C=O of urethane
1180	Stretching vibration of C-O-C=O in the case of PBAD (ester)
1100	Stretching vibration of C-O-C in the case of PPG (ether)

Annex 1.1. Vibration frequencies of the principal groups present in polyurethanes.

All polyurethane FTIR spectra have in common a band at 3300 cm^{-1} assigned to the N-H streching vibration associated by hydrogen bonding. Moreover, a band attributted to the streching vibration of carbonyl groups appears at 1720 cm^{-1} (Amide I). In some cases this band can present two contributions. In addition, all polyurethanes present a band at 1550 cm^{-1} (known as Amide II) attributable to a combination of C-N streching and N-H bending vibrations. Finally, due to the presence of polyether and polyester diols, an intense band assigned to C-O-C (1100 cm^{-1}) and C-O-C=O streching vibrations (1200 cm^{-1}) appears respectively.[1-4]

2. NUCLEAR MAGNETIC RESONANCE (NMR) ^{1}H, ^{13}C AND ^{29}SI

2.1. Introduction

^{1}H, ^{13}C and ^{29}Si NMR spectroscopies were used in order to characterize the reagents, the products obtained together with the reaction kinetics and mechanisms in the synthesis of waterborne polyurethanes.[5-6] All the NMR liquid spectra were recorded in acetone. Liquid Nuclear Magnetic spectra were obtained in a Fourier Transform Bruker 300 MHz spectrometer (model avance 300 DPX). 0.75 mL from the reactor was charged into the NMR tube and a small amount of deuterated acetone was added using tetramethylsilane (TMS) as internal standard.

2.2. Introduction to ^{29}Si NMR

^{29}Si NMR is becoming an important characterization technique in order to study compounds with silicon atoms. Lippmma et al[7-8] designed a model to name all the possible silicon atoms. The atom is called M, D, T or Q depending on the number of oxygen atoms linked to silicon and a subscript is added to give information about the number of oxygen atoms linked to another silicon atom (Annex 1.2).

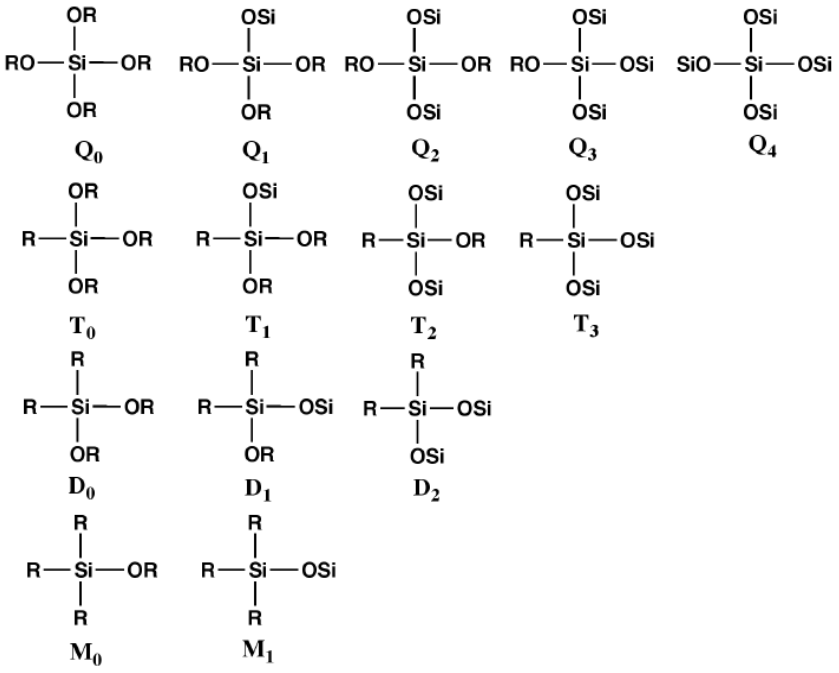

Annex 1.2. Structures coexisting in the Sol-Gel process, as called by Lippmaa et al[7-8].

2.3. Solid NMR technique

The cross polarization magic angle spinning (CP/MAS), is the most employed strategy when solid NMR spectroscopy is applied. In order to obtain a quantitative analysis experimental conditions must be appropriately chosen. Following the literature and according to previous experiments of the group, the solid NMR spectra were recorded using a 4 mm diameter rotor in a CP/MAS probe. The cross polarization contact time for the hybrid materials was fixed to 1.6 ms. Cross polarization inversion recovery experiments yielded a short relaxation delay of 2 seconds. The spectra were recorded at 59.6 MHz with a superconductor of 7 T.

The solid-state NMR technique, and particularly ^{29}Si CP/MAS NMR, was used to study the composition of both the coupling agent and inorganic precursor in the films and also to characterize the grafting of TEOS onto the functionalized polyurethane particles.[9-10]

3. TURBISCAN

Turbiscan Lab is an instrument for the optical characterization of liquid dispersions[11]. The dispersion is placed in a cylindrical glass measurement cell, which is completely scanned by a light source. Two synchronous detectors collect on the one hand the transmitted light (180 °C from the incident light) and on the other hand the backscattered light (45 °C from the incident radiation) by the sample. Both of them are directly dependent on the particle mean diameter and volume fraction.

The Turbiscan can work in scanning mode (measurements can be acquired every 40 μm) providing the transmitted and backscattered light fluxes as a function of sample height (in mm). In this work backscattering was employed to study the stability of the obtained final dispersions. This technique allows visualization of creaming (disperse phase due to the lower density goes to the top of the sample increasing the backscattering), sedimentation (the sample precipitates and an increase in the backscattering at the bottom of the samples is observed) or particles coalescence or flocculation (the particles merge and there is an increase in the droplet size decreasing the backscattering).

4. DYNAMIC LIGHT SCATTERING (DLS)

Light scattering (DLS) is one of the most used techniques for the determination of particle size and particle size distribution.[12] When a light beam impinges onto a solution or dispersion of particles, these particles scatter a fraction of light changing the wavelength of the incoming light. In this method the experiment duration is short and the sample preparation is easy. However, one of the main disadvantages is that in order to avoid multiple light scattering particles need to be diluted before performing the measurements.

This technique was used to estimate the diameters of the polymer particles, the inorganic particles and also the functionalized and hybrid particles. Particle size was measured using a Malvern Zetasizer. The analyses were carried out at 25 °C in deionised water. The results are the overage of three measurements, each of them consisting in twelve runs.

5. ZETA POTENTIAL MEASUREMENTS

Zeta potential is an important parameter in order to determine the surface of colloidal particles[13]. Most particles dispersed in an aqueous system will acquire a surface charge, principally either by ionization of surface groups, or adsorption of charged species. The development of a net charge at the particle surface affects the distribution of ions in the surrounding interfacial region, resulting in an increased concentration of counter ions (ions of opposite charge to that of the particle) close to the surface. Thus an electrical double layer exists around each particle (Annex 1.3).

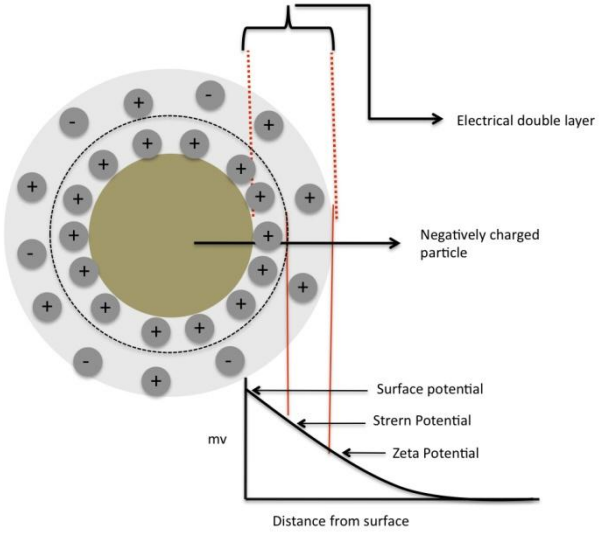

Annex 1.3. Schematic showing the distribution of ions around a charged particle.

The liquid layer surrounding the particle exists as two parts, an inner region, called the Stern layer, where the ions are strongly bound and an outer, diffuse, region where they are less firmly attached. Within the diffuse layer there is a notional boundary inside which the ions and particles form a stable entity. When a particle moves, ions within the boundary move with it, but any ions beyond the boundary do not travel with the particle. This boundary is called the surface of the hydrodynamic shear or slipping plane.

The potential that exists at this boundary in known as the zeta potential. In this work Zeta potential was determined through evaluation of the electrophoretic mobility measured by laser Doppler velocimetry. All measurements were recorded at 25 °C. Dispersions were prepared at 1 $g.L^{-1}$ in deionized water mixed with a background electrolyte (NaCl 0.01 M) in order to fix the ionic strength. pH was adjusted using 0.1 M NaOH or 0.1 M HCl.[14]

6. DIFFERENTIAL SCANNING CALORIMETRY (DSC)

DSC measurements were carried out in a TA INSTRUMENT Q 2000. The samples were dried for at least one week at 25 °C under vacuum and afterwards placed in the DSC pan and heated to 150 °C and kept for one week at room temperature before performing the heating ramp from -80 °C to 150 °C at 10 $°C.min^{-1}$. The Tm and the Tg values were corrected using the melting values of indium and dodecane as references.[15-17] All the DSC thermograms presented in this work correspond to the first scan results.

7. THERMO GRAVIMETRIC ANALYSIS (TGA)

TGA was employed to perform the thermal characterization of the materials analyzing the weight loss as a function of temperature and to determine the wt. % of SiO_2 in the final cured films. All the experiments were carried out in a TA instrument thermo balance Q 500. The samples were heated from 40 °C to 600 °C under nitrogen atmosphere (N_2 flow $75ml.min^{-1}$) and at a heating rate of 10 $°C.min^{-1}$ and Hi-res of six. In a second step the samples were cooled down to 300 °C and heated under air atmosphere to 800 °C in order to ensure the degradation of the polymer and to obtain the SiO_2 wt. %.

8. CONE PLATE VISCOMETER

The rheological behaviour of the different WPU systems was monitored during the phase inversion process using oscillatory flow measurements in cone-plate mode in a stress-controlled Thermo Haake Rheostress.[20] Experiments were performed at sufficiently low amplitudes to reach the linear viscoelastic regime using a cone-plate geometry (d=35mm, α=2º). 0.4 mL of sample were employed and three different temperatures used 25, 35 and 45 °C leaving 10 minutes of thermostatization before the measurements. The viscosity point was selected at 10 Hz of frecuency in all cases.

9. DYNAMIC MECHANICAL THERMAL ANALYSIS (DMTA)

Dynamic mechanical properties were analyzed in a Polymer Laboratories Mark III Dynamic Mechanical Analyzer DMTA in single cantilever mode. Scans of temperature from -60 to 150 °C at a frequency of 1 Hz, using a displacement of 0.050 and a heating rate of 2 °C.min^{-1} were carried out in bending mode, employing samples with dimensions of 2 mm length, between 4-9 mm of width and between 1–2 mm of thickness.

In this work, DMTA was employed to study the physical properties of the different materials[20-22] using the tan δ (storage modulus (E´)/loss modulus (E´)).

10. GAS CHROMATOGRAPHY (GC)

Gas chromatography (GC) was used (Shimadzu GC-14A) in order to study the polymerization of TEOS in water at different conditions.[23] GC experiments were carried out to study the reaction kinetics of TEOS in the presence of polyurethane particles through the quantification of the evolved ethanol during the polymerization process. The apparatus used was a Shimadzu GC-14A. The chromatographic columm was an Agilent 30 meters DB-waxetr capillary column of 0.53 mm internal diameter. The temperature of the detector and injector was set at 200 °C. The following temperature program was

used for the GC oven: isothermal at 45 °C for 5 min, temperature ramp at 10 °C.min^{-1} to 200 °C, where it was maintained for further 10 min. Nitrogen was used as the carrier gas at a pressure of 150 KPa. The analysis was performed in split mode with a ratio of 40:5 in a FID range of 100.

Methanol was used as the internal standard. A calibration curve was performed using known concentrations of ethanol and methanol in order to obtain the accurate ethanol concentration. The samples were prepared in a closed vial diluting 0.015-0.05 g of sample taken directly from the reactor in 10 grams of water using between 0.004-0.010 g of methanol.

At the pH of the system (9-10) it can be assumed that the condensation is favored respect to the hydrolysis. Assuming that the hydrolyzed alkoxy groups condense immediately, the conversion of the reaction can be determined using the expression below.

$$Conversion\ (wt.\ \%) = 100 * g_{exp.}/g_{max.}$$

Where g_{exp} is the weight of ethanol (g) of the sample measured by GC and $g_{max.}$ represents the maximum ethanol weight that can be formed during the Sol-Gel process.

11. TRANSMISSION ELECTRON MICROSCOPY (TEM)

In this work the TEM (Philips Tecnai 20, accelerating voltage 200 kV) was employed both for the study of the morphology of the dispersions and of the films in pure polyurethane, functionalized polyurethanes, polyurethane/silica hybrids and polyurethane/silica blends.

11.1. Dispersions

For the observation of particles (Annex 1.4), diluted samples of the dispersions (0.005-0.01 wt. % depending on the size) were prepared. Samples 0 wt. % APTES and 9.7 wt. % APTES were stained with phosphotungstic acid (PTA) in order to enhance the contrast[24].

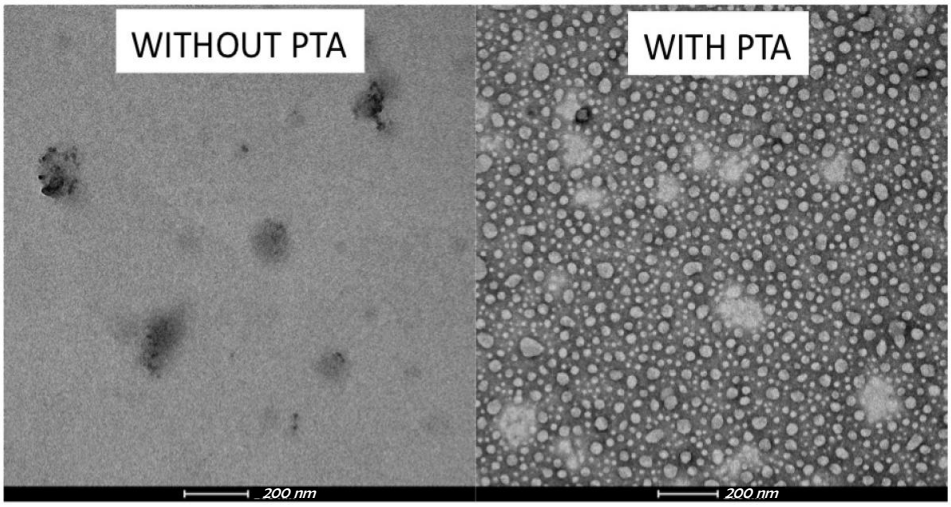

Annex 1.4. TEM images with and without PTA for a WPU containing 9.7 wt. % APTES and 8 wt. % SiO2 coming from TEOS.

11.2. Films

The films were prepared after drying the samples for at least one week. Moreover, ultrathin sections of the formed films were obtained with an ultramicrotome (LEICA ultracut EM UC6) using a diamond knife.

12. OXYGEN PERMEABILITY (P_{O2})

The oxygen gas permeability measurements were carried out using Mocon OXTRANS 2/21 equipment.

The oxygen permeability coefficient can be defined as the degree to which a polymer allows the passage of a gas or fluid. Oxygen Permeability of a material is a function of the diffusivity (D) (the speed at which oxygen molecules traverse the material) and the solubility (S) (amount of oxygen molecules absorbed per volume). Annex 1.5 shows a schematic representation of the permeator.

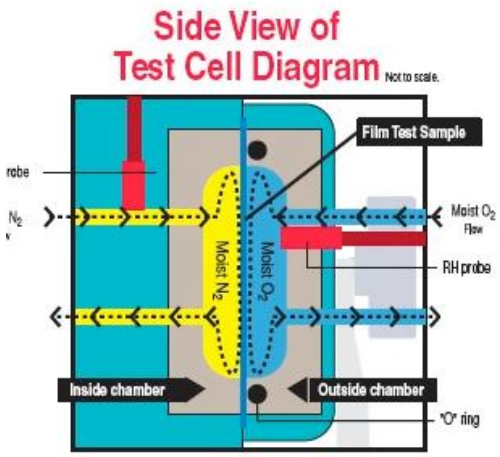

Annex 1.5. Schematic representation of oxygen permeator.

The permeation analysis was performed after drying the films at room temperature for one week and for an extra week at 30 °C under vacuum. The measurements were carried out at 23 °C under 760mmHg pressure and 0 % of relative humidity using air as permeant gas.

13. BIBLIOGRAPHY

1 Chen, J., Zhou, Y., Nan, Q., Sun Y., Ye, X. & Wang Z. Synthesis, characterization and infrared emissivity study of polyurethane/TiO2 nanocomposites. Applied Surface Science 253, 9154-9158 (2007).

2 Irusta, L., Iruin, J. J., Fernández-Berridi, M. J., Sobkowiak, M., Painter, P. C. & Coleman, M. M. Infrared spectroscopic studies of the self-association of ethyl urethane. Vibrational Spectroscopy 23, 187-197 (2000).

3 Bandekar, J. & Klima, S. FT-IR spectroscopic studies of polyurethanes Part I. Bonding between urethane C-O-C groups and the NH Groups. Journal of Molecular Structure 263, 45-57 (1991).

4 Bandekar, J. & Okuzumi, Y. FT-IR spectroscopic studies of polyurethanes: Part 3. Quantum chemical studies of the carbamate group and the urethane C-O-C hydrogen bonding in polyurethanes. Journal of Molecular Structure: THEOCHEM 281, 113-122 (1993).

5 Prabhakar, A., Chattopadhyay, D. K., Jagadeesh, B. & Raju, K. V. S. N. Structural investigations of polypropylene glycol (PPG) and isophorone diisocyanate (IPDI)-based polyurethane prepolymer by 1D and 2D NMR spectroscopy. Journal of Polymer Science Part A: Polymer Chemistry 43, 1196-1209 (2005).

6 Rochery, M., Vroman, I. & Lam, T. M. Kinetic model for the reaction of IPDI and macrodiols: study of the relative reactivity of isocyanate groups. Journal of Macromolecular Science, Part A: Pure and Applied Chemistry 37, 259-275 (2000).

7 Lippmaa, E., Maegi, M., Samoson, A., Engelhardt, G. & Grimmer, A. R. Structural studies of silicates by solid-state high-resolution silicon-29 NMR. Journal of the American Chemical Society 102, 4889-4893 (1980).

8 Magi, M., Lippmaa, E., Samoson, A., Engelhardt, G. & Grimmer, A. R. Solid-state high-resolution silicon-29 chemical shifts in silicates. The Journal of Physical Chemistry 88, 1518-1522 (1984).

9 Baccile, N., Laurent, G., Bonhomme, C., Innocenzi, P. & Babonneau, F. Solid-State NMR Characterization of the surfactant–silica interface in templated silicas: acidic versus basic conditions. Chemistry of Materials 19, 1343-1354 (2007).

10 Azaïs, T. Coury, L.B., Vaissermann, J., Bertani, P., Hirschinger, J., Maquet, J. & Bonhomme, C. Advanced solid state NMR techniques for the characterization of Sol–Gel-derived materials. Accounts of Chemical Research 40, 738-746, (2007).

11 http://www.formulaction.com/public_download/TurbiScan%20Lab%20brochure.pdf.

12 http://www-physics.ucsd.edu/neurophysics/courses/physics_173_273/dynamic_light_scattering_03.pdf.

13 Delgado A. V. González-Caballero F. Hunter R.J. Koopal L.K. & Kyklema J. Measurement and interpretation of electrokinetic phenomena. Pure and Applied Chemistry 77, 1753-1805 (2005).

14 Svecova, L. Cremel, S., Sirguey, C., Simonnot M. O., Sardin, M., Dossot, M. & Mercier-Bion, F. Comparison between batch and column experiments to determine the surface charge properties of rutile TiO2 powder. Journal of Colloid and Interface Science 325, 363-370 (2008).

15 Wunderlich, B. in Thermal analysis of polymeric materials (ed Spinger) (Springer, 2005).

16 Gabbott, P. A practical introduction to differential scanning calorimetry. (Blackwell Publishing Ltd, 2008).

17 Bagdi, K., Molnár, K. & Pukánszky, B. Thermal analysis of the structure of segmented polyurethane elastomers. Journal of Thermal Analysis and Calorimetry 98, 825-832 (2009).

18 Bottom, R. Thermogravimetric analysis. (Blackwell Publishing Ltd, 2008).

19 Furniss, D. & Seddon, A. B. Thermal analysis of inorganic compound glasses and glass-ceramics. (Blackwell Publishing Ltd, 2008).

20 Navarro-Bañón, V., Vega-Baudrit, J., Vázquez, P. & Martín-Martínez, J. M. Interactions in nanosilica-polyurethane composites evidenced by plate-plate rheology and DMTA. Macromolecular Symposia 221, 1-10 (2005).

21 Jena, K. K. & Raju, K. V. S. N. Synthesis and characterization of hyperbranched polyurethane–urea/silica based hybrid coatings. Industrial & Engineering Chemistry Research 46, 6408-6416 (2007).

22 Xiong, J., Zheng, Z., Jiang, H., Ye, S. & Wang, X. Reinforcement of polyurethane composites with an organically modified montmorillonite. Composites Part A: Applied Science and Manufacturing 38, 132-137 (2007).

23 Blum, J. B. & Ryan, J. W. Gas chromatography study of the acid catalyzed hydrolysis of tetraethylorthosilicate [Si(OC2H5)4]. Journal of Non-Crystalline Solids 81, 221-226 (1986).

24 Li, C. Y., Chiu, W. Y. & Don, T. M. Morphology of PU/PMMA hybrid particles from miniemulsion polymerization: Thermodynamic considerations. Journal of Polymer Science Part A: Polymer Chemistry 45, 3359-3369 (2007).

LABURPENA

Poliuretanoak, beraien ezaugarriengatik oso propietate desberdinak azal ditzaketen materialak dira. Honen ondorioz aplikazio-mundu zabala dute. Batzuetan material bigunak izan daitezke (itsasgarri bezala erabiltzen direnean adibidez) eta beste batzuetan, material gogorrak. Propietate desberdinak lortzeko gaitasun honen jatorria beraien bloke-kopolimero izaeran dago. Honela, Poliuretanoak bloke zurrun (poliuretanoa) eta malguez (Polieter, Poliester,...) osaturiko kopolimeroak dira.

Poliuretanoen erabilera garrantzitsuenetakoen artean gainestaldurak eta itsasgarriak aipa daitezke. Erabilera hauetan, polimeroa disolbatzaile organikoetan disolbatua aurkitzen da, eta jakina denez disolbatzaile hauen erabilera oztopo bat da ingurumenarentzat, suposatzen duten kaltearen ondorioz.

Arazo hauek konpontzeko asmotan, azken urteotan uretan dispertsatutako poliuretanoak garatu dira. Sistema hauen abantailak argiak dira disolbatzaileak erabiltzen dituzten sistemekin konparatuz. Poliuretano/ur sistemen lorpena ez da inolaz ere erraza, isozianato taldeek urarekiko azaltzen duten erreaktibotasun altua dela eta. Honen ondorioz, sintesi-prozesu berritzaileak erabil behar izaten dira poliuretanoak uretan lortu ahal izateko. Zoritxarrez, poliuretano/ur dispertsioen propietateak, disolbatzaile organikoetan lortutako poliuretanoenak baino xumeagoak dira. Beraz, disolbatzaile organikoetan oinarritutako poliuretanoak uretan dispertsatutakoez ordezkatu nahi badira azken hauek kimikoki moldatu behar dira antzeko propietateak lortzeko.

Tesi honen helburu orokorra propietate egokiak dituzten uretan dispertsatutako poliuretanoen garapena izan da. Sistema hauen propietateak hobetzeko asmotan poliuretanoak material ez-organiko batekin (silizearekin) eraldatuak izan dira. Ezaguna da material ez-organikoek polimeroen propietate mekaniko, termiko eta abar hobetzeko duten gaitasuna. Hala ere, polimero eta material ez-organikoen bateragarritasuna ahula denean (kasu gehienetan), propietateen hobetzea ez da espero litzatekeena. Honen ondorioz, bi material hauen artean bateragarritasun egokia lortzea beharrezkoa da propietateen hobekuntza lortu ahal izateko.

Tesi honetan lortutako emaitzak azaltzeko memoria hau, 5 kapitulutan zatitu dugu. Lehen kapituluan, poliuretanoen ezaugarri nagusiak azaldu ondoren, poliuretano dispertsioak lortzeko beharrezkoak diren erreakzio-baldintzak deskribatzen dira. Bukatzeko, konposatu organiko/ez-organikoei inguruko azalpen bat burutzen da, lortzeko aukera desberdinak eta bateragarritasuna hobetzeko teknikak aztertuz.

Bigarren kapituluak, poliuretano dispertsioak sintetizatzea eta karakterizazioa du helburutzat. Atal honetan sintesi prozesuaren, hots, azetona prozesuaren puntu nagusiak argitzen dira. Hala nola, poliuretano dispertsio egonkorrak lortzeko eragina duten faktoreak azaltzen dira.

Hirugarren kapituluan, poliuretano silize material hibridoen sintesi eta karakterizazioa lantzen dira bereziki. Komentatutakoaren arabera, poliuretanoen modifikazioa, konposatu ezorganikoak erabiliz, oso komenigarria da lortutako dispertsioen propietateak hobetzeko eta bide batez, dispertsio hauek disolbatzaile sistemekin lehiakorrak izateko. Hala ere, kontuan hartu beharrekoa da, konposatu organiko/ezorganikoen bateragarritasuna egokia ez denez, poliuretanoa akoplamendu agente batekin (3-aminopropiltrietoxisilanoarekin (APTES)) eraldatu behar dela propietateak hobetu nahi badira. Honela, gure lanean, APTES-aren eragina dispertsioaren egonkortasunean aztertzen da eta faseen arteko bateragarritasun egokia lortzeko behar den APTES kantitatea finkatzen da. Behin kantitate hau finkatua, hiru silize mota desberdin txertatzen dira poliuretano dispertsioan. Lehenik eta behin bi silize komertzial (CAB-O-SIL eta KLEBOSOL) zuzenean nahastu ziren eraldatutako poliuretano dispertsioarekin. Bestalde, hirugarren kasuan, silizea dispertsioan bertan ("in situ") sintetizatu zen tetraetoxisilano (TEOS) konposatutik abiatuz. TEOS-ak, Sol-Gel deritzon prozesua dela medio, silizea tenperatura baxuan eratzeko gaitasuna azaltzen du, material hibridoaren sintesia ahalbideratuz. Atal honetan dispertsio egonkorrak lortzeko lan sakona garatu da, batez ere, parte ezorganikoa gehitzeko baldintza egokienak aukeratzeko.

Behin poliuretano/silize dispertsio egonkorrak edukita, lortutako propietateak neurtzea izan zen gure helburua eta lortutako lanaren emaitzak laugarren kapituluan laburturik daude. Dispertsio hauen aplikazio garrantzitsuenak gainestaldura eta itsasgarrien arloan daudenez, erabakigarriak diren propietateak neurtu ziren. Honela, APTES eta silizearen eragina propietate desberdinetan (termiko eta mekanikoak, atxikidura-indarra, eta oxigenoarekiko permeabilitatea) azaltzen da.

Lan honetan zehar, Poliuretano/silize dispertsio egonkorren sintesia lortu da. Dispertsio hauek azaldu dituzten propietate interesgarriak direla-eta komertzialki garatzeko hautagarri interesgarriak izan daitezke. Lanaren ondorio nagusiak bosgarren kapituluan laburtzen dira.